Stony Brook University

The official electronic file of this thesis or dissertation is maintained by the University Libraries on behalf of The Graduate School at Stony Brook University.

Electrospun Conducting Polymer Composites for Chemo-Resistive Environmental and Health Monitoring Applications

A Dissertation Presented

by

Aisha Suzette Haynes

to

The Graduate School

in Partial fulfillment of the

Requirements

for the Degree of

Doctor of Philosophy

In

Materials Science and Engineering

Stony Brook University

May 2008

Stony Brook University

The Graduate School

Aisha Suzette Haynes

We, the dissertation committee for the above candidate for the

Doctor of Philosophy degree, hereby recommend

acceptance of this dissertation.

Pelagia I. Gouma - Dissertation Advisor
Associate Professor, Materials Science and Engineering

Gary Halada
Professor, Materials Science and Engineering

Miriam Rafailovich
Professor, Materials Science and Engineering

Dr. Xiao-Dong Zhang
Bose Corporation

This dissertation is accepted by the Graduate School

Lawrence Martin
Dean of the Graduate School

Abstract of the Dissertation

Electrospun Conducting Polymer Composites for Chemo-Resistive Environmental and Health Monitoring Applications

By

Aisha Suzette Haynes

Doctor of Philosophy

In

Materials Science and Engineering

Stony Brook University

2008

The focus of this dissertation is the development of polyaniline based hybrid systems for selective room temperature detection of NO_2. The electrospinning technique has been employed to produce highly dispersed nanocomposites of leucoemeraldine base polyaniline (LEB-PANI) with poly-vinyl-pyrrolidone (PVP) and cellulose acetate (CA) as secondary components. The nanocomposites exhibit relatively high sensitivity and selectivity to NO_2 down to 0.5 ppm with response times down to 40 s and recovery times down to 155 s at varying levels of humidity.

DC electrical resistance measurements reveal that the responses of the LEB-PANI composites have dependence on the humidity level and concentration of LEB-PANI in the composite matrix, whereas at low concentrations the resistance decreases on exposure

iii

to NO_2, for a 1:1 PVP LEB-PANI ratio there was no response to NO_2, and for high LEB-PANI concentrations the resistance increased on exposure to the analyte. The varying response mechanisms are attributed to the oxidation state and degree of water absorption by PVP and LEB-PANI. DC electrical resistance measurements of the CA LEB-PANI composite during exposure to the analyte suggest that the response mechanism has dependency on the humidity level in the gas chamber such that on exposure to NO_2 the electrical resistance of the film decreases. This is partly attributed to the hydrolysis of CA yielding acetic acid which lightly dopes polyaniline and acts as an additional reactant site along the polymer backbone for NO_2.

An in-situ gas sensing ultraviolet-visible spectroscopic technique was developed to analyze the effects of processing and the sensoric nature of the LEB-PANI composites. Absorption spectra of the PVP LEB-PANI composites reveal that as the concentration of LEB-PANI increased the oxidation level increased from the reduced state to the emeraldine oxidation state, as evaluated against the work of MacDiarmid et al. The oxidation level of the CA LEB-PANI composite films also exhibited an increase in the oxidation level to the emeraldine oxidation state.

The evolution of the electronic transitions in the films were analyzed at different levels of humidity and under exposure to NO_2 revealing that for the PVP LEB-PANI composites, water vapor absorbed into the electrospun mat and adsorbed on LEB-PANI (via H- bonding and protonation of amine and imine sites, respectively) acts as a primary charge carrier for polyaniline (through the formation of polarons and bipolarons). This charge transport mechanism of hydrated LEB-PANI is shown to be analogous to the Grotthus mechanism for proton transport.

The observations relative to effects of NO_2 exposure reveal the existence of several reaction mechanisms between LEB-PANI and NO_2: 1) NO_2 can oxidize the polymer transferring an electron from the N center to the gas, and 2) NO_2 can be dissolved by the water vapor producing H_3^+O, HNO_2, and NO_2^- which can both reduce and protonate imine sites of LEB-PANI. The latter affects to the stability of the sensors.

These studies coupled with x-ray photoelectron spectroscopy (XPS) and infrared spectroscopy (FTIR) of the films, are used to determine the proper paradigm for NO_2 detection with LEB-PANI.

Dedicated to

My beautiful mother and daughter

Table of Contents

LIST OF FIGURES

LIST OF TABLES

ACKNOWLEDGEMENTS

The work presented in this dissertation would and could not have been initiated or completed without the support of family, friends, and co-workers.

First I'd like to thank God for answering all of my prayers in these last years and for all the blessings he's bestowed on me.

I thank my mom, Suzette Bishop, who has always provided the love and support necessary for me to progress to this stage in my life. Rightfully my thesis is dedicated to her because she is always in my corner. I'd also like to thank my sisters, Shelley and Amanda, for their love and confidence in my ability to complete this chapter of my life.

I thank my husband for putting up with my late nights, my messiness, and my stress. Thank you Kenny, for taking care of our beautiful daughters (Kianah and Kandice) and making sure I had space and time to complete my work. I am grateful for your love and support. Thank you for your understanding and for my beautiful daughter Kandice to whom I dedicate this work to - my darling you have motivated me to do so much more!

I am grateful to Dr. Perena Gouma, my advisor, my mentor, my friend, you have believed in me since day one even when I'm sure there were times you were unsure of what I was doing or thinking. I'm so fortunate to have had you mentor me throughout my research and in the last few years. You have provided me with so many opportunities from being creative with my research to touring the world. No words can express how grateful I am for all of your support and all of your advice. Thank you.

To my lab mates (old and new), Krithika Kalyanasundaram, Lisheng Wang, Smita Gadre, Kasia Sawicka, and Prashant Jha, thank you for your help in the lab and thank you for your support through my research. Thank you Krithika for being a dear friend as well as my colleague.

I'd like to thank the Materials Science Department, namely, Debbie, Lynn, and Jim and my defense committee, thank you for your time, patience, and understanding. Dr. Zhang thank you for taking the time to attend my presentations and review my work.

Thank you Benet labs and Analysis and Evaluation Technology at ARDEC for your support, and especially for *all* the time you gave me to complete this work.

Finally I would like to thank Dr. Elisabetta Comini, Dr. Dave Kubinski, and Dr. Namita Choudhury for their expertise and countless support throughout my studies. Especially Dr. Comini, to whom conducted a great deal of sensing experiments for me; thank you for your patience and time with me.

VITAE

Aisha Suzette Haynes
Materials Engineer
Email Address: aisha.s.haynes@us.army.mil

I. Education

State University of New York at Stony Brook, Stony Brook, NY　　May 2008
PhD in Materials Science and Engineering　　GPA: 3.74

Rensselaer Polytechnic Institute, Troy, NY　　Dec. 2001
Bachelor of Science in Engineering Physics　　GPA: 3.04
Minor in Applied Mathematics

II. Employment

Oct. 2007 – Present　　*GS-12 Materials Engineer,* US ARMY ARDEC
　　Picatinny Arsenal, Picatinny, NJ
　　Clearance: Secret

- Lead Materials Engineer for Fuze Precision and Armaments Technology - Analysis and Evaluation Division.

Aug. 2004 - Present　　*Research Fellow,* Materials Science & Engineering, State University of New York, Stony Brook, NY

May 2001 – Oct. 2007　　*YD-2 Materials Engineer,* US ARMY RDECOM, Benet Laboratories, Watervliet, NY
　　Clearance: Secret

Performed as Project Leader for:
- U.S. ARMY Strategic Environmental Research and Development Program – University of California at Riverside: "Zeolite Coating System for Corrosion Control to Eliminate Hexavalent Chromium from DOD Applications", 2003-2004
- U.S. ARMY Strategic Environmental Research and Development Program – NAVAIR China Lake: "Novel Electroactive Polymers as Environmentally Compliant Coatings for Corrosion Control", 2002-2004

Performed as Principle Investigator for
- In-House Laboratory Research: "H_2O Doped Polyaniline for Gas Sensing Applications", 2006-2007
- In House Laboratory Research: "Investigation of Chemical Warfare Agent (CWA) Sensor Polymer Coating-Simulant / Interferent Interactions by Atomic Force Microscopy", 2003-2004

Developed and facilitated Test Service Agreements (TSAs) and Cooperative Research and Development Agreements (CRADAs) with:

- New Jersey Institute of Technology for collaboration on the study of Smart Materials developed through the Army's Smart Material Program (TSA)
- GE Silicones – Confocal Microscopy of Human Hair (TSA)
- Strong Epilepsy Center of University of Rochester Medical Center – for the development of a Seizure Monitor (CRADA)
- State University of New York at Stony Brook for collaboration on the study of novel polymer based chemical and biological sensors for homeland defense technologies (CRADA)

III. Scholarships & Awards
2007: NSF Travel Award to attend NATO Advanced Study Institute
2006: NSF Fellow, U.S. Delegate for 56th Meeting of Nobel Laureates in Chemistry in Lindau, Germany
2004: W. Burghardt Turner Fellowship
1997: Rensselaer Medalist

IV. Affiliations:
Materials Research Society
American Ceramic Society
The Minerals, Metals & Materials Society
American Society for Metals

V. Presentations
Government

Invited
1. NATO Advanced Studies Institute on Sensors for Environment, Health and Security: Advanced Materials and Technologies, Vichy France 9-25 September 20072007

Contributed
1. US DTRA Nanoelectronic Devices for Defense and Security, Crystal City VA, 18-19 June 2006

Non-Government

Invited
1. NitroEurope/NinE summer school, Seminar on   , Federal Research and Training Centre for Forests, Natural Hazards and Landscape (BFW), Vienna Austria, 2-5 Oct 2006

Contributed
1. 11th International Meeting on Chemical Sensors, Brescia, Italy, 16-19 July, 2006
2. ACUN-5 International Conference, Sydney, Australia, 11-14 July 2006
3. Material Research Society Symposium - Fall Meeting, Boston, MA, 28 November, 2005

VI. Publications

[1] **A. Bishop** and C. Mulligan, "Effects of Surface Preparation Techniques on the Adhesion of Tantalum Sputtered Coatings", ARCCB-TR-03015, 2003

[2] **A. Bishop** and P. Gouma, "Electrospun bio-nano-composites for electronic pathogen detection devices", Proceedings of the International Conference on Bio-Nano-Informatics (BNI) Fusion, Marina del Rey, CA, USA, July 20-22, 2005

[3] **A. Bishop** and P. Gouma – "Leucoemeraldine Based Polyaniline-Poly-vinyl-pyrrolidone Electrospun Composites and Bio-composites: A preliminary Study of Sensing Behavior", Reviews on Advanced Materials Science **10** (3), 2005

[4] **A. Bishop**, C.S. Balazsi, and P. Gouma, "Hydroxyapatite Biocomposite Coatings Prepared by Electrospinning for Advanced Prosthetics", Proceedings of the 8th International Symposium on Polymers for Advanced Technologies, Budapest, Hungary, September 13-16, 2005

[5] **A. Bishop** and P. Gouma, "Self Assembly in Biologically Synthesized Electrospun Electroactive Polymers", Electroresponsive Polymers and Their Applications, edited by Vivek Bharti, Yoseph Bar-Cohen, Zhong-Yang Cheng, Qiming Zhang, John Madden, Materials Research Society Symposia Proceedings, v. **889**, 0889-W01-06, Warrendale, PA, 2006

[6] P. Gouma, K. Kalyansundaram, and **A. Bishop**, "Electrospun single-crystal MoO_3 nanowires for biochemistry sensing probes", Journal of Materials Research, v. **21** (11), pp. 2904-2910, 2006

[7] **A. Bishop**, C.S. Balaszi, J.C. Yang, and P. Gouma, Biopolymer-Hydroxyapatite Composite Coatings Prepared by Electrospinning" Polymers for Advanced Technologies, v. **17** (11-12), pp. 902-906, 2006

[8] **A. Bishop**, D. Kubinski, and P. Gouma, "Polyaniline Based Hybrids for NH_3 Sensing", Proceedings of the 11th International Meeting on Chemical Sensors, Brescia, Italy, July 16-19, 2006

[9] **A. Bishop** and P. Gouma, "Electrospun Polyaniline Composites for NO_2 Detection", Proceedings of the ACUN-5 International Composites Conference: Advanced, Infrastructure, Natural and Nanocomposites, Sydney, Australia, July, 11-14, 2006

[10] P. I. Gouma, **A. Bishop**, K. K. Iyer, "Single Crystal Metal Oxide Nanowires as Bio-Chem Sensing Probes", Rare Metal Materials and Engineering, v. **35**, p. 295-298, 2006.

[11] **A. Bishop-Haynes** and P. Gouma, "Electrospun Polyaniline Composites for NO_2 Detection", Materials and Manufacturing Processes, v. **22** (5-6), pp. 764-767, 2007

[12] **A. Haynes** and P. Gouma, "Polyaniline Based Environmental Gas Sensors", NATO Science Series, Accepted **-** 2008

[13] **A. Haynes** and P. Gouma, "Electrospun Conducting Polymer Based Sensors for Advanced Pathogen Detection, IEEE Sensors Journal, Accepted - 2008

CHAPTER 1

1. Introduction

Gaseous agents such as NH_3, CO, SO_2, CO_2, and NO_2 are detrimental to human health and the environment. The most common source for these analytes is automobiles. Automotive emissions alone contribute 50-70% of these gases in the atmosphere [1-2]. Other sources include industrial and residential processes that burn fuel (i.e. utilities), farming, metals processing, and mining. The environmental impact of increased levels of these analytes ranges from low ozone/smog formation to global warming. Moreover, many of these gases can react with each other resulting in changes in climate, temperature, and air quality. Inhalation of gas concentrations above normal (in ambient air) may provoke the development of respiratory illnesses (i.e. bronchitis and emphysema), skin, eye, and nose irritations, cardiovascular problems, a weakened central nervous system, and can even be fatal after long term exposures [2].

In order to monitor these analytes in ambient air, federal and state agencies (Environmental Protection Agency, Department of Defense, Department of Energy, National Science Foundation, etc.,) have been sponsoring research and development of environmental and health monitoring systems. Among the plethora of sensors currently under development, resistive ceramics or polymer based technologies have shown to be very promising. Ceramic chemoresistors offer high sensitivity to many of the target analytes; however, these sensors are only operable at high temperatures, thus needing more power for operation which yields increase in costs of manufacturing devices made

from these materials. Polymer chemoresistors on the other hand operate at room temperature and so are more likely to be more economical to manufacture in mass quantities. However, many of the available polymers based sensor technologies inherently lack selectivity. The focus of this dissertation will be the development of novel room temperature gas sensing system for the selective detection of NO_2 based on electroactive (conducting) polymers: and to understand the sensing mechanism involved.

1.1. ENVIRONMENTAL AND HEALTH IMPACTS OF NO_2

Nitrogen dioxide belongs to a myriad of toxic gases created from combustion systems as discussed above. The health impacts of inhaling NO_2 gas above concentrations in ambient air (according to the U.S. environmental protection agency's - EPA - air quality trends studies from 1990-2006, the concentration is typically less than 0.053 ppm) may range from bronchoconstriction in asthmatics (occurring at concentrations >0.1 ppm - people who suffer from asthma are more sensitive to changes in air quality) to irritation of eyes, nose, and throat (occurring at concentrations >1 ppm), to a decrease in cardiovascular and pulmonary function, lung damage and lung edema, and the onset of diseases such as bronchitis and emphysema (occurring at concentrations >5 ppm) [3-4].

The environmental impact of elevated NO_2 concentrations may stem from upsetting the concentration of reactive N_2 which affects the natural nitrogen cycle and overall air, land, and water quality. Reactions between NO_2 with other toxic agents (such

as SO_2) causes changes in climate, temperature, air, and water quality through the formation of smog or low level ozone, acid rain (which can destroy plant and aquatic life), and green house gases which contribute to global warming.

1.1.1. *NO₂ in Exhaled Breath*

Medical studies have associated certain constituents of the human breath with specific types of diseases, and have addressed the importance of diet, dental pathology, smoking, etc. on determining the physiological levels of bio-marker concentrations in exhaled breath [5-6]. Inflammation and oxidative stress in the lungs can by monitored by measuring the changes in the concentration of the following gases [7-9]: NO (which has been widely studied as a bio-marker), and it's related products NO_2- (nitrite) NO_3- (nitrate); exhaled CO (also a marker for cardiovascular diseases, diabetes, nephritis, bilirubin production); exhaled hydrocarbons of low molecular mass, such as ethane, n-pentane; ethylene, isoprene (hydrocarbon affected by diet which is a marker for blood cholesterol levels) [9]; acetone; formaldehyde; ethanol; hydrogen sulfide, carbonyl sulfides, and ammonia /amines [10].

Changes in NO concentration in human breath can be directly monitored through detection of its end products NO_2 and NO_3. For healthy adults the concentration can be as low as 0.2 ppm. In the event of oxidative stress, pulmonary distress, or asthma the concentration of NO_x increases. For example, in the latter the concentration of NO_x can increase to 0.38 ppm [11].

Several requirements for a successful NO_2 sensor include high sensitivity (the sensor needs to detect NO_2 concentrations as low as 1 ppm as the standards set by the occupational health and safety administration are 1 – 3 ppm for long term exposures which are greater than 8 hours, and 5 ppm for short term exposures, which are less than 15 minutes [4]), high selectivity to low concentrations of NO_2 in the presence of other gases (i.e.NH_3 and CO for environmental monitoring; isoprene, acetone, ethanol, and NH_3 for breath analysis), fast response and recovery times, and good stability over extended and repeated exposures.

1.2. CHEMICAL SENSORS FOR NO_2

Typically for any chemical sensing material, analyte molecules interact with the sensing element resulting in a physical or chemical change on its surface which is converted by a transducer to a physical (surface acoustic wave), chemical (pH), optical (color), or an electronic (resistance, conductance, voltage etc.,) [12] output signal, figure 1.2.1. Table 1.2.1 outlines current NO_2 gas sensor technologies and sensor elements commonly employed.
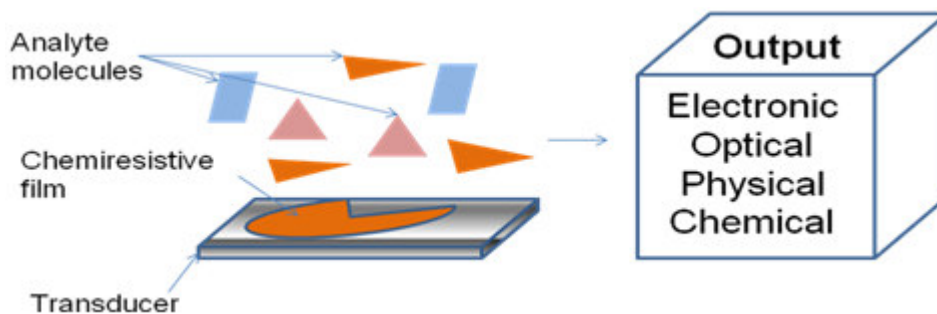
Figure 1.2.1 Chemical Sensor Setup

Table 1.2.1 Current NO_2 chemical sensor technologies and the materials employed

Sensor Output	Material	Ref.
Electronic		
Resistive	Indium acetylacetonate (InAcAc), nickel phthalocyanine (NiPc), copper(II) para-tetratolylmethylporphyrine (CuTTMP), poly(3,4-ethylenedioxyphioene, n-InP, Cu_2O	13-16
Conductimetric	Carbon nanotubes, SnO_2, Fe_2O_3, SiO_2-NiO and SiO_2-Co_3O_4	17-19
Potentiometric	Pt-loaded zeolite, WO_3	20
Optical	poly (3-octylthiophene), single wall carbon nanotubes (SWCNT), quartz, phthalocyaninato-iron(II); SiO_2-NiO and SiO_2-Co_3O_4	19, 21-24
Physical	SWCNT, TiO_2; ZnO_2, polyaniline, polyacrylic acid, DNA, In_2O_3, TiO_2, $Pt/TaSi_x/SiO_2/SiC$, barium carbonate ($BaCO_3$)	22, 25-31
Chemical - Electrochemical	Oxide-potassium nitrate, WO, $NaNO_2$, NASICON	32-36

Of these, resistive sensors (chemoresistors) provide a direct output of changes in the electronic properties of the sensor material in the presence of a chemical analyte. The

output signals of chemoresistors are manifested as changes in electrical resistance of the sensing element which can be directly correlated to analyte concentration.

1.2.1. *Chemoresistive Sensors*

For a chemoresistive sensor, the sensing element exhibits a change in its electrical resistance upon exposure to a gas or liquid. This change is attributed to the nature of the charge carriers inherent in the sensing element and the exchange and mobility of charges between the analyte and the sensor. If the charge carriers are positive (i.e. holes) than on removal of an electron the electrical resistance of the film will decrease, this is also the case in the event where the analyte contributes a positive charge (i.e. H^+). If the analyte contributes an electron to the molecular matrix of the sensor than an increase in resistance is observed. On the contrary, if the charge carriers are negative (i.e. electrons) than on the removal of an electron the resistance will increase, and on addition of an electron from the analyte to the sensing element the electrical resistance of the sensor would decrease. The type of charge carriers inherent in the sensor matrix is dependent on a processing mechanism called doping. Doping is defined as the introduction of impurities into a pure material inducing changes in the materials electrical properties. A material can be p (positively) or n (negatively) doped, that is the dopant can remove or add electrons from the material, respectively. Traditionally the material can be doped with a chemical (i.e. acid or base) or in more advanced efforts molecularly doped with metals and or ceramics to induce specific electronic properties within the host's matrix. The impurity dopant thus transforms the material from an insulating matrix to a semi-

conducting or conducting system for which the new charge carriers can react with the target chemical analyte.

Chemoresistive sensors are designed to optimize the five key elements of a sensor: sensitivity, selectivity, response time, recovery time, and stability. Sensitivity is defined as the magnitude of the change in electrical resistance of the sensor on exposure to an analyte. The response of the sensor can be translated to sensitivity via the following relation, (1.1):

$$S = \frac{\Delta R}{R_o} \qquad (1.1)$$

where ΔR is, the change in electrical resistance of the sensor denoted by R_g - R_o, R_g is the resistance of the film during exposure to the analyte, and R_o is the resistance of the film in air. The magnitude of the response can also be reported as the normalized resistance i.e. $\frac{R_g}{R_o} or \frac{R_o}{R_g}$ depending on whether or not the analyte is as oxidizing agent or reducing agent, respectively.

The response time is defined as the time it takes for the sensor resistance to change from baseline to 90% of the saturated response during exposure to the analyte. And the recovery time is defined as the time it takes the electrical resistance of the sensor to return to 90% of its baseline after removal of the analyte.

Stability is related to the consistency and steadiness of the sensor response after extended and repetitive exposures to an analyte. In the event the sensor becomes poisoned by the analyte, a drift in the sensor's baseline resistance can be observed. Moreover this drifting can translate to changes in the amplitude of the response the more poisoned the sensor becomes.

Selectivity reflects how the sensor operates or is affected by interfering analytes of similar and dissimilar nature (i.e. reducing gases vs. oxidizing gases, or an oxidizing gas in the presence of other oxidizing gases) If the sensor only responds to the target analyte in the presence of these interferents than it is said to be selective.

1.3. POLYMER BASED CHEMORESISTIVE SENSORS

As discussed previously, polymer based chemoresistors offer the advantage of being operable at room temperature and are more economical to manufacture compared to their ceramic counter parts. In this section, a description of a class of polymers termed 'conducting polymers' employed for chemoresistive sensing applications will be given.

Polymers are repeating units of carbon chains with immobile electrons bound by covalent bonds formed between carbon and other atoms making them insulating by nature. A class of polymers termed '*electroactive*' consists of conjugated chains, whereas the system is comprised of atoms with alternating single and double bonds with the latter consisting of p orbitals. The structure is said to consist of delocalized π bonds (the superposition of 2p atomic orbitals between atoms in a covalent double bond [37])

which can be manipulated by chemical or electrochemical means to alter the density of charge (i.e. electrons or protons) within the conjugated species. Manipulation of these chains by reduction/oxidation mechanisms (via changes in number of electrons) and in the case of polyaniline, protonation/deprotonation (change in number of protons while the number of electrons remain unchanged) has led to the development of intrinsically conducting polymers - ICPs.

ICPs are '*electroactive*' polymers that possess electronic and magnetic properties while retaining their structural characteristics [38]. It has been demonstrated by the Nobel laureates A. Heeger, A. MacDiarmid and H. Shirakawa that charges can be added or removed from the polymer chain electrochemically or chemically by introducing acidic or basic solutions (i.e. doping) during the polymerization or post processing of the polymer. The negative or positive (holes) ions formed are then free to move throughout the polymer chain creating current throughout transport. ICPs are a class of polymers that can be made conducting without the use of conductive additives. Examples of conducting polymers studied for sensing applications are polypyyrole, polythiophene, poly (3,4-ethylenedioxythiophene), poly(phenyl vinlene), and polyaniline, figure 1.3.1.
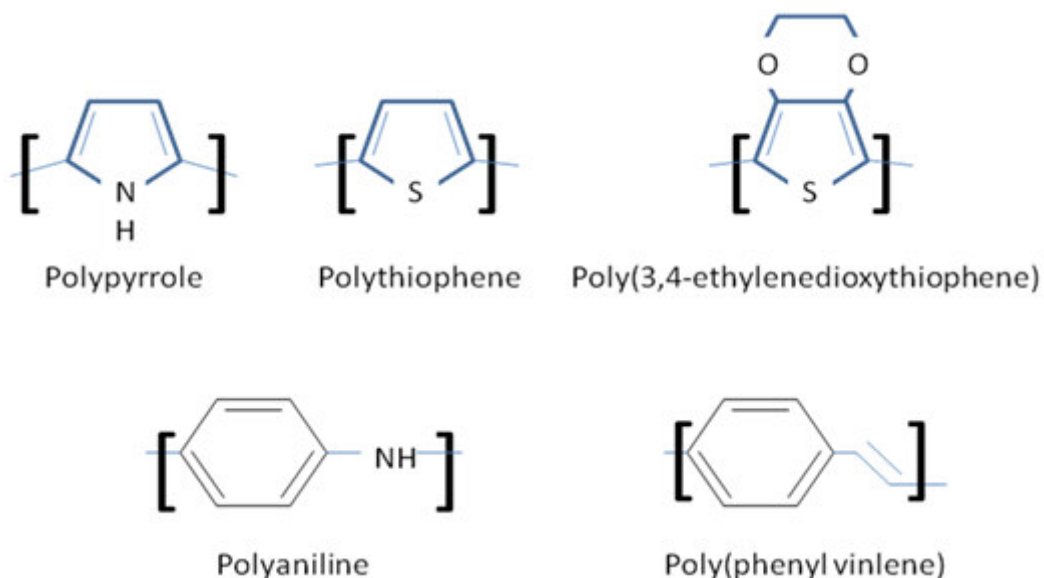
Figure 1.3.1 Structures of popular intrinsically conducting polymers used in resistive sensing applications
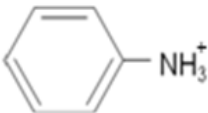
During sensing the polymer can exhibit swelling due to absorption of the analyte, but more importantly the analyte molecules can adsorb and react with active sites along the molecular structure of the polymer inducing conformational and electronic changes in the polymer that translate to a change in the films electrical resistance. These changes can also be manifested as optical, physical, chemical, electrochromic, or magnetic changes in the polymer.

Conducting polymers such as polypyrrole and polyaniline have been widely researched for NO_2 detection. According to literature however, chemoresistors based on polyaniline has shown to uphold higher sensitivities (down to 0.5 ppm of NO_2) [39-40] as compared to polypyrrole based chemoresistors (down to 20 ppm of NO_2) [41]. Due to the enhanced sensitivity of polyaniline to NO_2, polyaniline was chosen as the optimum
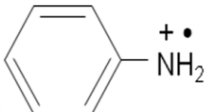
ICP for the NO$_2$ detection studies presented in later chapters. A brief background on the structure of the polymer will be discussed in the next section.

1.3.1. *Polyaniline: Background and Structure*

The monomer aniline was first reported in 1862 by Letheby [42] and was synthesized to form different oxidation states by [43-46] in the early 20th century. It was later sought in the late 70's by [47] that the polymer polyaniline can be made conducting via chemical or electrochemical doping mechanisms. The traditional routes for producing polyaniline are chemical oxidative polymerization and electrochemical oxidative polymerization (which occurs in an electrochemical cell – two or three electrode). Generally, the synthesis of polyaniline can be expressed as follows: the aniline monomer is first dissolved in an acidic solution (i.e. dopant solution such as HCl)

to form (in this case a proton is transferred from HCl to the monomer). An oxidant (such as ammonium peroxydisulphate) transforms it to the anilium cation , which then reacts with other units through hydrogen bonding to form diamine chains which react with other chains to form the extended conjugated network. This process produces the highest oxidation form (pernigraniline - to be discussed later in the section). A reductant (i.e. NaOH) can then be employed to produce the other polymer forms.

11

The base structure of polyaniline, as depicted in figure 1.3.2, consists of a reduced unit or benzenoid attached to an amine (-NH-), and an oxidized unit or quinoid attached to an imine (-N=). The amines and imines are the nitrogenous centers of polyaniline which may react with dopant agents and/or analyte and the ratio of amines to imines dictates the oxidation state. Polyaniline exists in several oxidized forms. The most studied and widely accepted are the leucoemeraldine which is the fully reduced form, $y = 1$, the emeraldine form which is half oxidized, half reduced, $y = 0.5$, and the pernigraniline form which is the fully oxidized form, $y = 0$.

Transformations between oxidation states are reversible and controlled using reducing or oxidizing mechanisms. During oxidation of leucoemeraldine base the oxidant removes an unbound electron from the amine nitrogen center, a proton is liberated, and the lone unbound electron resonates to a neutral position, forming an imine. Leucoemeraldine can be oxidized to emeraldine and then pernigraniline. From pernigraniline, leucoemeraldine can again be obtained by reducing pernigraniline to emeraldine and finally back to leucoemeraldine with an alkaline solution (i.e. NaOH). The emeraldine base is deemed the most stable form of polyaniline that is because further oxidation of the pernigraniline state results in degradation of the polymer back to emeraldine and leucoemeraldine can be easily oxidized in air. Thus the most widely used and widely studied form of polyaniline is the emeraldine form.
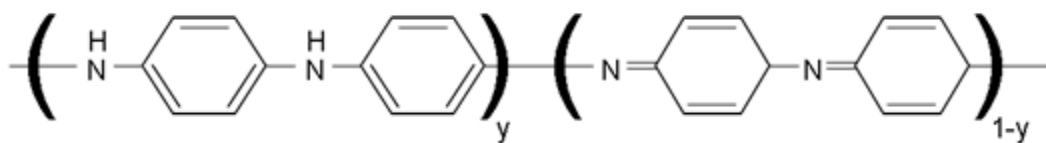
Figure 1.3.2 Base structure of polyaniline for y=1 the oxidation state is leucoemeraldine, for y=0 the polymer is in the pernigraniline oxidation state and for y=0.5 the polymer is in the emeraldine oxidation state

1.3.2. *Doping Mechanisms*

All three states can exist in the base and salt form. In the former the polymer is insulating and upon doping can be transformed into a conducting salt. The highest conducting form is the emeraldine salt (ES-PANI). The two most common methods used to produce ES-PANI are oxidative doping of leucoemeraldine base (LEB-PANI) and protonic acid doping, of emeraldine base (EB-PANI). Figures 1.3.3 and 1.3.4 detail both mechanisms to producing ES-PANI. Both methods result in the creation of reactive sites delocalized along the polymer backbone through which charge transport can occur.

Oxidative or p doping is a two step process which starts with oxidation (a example of an oxidant is H_2O_2) of LEB-PANI yielding the partial removal of electrons from the polymer chain and doping with an acid (i.e. camphorsulfonic acid or HCl) to incorporate molecular impurities at the same sites through the addition of holes and anions (in the case of HCl, H^+ is the hole or positive charge and Cl^- is the anion) [48]. During doping the polymer becomes positively charged and anions provide charge neutrality. Theoretically pernigraniline base (PB-PANI) can also undergo reduction or n doping to produce ES-PANI, where cations are inserted at the sites where electrons are

added imparting a negative charge on the polymer chain. Reductive or n doping however is not commonly employed for preparing ES-PANI. The impurities added to the polymer can inflict localized distortions (associated with the charge on the site) in the conformational structure (i.e. ring torsion). These distortions are coupled with defects called polarons (primary charge carriers formed during doping and oxidation; a positive polaron is formed when a hole is coupled with an anion -typically resembles the form of an amine) and bipolarons (charge carriers formed when secondary charges are removed from the electronic structure; not energetically stable and is typically centered around a quinoid di-imine group). The effects of these defects on the conductivity and structure of polyaniline will be discussed later in this chapter.

Protonic acid doping of EB-PANI can yield a positively charged polymer from the addition of protons (coupled with an anion) at imine sites along the polymer chain while the number of electrons in the π system remains unchanged. The protons and anions added to the system also inflict distortions coupled with polarons and bipolarons along the polymer chain. The emeraldine salt form produced through this mechanism consists of -N^+H- units throughout the matrix. H^+Cl^- is also a common protonic acid employed for this process. Currently protonic acid doping is the more popular doping mechanism employed for producing ES-PANI.

The defect sites act as charge carriers and tunneling bridges for ions. Moreover the dopant anions (cations for n doped materials) can react with analyte molecules with higher sensitivity and selectivity depending on the anion and target analyte [49]. These mechanisms can impart electrical conductivities in polyaniline up to 10^{-1} S/cm [48]. The

electronic nature of polyaniline (i.e. conduction mechanism) will be discussed in the next

section.
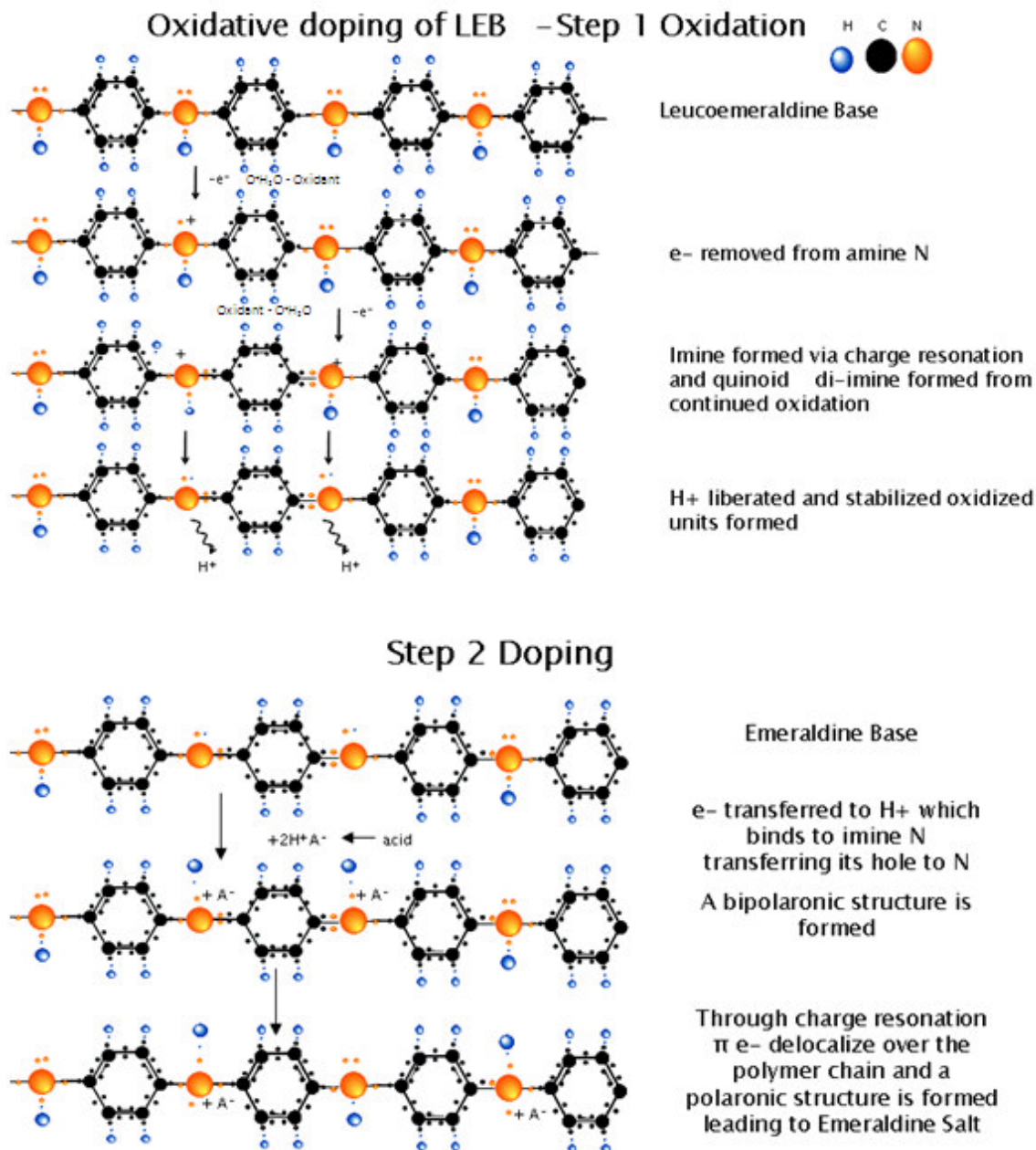
Figure 1.3.3 Oxidative doping mechanism from LEB-PANI to ES-PANI. The steps are interchangeable and either one can occur 1st during the chemical/electrochemical reaction.

Protonic acid doping of EB
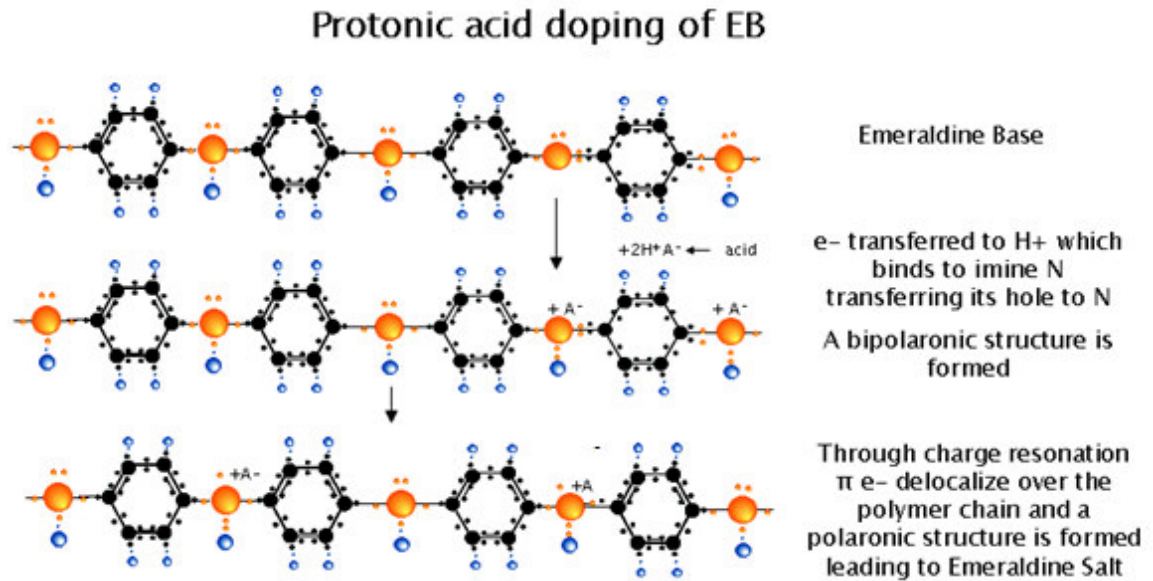
Figure 1.3.4 Protonic acid doping of EB-PANI to ES-PANI

1.3.3. *Conduction in Polyaniline*

Electronic conduction in polyaniline is a function of interchain, interdomain, and intrachain charge transport where

$$\sigma = nq\mu = f(\text{int }erdomain) : f(\text{int }erchain) : f(\text{int }rachain) \qquad (1.2)$$

and n is the number of carriers, q is the charge on the electrons and µ is the mobility. Intrachain electrical conductivity has dependence on conjugation length and number of defects in the system. Interchain and inter-domain electrical conductivity has dependence on degree of crystallinity (the increase in crystallinity allows for an increase in charge hopping sites). The transport routes have been depicted in figure 1.3.5.

16
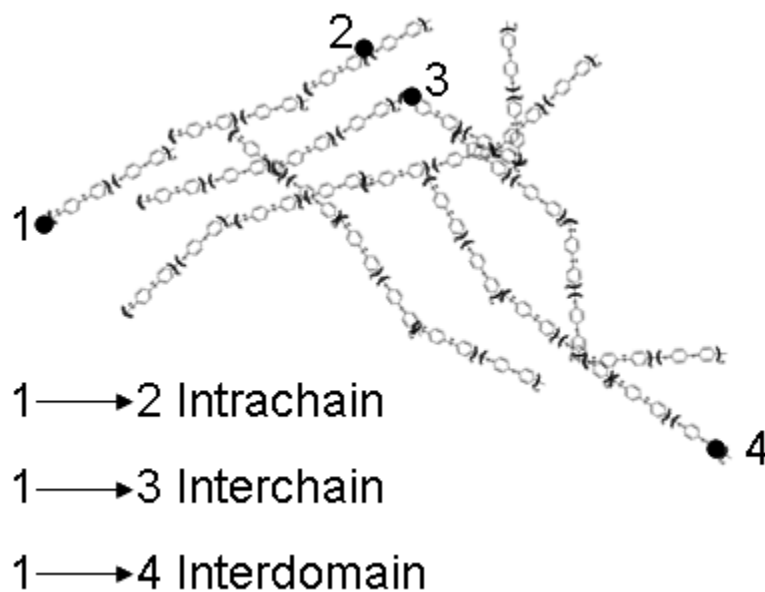
Figure 1.3.5 *Intra*-chain, *Inter*-chain, and *Inter*-domain charge transport routes

Researchers have developed models to explain the electron-phonon interactions in polyaniline as ions move through its matrix. For low doped polyaniline (where few sites along the chain have been doped – not highly conducting) the popularly accepted variable range hopping mechanism [50-51] has been employed to prove that at low temperatures, in a disordered system (such as a conducting polymer) the charge transport mechanism is governed by hopping and/or tunneling mechanisms along doped/conducting sites. As the doping and oxidation level increases, molecular chain arrangements resulting in interchain coupling and intrachain order [52-54] can cause phase segregation of the polymer into crystalline conducting regions and amorphous insulating regions [55]. It has been shown [55] that charge transport for these materials depends on the crystalline moieties formed such that ion transport occurs macroscopically through these regions

(surrounded by insulating charge barriers) as opposed to the molecular charge transport mechanism of lightly doped conducting polymers.

The level of crystallinity may also influence the color of the polymer. In the reduced form (LEB-PANI) it has been observed that changes in color from colorless (or opaque) to dark blue can be attributed to the presence of partially crystalline regions [56-57] as a consequence of the polymer's ease of oxidation in air. Commercial LEB-PANI powders can be found with this character. As the oxidation level and doping level increases the level of crystallinity or chain ordering also increases and the pigmentation traverses from dark blue to dark green.

Conducting polymers such as polyaniline are termed '*disordered semiconductors*'. That is because during doping an electron is removed from the 'top of the valence band' and excited to a higher transition, the highest of course being a transition to the conduction band. Many researchers have idealized band theory of inorganic semiconductors such as Si and GaAs to describe doping effects and the basic electronic conduction properties of ICPs. Alternatively the valence and conduction bands in inorganic semiconductors translates to π or bonding and π^* or anti-bonding bands in conducting polymers, respectively. Electrons (π electrons -electron from π bond created between two atoms in a conjugated system, i.e. C=C, C=N, C=O) can nucleate through the conjugated system via the π bonds (C=C consists of 1 σ bond and 1 π bond, the latter of which needs less energy to break) between C and N and C and C (for polyaniline). Once this happens the charge is said to be excited from a lower energy (bonding molecular orbital) to a state of higher energy (anti-bonding molecular orbital) within the

molecular matrix. Once excited, the electron can be easily removed (i.e. by an oxidizing gas).

During doping (looking at p doping for simplicity) distortions formed along the polymer chain translate to intermittent states (localized electronic states) within the band gap to which electrons can transition to once excited from the π band.   This results in distortion of the highest occupied molecular orbital (HOMO) upward and relaxation of the lowest unoccupied molecular orbital (LUMO) downward within the band gap. These localized states can be conceived as the polarons and bipolarons formed within the physical structure of the polymer. The electronic states created just below the π^* band and just above the π band remain completely empty and completely full, respectively until an electron is excited. It should be noted that electrons once transitioned to these mid gap states can be removed and excited from these energy band to higher energy bands. Polaronic bands are formed initially and if further electrons are removed (from the polaron as well as the π band) the formation of bipolaronic bands transcends. With further doping, the electronic states can coalesce into new electronic bands. The result is a smaller band gap (electronic bands move closer to the Fermi energy) and evolution of the polymer from an insulator to an organic metal transpires. Figure 1.3.6 depicts the formation of these localized states and the transition of the HOMO and LUMO. The width of electronic band gap in polyaniline ranges from 3.6 eV for leucoemeraldine to 1.4 eV for pernigraniline [58].

Both the polarons and bipolarons act as charge carriers for delocalized electrons to tunnel through the monomer units inducing a flow a charge along the polymer chain.

Physically polarons are de-localized charge carriers and bipolarons are localized charge carriers, with the former being the more energetically favorable defect.
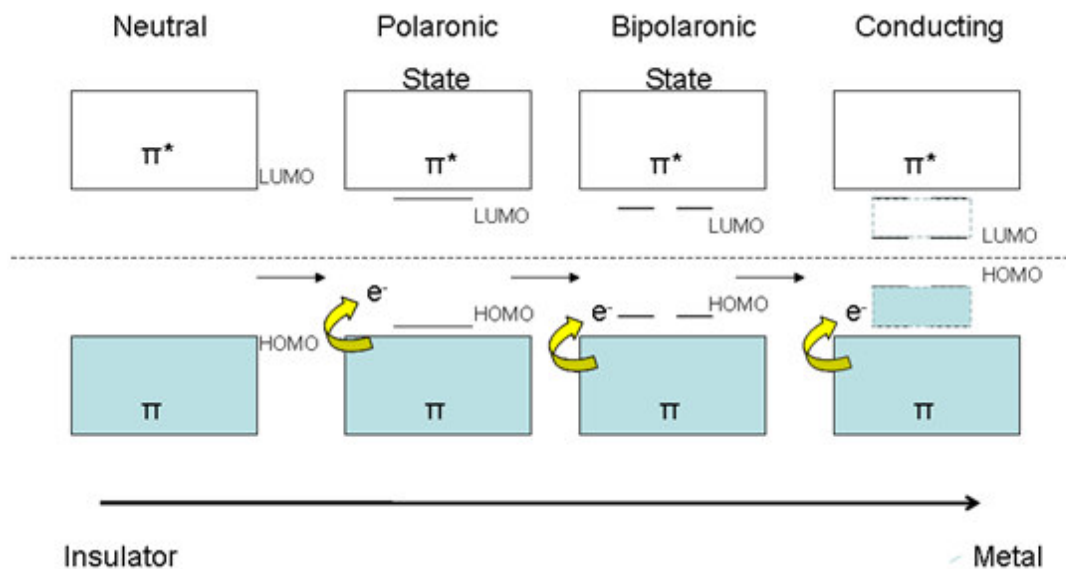
Figure 1.3.6 Band Theory evolution of polyaniline from insulating to metallic regime. With continued doping, localized states formed in the band gap (polarons and bipolarons) transcend the molecular orbitals from higher energies to lower energies The polarons and bipolarons eventually coalesce into the π and π^* bands.

The electronic transitions are observable by spectroscopic techniques such as ultraviolet visible (UV-Vis) spectroscopy. During this analysis, ultraviolet light absorbed by the material irradiates the molecules in the polymer structure inducing photochemical reactions which excite π electrons to different energy states. This technique can prove valuable for determining the extent of conjugation, the oxidation level [59], and dopant effects on the conformational structure of the polymer.

1.4. POLYANILINE FOR GAS SENSING APPLICATIONS

In the presence of gases, for polyaniline, both redox and protonating/ deprotonating conduction mechanisms play a role in the material's sensing mechanism. Interactions between the surface of polyaniline and the adsorbate may induce further doping/de-doping of the polymer resulting in an increase or decrease in electrical resistance.

1.4.1. *Current Research in Polyaniline Gas Sensors*

Current advancements in polyaniline based environmental gas sensors are outlined in Table 1.4.1. Researchers have employed various techniques to chemically and physically alter the molecular structure of polyaniline in an effort to enhance the selectivity and sensitivity of the polymer to analytes such as CO_2, CO, SO_2, NO_2, and NH_3. This section will provide a brief review of current research in polyaniline gas sensors and the complimentary techniques involved in producing such.

1.4.1.a. Dopants

Choice of dopant can manipulate the overall sensor response to target analytes. Novel alternative dopants employed include poly (4-styrenesulfonate-co-maleic acid) for templating and synthesizing for NH_3 detection [60], maleic acid for CO detection [61-62], and acetic acid [63] for NO_2 detection.

1.4.1.b. Polyaniline Composites

Researchers have observed that polyaniline hybrids with insulating polymers show enhanced structural and electronic stability in different gas atmospheres. The insulating base polymers employed enhances the overall reaction and adsorption kinetics of the hybrid by acting as adsorbents for the gas and filters for interferents. The choice of matrix polymer depends on stability of the polymer in varying gas atmospheres, vapor transport ability, and affinity of the polymer to the encapsulated material. Several popularly used matrix polymers employed are poly (vinyl acetate) [64], poly (vinyl alcohol) [65-66], poly (methyl methacrylate) [67], and polystyrene [67]. Solution and powder blending of polyaniline with these base polymers are common routes employed in enhancing the processibility of polyaniline for sensing applications. Charge transport in these polymers is dependent on the concentration of polyaniline and morphology of the matrix composite [38]. The transition of the composite from insulating to conducting follows with an increase in the concentration, doping, and oxidation level of the conducting filler, polyaniline. A decrease in percolation length between neighboring particles corresponds to the increase in polyaniline concentration. This effects hopping and/or tunneling mechanisms of the electron as it traverses from $\pi \rightarrow \pi^*$ and from one conducting grain to the other.

In other efforts to enhance sensitivity and selectivity of polyaniline, researchers have impregnated polyaniline with nanoparticles such as carbon nanotubes [61], SnO_2 [39], TiO_2 [39, 68], In_2O_3 [69], Fe-Al [70], Ni [71], Au [72], Nafion [72], and zeolite [62] to form specific binding sites for chemical interactions. The inorganic nanoparticles

implanted in the polymer matrix catalyze the reactions between the polymer and the gas resulting in an improvement in response time as well as an increase in the overall electrical conductivity of the film.

1.4.1.c. Deposition Techniques

One major factor influencing sensitivity is the dispersion quality of polyaniline in the sensor matrix. The more dispersed the polyaniline powders, the better the diffusivity of the gas agent into the polymer matrix yielding enhanced film sensitivity. A primary factor that may influence the dispersion quality is the deposition technique employed. Typical polyaniline deposition techniques include electrochemical deposition, spin coating, dip coating, and drop- coating [72]. Some of the newer and more novel methods include self assembly [39-40, 69], templating, Langmuir Blodgett [63], and thermal [73] and vacuum evaporation [70]. Some of the more novel techniques involve in-situ polymerization (chemical or electrochemical) of polyaniline on the transducer (yielding high surface area nanofibers) [40, 74, 77] or with nanoparticles seeded into the polymer matrix [39, 61, 69-72]. Table 1.4.1 outlines the effects of polyaniline processing on the sensitivity to analytes such as NO_2.

Researchers have shown that through manipulation of polyaniline's microstructure, via novel processing and synthesis techniques as described above, polyaniline becomes a suitable candidate for gas sensing applications. Many of the mentioned systems employ the emeraldine base or salt form of polyaniline for gas

detection. To date, sensors based on polyaniline for NO_2 detection have shown to be non-selective and in many cases unstable (unrecoverable). The focus of this research is to employ leucoemeraldine base polyaniline for selective NO_2 detection due to its oxidation sensitive structure (the benzenoid amine structure are vulnerable to oxidizing species like NO_2), based on this it should prove to have higher sensitivity and selectivity over current sensor designs. Leucoemeraldine was first introduced by [75] for NO_2 detection. In this work the claim was that leucoemeraldine base polyaniline produced during vacuum evaporation of emeraldine base polyaniline and deposited onto Au plated Cu electrodes could be employed for chemoresistive gas sensing. The reported minimum concentration of NO_2 that these films could detect was 4 ppm [76]. However, after the thin films were prepared they were exposed to air and it was not determined whether or not after air exposure if the LEB-PANI reduced state was achieved or maintained (it is plausible that the films may have been re-oxidized by volatiles and water vapor during laboratory air exposure transitioning the polymer to a higher oxidation state).

It will be attempted in this study to employ the electrospinning technique for producing dispersed polyaniline matrices. The application of electrospinning to produce LEB-PANI chemo-resistive sensors has not been studied. It is expected that the morphology of the matrix should allow for enhanced diffusion of the gaseous analyte due to the increased number of accessible reactant sites according to [79].

Table 1.4.1 Employed Polyaniline Sensor Deposition Techniques

Deposition/Processing Technique	Dopant/ Composite	Gases	Detection Limit	Response Time
Spin Coating[60]	Poly (4-styrenesulfonate-co-maleic acid)	NH_3	5 ppm	60 sec
Langmuir Blodgett[63]	EB/Acetic Acid	NO_2	20 ppm	10 sec
Cyclic Voltammetry[72]	$HClO_4$, H_2SO_4, HCl/PANI /Au/Nafion	NO_2	20 ppm	18 min
Constant Current[72]	$HClO_4$, H_2SO_4, HCl/PANI /Au/Nafion	NO_2	20 ppm	19 min
Constant Potential[72]	$HClO_4$, H_2SO_4, HCl/PANI /Au/Nafion	NO_2	20 ppm	14 min
Interfacial Polymerization[77]	HCl	NO_2	10ppm	104 sec
Solution Casting[61,78]	EB/ Poly vinyl alcohol composite; Maleic Acid/Carbon Nanotubes	CO_2/CO	100 ppm/ 167 ppm	5 min/ 0.6 min
Self Assembly[39-40]	HCl/SnO_2, TiO_2; amino-silane for templating	CO/NH_3	1ppm/0.5ppm	80 sec/60 sec
Drop Cast[69]	camphorsulfonic acid (CSA)/In_2O_3	CO, NO_2	60 ppm CO, and 0.51ppm NO_2	24 and 30 sec respectively
Vacuum Deposition[70]	Fe-Al	CO	10 ppm	5 sec
Pressed Pellets[62]	Maleic Acid/Zeolite	CO	7.8 ppm	169 min

1.5. STATEMENT OF WORK

Many polymer based sensor systems offer non-selective detection of the toxic gases mentioned above leaving room for ambiguity and false alarms. There is a strong requirement for selective films that show sensitivity to specific analytes. Specifically, detection of NO_2 is of continuous importance due to effects of the gas on the environment and public health. Several requirements for developing a NO_2 sensor include high sensitivity to low gas concentrations (the American Occupational Safety and Health Administration standard for NO_2 is $1-3$ ppm for long exposures (>8 hours) and 5 ppm for short exposures (<15min)), high selectivity to NO_2 in the presence of other interfering gases, fast response and recovery times, and stability of the response during extended and repetitive exposures.

This thesis explores nano-manufacturing leucoemeraldine base polyaniline (LEB-PANI) nanocomposites using the electrospinning technique as a new sensing material and water vapor as a catalyst for room temperature selective NO_2 detection. The proposed hybrids are anticipated to provide high sensitivity and selectivity to NO_2 and fast response and recovery times with gas exposure.

Traditionally when working with conducting polymers, scientists employ strong acidic agents such as HCl or H_2SO_4 in reductive/oxidative or protonic acid doping mechanisms to generate charge flow in the polymer matrix. However over time the acid may volatilize to the surface of the film blocking further reactions. Since the primary contributor of the protonic agent is the H^+ ion, water vapor might prove suitable as a primary dopant for LEB-PANI. The effects of this dopant on the sensor response to NO_2 can be assessed using optical, infrared, and x-ray spectroscopic techniques.

It is well conveyed throughout the sensing literature that the response mechanism of polyaniline is dictated primarily by redox and/or protonation/deprotonation mechanisms between the gas and sensing element. In order to detail the properties and effects of NO_2 and H_2O on the proposed films, the evolution of the polymer as it is exposed to varying mixed analyte environments needs to be assessed. A technique has been developed which employs ultraviolet-visible spectroscopy to do as such. In-situ experiments will be conducted before and during exposure to NO_2 and H_2O to determine the sensing mechanism(s) of LEB-PANI.

REFERENCES

1. U.S. Environmental Protection Agency, National Ambient Air Quality Standards, *http://www.epa.gov/air/criteria.html*, 1990

2. U.S. Environmental Protection Agency, Six Common Pollutants, *http://www.epa.gov/air/urbanair/6poll.html*, 2007

3. U.S. Environmental Protection Agency, Nitrogen dioxide http://www.epa.gov/airtrends/nitrogen.html, 2007

4. U.S. Department of Labor, Occupational Safety and Health Administration, Chemical Sampling information: Nitrogen Dioxide, http://www.osha.gov/dts/chemicalsampling/data/CH_257400.html, 2005

5. S.A. Kharitonov and P.J. Barnes, "Exhaled markers of pulmonary disease",*American Journal of Respiratory and Critical Care Medicine*, vol. 163 no. 7, pp. 1693-1722, 2001.

6. S.A. Kharitonov and P.J. Barnes, " Biomarkers of some pulmonary diseases in exhaled breath ", *Biomarkers*, vol. 7, no. 1, pp. 1-32 , 2002

7. P. Montuschi, S.A. Kharitonov, and P.J. Barnes, "Exhaled carbon monoxide and nitric oxide in COPD", *Chest*, vol. 120, no. 2, pp. 496-501, 2001

8. D. Gelmont , R.A. Stein, and J.F. Mead, "Isoprene-the main hydrocarbon in human breath", *Biochem Biophys Res Commun , vol.* 99, pp. 1456-60, 1981

9. M. Phillips, K. Gleeson, J. M. B. Hughes, J. Greenberg, R. N. Cataneo, L. Baker, and W. P. McVay, "Volatile organic compounds in breath as markers of lung cancer: a cross-sectional study", *Lancet*, vol. 353, pp. 1930–33, 1999

10. C.D.R. Dunn, M. Black ,D.C. Cowell, C. Penault , N.M. Ratcliffe, R. Spence, and C. Teare, "Ammonia vapour in the mouth as a diagnostic marker for Helicobacter pylori infection: preliminary proof of principle pharmacological investigations", *British J. of Biomedical Sci.,* vol. 58, no. 2, pp. 66-75, 2001.

11. Ratnawati, J. Morton, R. Henry, and P. Thomas, "Exhaled Breath Condensate Nitrite/Nitrate and pH in Relation to Pediatric Asthma Control and Exhaled Nitric Oxide", *Pediatric Pulmonology*, vol. 41, no. 10, pp. 929-36, 2006

12. J. Planes, A. Wolter, Y. Cheguettine, A. Pron, F. Genoud, and M. Nechtschein, "Transport properties of polyaniline-cellulose-acetate blends", *Physical Review B,* vol. 58, no. 12, pp. 7774-85, 1998

13. R. Frycek, F. Vyslouzil, V. Myslik, M. Vrnata, D. Kopecky, O. Ekrt, P. Fitl, M. Jelinek, T. Kocourek, and R. Sipula, "Deposition of organic metalocomplexes for sensor applications by MAPLE", *Sensors and Actuators B- Chemical*, vol. 125, no. 1, pp. 189-194, 2007

14. H.J. Zheng, Y.D. Jiang, G.Z. Xie, J.S. Yu, and C.P. Chen, "Preparation and characterization of PEDOT films for NO_2 gas sensors", *Rare Metal Materials and Engineering*, vol. 35, pp. 178-179, 2006

15. K. Wierzbowska, A. Pauly, B. Adamowicz, and L. Bideux, "Studies of gas sensing, electrical and chemical properties of n-InP epitaxial surfaces", *Physica Status Solidi A – Applications and Materials Science*, vol. 203, no. 9, pp. 2281-2286, 2006

16. S.T. Shishiyanu, T.S. Shishiyanu, and I.O. Lupan, "Novel NO_2 gas sensor based on cuprous oxide thin films", *Sensors and Actuators B- Chemical*, vol. 113, no 1, pp. 468-476, 2006

17. O. Kuzmych, B.L. Allen, and A. Star, " Carbon nanotube sensors for exhaled breath components", *Nanotechnology*, vol. 18, no 37, 375502, 2007

18. M. Rumyantseva, V. Kovalenko, A. Gaskov, E. Makshina, V. Yuschenko, I. Iwanova, A. Ponsoni, G. Faglia, and E. Comini, "Nanocomposites SnO_2/Fe_2O_3: Sensor and catalytic properties", *Sensors and Actuators B-Chemical,* vol. 118, no 1-2, pp. 208-214, 2006

19. C. Cantalini, M. Post, D. Buso, A. Guglielmi, and A. Martucci, "Gas sensing properties of nanocrystalline NiO and Co_3O_4 in porous silica sol-gel films", *Sensors and Actuators B-Chemical*, vol. 108, no 1-2, pp. 184-192, 2005

20. H.C. Yang and P.K. Dutta, "Promoting selectivity and sensitivity for a high temperature YSZ-based electrochemical total NO_x sensor by using a Pt-loaded Zeolite Y filter", *Sensors and Actuators B-Chemical,* vol. 125, no 1, pp 30-39, 2007

21. J.C. Solis, E. de la Rossa, and E. P. Cabrerra, "Fiber-optic chemical sensor for detection of NO$_2$ using poly (3-octylthiophene)", *Fiber and Integrated Optics*, vol. 26, no 6, pp 335-342, 2007

22. M. Consales, S. Campopiano, A. Cutolo, M. Penza, P. Aversa, G. Cassano, M. Giordano, and A. Cusano, "Carbon nanotubes thin films fiber optic and acoustic VOCs sensors: Performances analysis", *Sensors and Actuators B-Chemical,* vol. 118, no 1-2, pp. 232-242, 2006

23. Y. Takabayashi, M. Uemoto, K. Aoki, T. Odake, and T. Korenaga, "Development and optimization of a lab-on-a-chip device for the measurement of trace nitrogen dioxide gas in the atmosphere", *Analyst,* vol. 131, no 4, 573-578, 2006

24. J.F. Fernandez-Sanchez, T. Nezel, R. Steiger, and U.E. Spichiger-Keller, "Novel optical NO$_2$-selective sensor based on phthalocyaninato-iron(II) incorporated into a nanostructured matrix", *Sensors and Actuators B-Chemical*, vol. 113, no 2, pp 630-638, 2006

25. M. Penza, P. Aversa, G. Cassano, W. Wlodarski, and K. Zadeh-Kalantar, "Layered SAW gas sensor with single-walled carbon nanotube-based nanocomposite coating", *Sensors and Actuators B-Chemical*, vol. 127, no 1, pp 168-178, 2007

26. G.Z. Xie, J.S. Yu, H.L. tan, W.S. Suo, Y.D. Jiang, and B.C. Yang, "Study on ChemFET NO$_2$ gas sensor array" *Rare Metal Materials and Engineering*, vol. 35, pp 104-105, 2006

27. A.T.C. Johnson, C. Stali, M. Chen, S. Khamis, R. Johnson, M.L. Kleing, and A. Gelperin, "DNA-decorated carbon nanotubes for chemical sensing", *Physica Status Solidi B-Basic Solid State Physics,* vol. 243, no 12, pp 3252-3256, 2006

28. A.Z. Sadek, W. Wlodarski, K. Shin, R.B. Kaner, and K. Zadeh-Kalantar, "A layered surface acoustic wave gas sensor based on a polyaniline/$_{In2O3}$ nanofibre composite", *Nanotechnology*, vol. 17, no 17, pp. 4488-4492, 2006

29. Z.M. Qi, I. Homma, and H.S. Zhou, "Chemical gas sensor application of open-pore mesoporous thin films based on integrated optical polarimetric interferometry", *Analytical Chemistry,* vol. 78, no 4, pp 1034-1041, 2006

30. O. Casals, B. Barcones, A. Rodrigues-Romano, C. Serre, A. Rodriguez-Perez, J.R. Morante, P. Godignon, J. Montserrat, and J. Millan, "Characterisation and stabilisation of Pt/TaSi$_x$/SiO$_2$/SiC gas", *Sensors and Actuators B-Chemical,* vol. 109, no 1, pp 119-127, 2005

31. H. She, T. Hyodo, and H.L. Tuller, "Bulk acoustic wave resonator as a sensing platform for NO$_x$ at high temperatures", *Sensors and Actuators B-Chemical,* vol. 108, no 1-2, pp 547-552, 2005

32. S. Tamura and N. Imanaka, "Nitrogen oxide gas sensor based on multivalent ion-conducting solids", *Sensors and Materials,* vol. 19, no 6, pp 347-363, 2007

33. I.G. Casella and M. Contursi, "Electrochemical and spectroscopic characterization of a tungsten electrode as a sensitive amperometric sensor of small inorganic ions", *Electrochimica Acta,,* vol. 50, no 20, pp 4146-4154, 2005

34. Z.Y. Fan, and J.G. Lu, "Gate-refreshable nanowire chemical sensors", *Applied Physics Letters*, vol. 86, no 12, 123510, 2005

35. K. Miura, M. Ono, K. Shimanoe, and N. Yamazoe, "A compact solid-state amperometric sensor for detection of NO2 in ppb range", *Sensors and Actuators B-Chemical,* vol. 49, no 1-2, pp 101-109, 1998

36. M. Ono, K. Shimanoe, N. Miura, and N. Yamazoe, Amperometric sensor based on NASICON and NO oxidation catalysts for detection of total NO_x in atmospheric environment", *Solid State Ionics*, vol. 136, SI, pp 583-588, 2000

37. W. Brown and C.S. Foote, *Organic Chemistry 3rd Ed.*, Thomas Learning Inc., p. 38, 2002

38. V. Sreejith, "Structure and Properties of Conductive Polyaniline Blends", Doctoral Thesis, University of Pune, 2004

39. M. Kumar Ram, O. Yavuz, V. Lahsangah, and M. Aldissi, "CO gas sensing from ultrathin nano-composite conducting polymer film", *Sensors and Actuators B*, vol. 106, pp. 750-757, 2005

40. D.S. Sutar, N. Padma, D.K. Aswal,S.K. Deshpande, S.K. Gupta, and J.V. Yakhmi, "Preparation of nanofibrous polyaniline films and their application as ammonia gas sensor", *Sensors and Actuators B,* vol. 128, 286-292, 2007

41. C.N Van and K Potje-Kamloth, "Electrical and NO_x gas sensing properties of metallophthalocyanine-doped polypyrrole/silicon heterojunctions". *Thin Solid Films*, vol. 392, pp. 113-121, 2001

42. H. Letheby," On the production of a blue substance by the electrolysis of sulphate of aniline", *J. Chemical Society*. Vol. 15, p. 161,1862

43. R. Willstatter and C. W. Moore, "Black Aniline", *Berichte Der Deutschen Chemischen Gesellschaft*, vol 40, no 2, pp. 2665-2689, 1907

44. R. Willstatter and S.Dorogi, "Aninline black III", *Berichte Der Deutschen Chemischen Gesellschaft*, , vol 42, no 3, pp. 24118-4135, 1909

45. A.G. Green and A.E. Woodhead, "Aniline black and allied compounds Part I", *J Chemical Society*, vol 97, pp. 2388-2403, 1910

46. A.G. Green and A.E. Woodhead, "Aniline black and alied compounds Part II" *J Chemical Society*, vol 101, pp 1117-1123. 1912

47. R. de Surville, M. Jozefowicz, L.T. Yu, J. Perchon, and R. Buvet, "Electrochemical chains using protolytic organic semiconductors", *Electrochima Acta*, vol. 13, no 6, pp1451-1458, 1968

48. A.G. MacDiarmid, "Synthetic metals: a novel role for organic polymers", *Synthetic Metals,* vol. 125, no 1, pp.11-21, 2001

49. E.S. Matveeva," Residual water as a factor influencing the electrical properties of polyaniline. The role of hydrogen bonding of the polymer with solvent molecules

in the formation of a conductive polymeric network", *Synthetic Metals*, vol. 79, pp. 127 -139, 1996

50. N. Mott and E. David, *Electronic Processes in Non-crystalline materials 2nd Ed.*, Clarendon, Oxford, 1979

51. B. I. Shklovskii and A. L. Efros, *Electronic Properties of Doped Semiconductors*, Springer-Verlag, Berlin 1984

52. J.P Pouget, M. Laridjani, M.E. Jozefowicz, A.J. Epstein, E.M. Scherr, and A.G. MacDiarmid, "Structural aspects of the polyaniline family of electronic polymers", *Synthetic Metals*, vol. 51, no. 1-3, pp. 95-101, 1992

53. M.E. Jozefowicz, A.J. Epstein, J.P. Pouget, J.G. Masters, A. Ray, Y. Sun, X. Tang, and A.G. MacDiarmid, "X-ray structure of polyanilines", S*ynthetic Metals*, vol. 41, no. 1-2, pp. 723-726, 1991

54. W. Fosong, T. Jinsong, W. Lixiang, Z. Hongfang, and M. Zhishen, "Study on the crystallinity of polyaniline", *Molecular Crystals and Liquid Crystals*, vol. 160, no. 1, pp. 175-184, 1988

55. S. Stafstrom, J.L. Bredas, A.J. Epstein, H.S. Woo, D.B. Tanner, W.S. Huang, and A.G. MacDiarmid, "Polaron lattice in highly conducting polyaniline: Theoretical and optical studies", *Physics Review Letters,* vol. 59, no. 13, pp. 1464-1467, 1987

56. A.G. MacDiarmid and A.J. Epstein, "Polyanilines: A novel class of conducting polymers", *Faraday Discussions of the Chemical Society,* vol. 88, pp. 317-332, 1989

57. A.G. MacDiarmid, J.C. Chiang, A. F. Richter, and A.J. Epstein, "Polyaniline: A new concept in conducting polymers", *Synthetic Metals*, vol. 18, no. 1-3, pp. 285-290, 1987

58. E.Z. Kurmaev, M.I. Katsnelson, A. Moewes, M. Magnuson, J.-H. Guo, S.M. Butorin, J. Nordgren, D.L. Ederer, and M. Iwami," Spectroscopic observation of polaron-lattice band structure in the conducting polymer polyaniline" *J. Physics: Condensed Matter,* vol. 13, pp. 3907-12, 2001

59. J.E. Albuquerque, l.H.C. Mattoso, D.T. Balogh, R.M. Faria, J.G. Masters, and A.G. MacDiarmid, "A simple method to estimate the oxidation state of polyanilines", *Synthetic Metals*, vol. 113, pp 19-22. 2000

60. G.K. Prasad, T.P. Radhakrishnan, D. Sravan Kumar, and M. Ghanashyam Krishna, "Ammonia sensing characteristics of thin film based on polyelectrolyte templated polyaniline", *Sensors and Actuators B*, vol. 106, pp. 626-631, 2005

61. Y. Wanna, N. Srisukhumbowornchai, A. Tuantranont, A. Wisitsoraat, N. Thavarungkul, and P. Singjai, "The effect of carbon nanotube dusperion on CO gas sensing characteristics of polyaniline gas sensor", *Journal of Nanosicence and Nanotechnology*, vol. 6, pp. 3893-3896, 2006

62. N. Densakulprasert, L. Wannatong, D. Chotpattananont, P. Hiamtup, A. Sirivat, and J. Schwank, "Electrical conductivity of polyaniline/zeolite composites and synergetic interaction with CO", *Materials Science and Engineering B* , 117, 276-282 (2005)

63. D. Xie, Y. Jiang, W. Pan, D. Li, Z. Wu, and Y. Li, "Fabrication and characterization of polyaniline-based gas sensor by ultra-thin film technology", *Sensors and Actuators B*, vol. 81, pp. 158-164, 2002

64. S.A. Kanhegaokar, "Charge transport and conductivity measurement in polyaniline-polyvinyl acetate blends", *E-Polymers*, vol. 63, 2007

65. M. Irimia-Vladu and J.W. Fergus, "Suitability of emeraldine base polyaniline-PVA composite film for carbon dioxide sensing", *Synthetic Metals*, vol. 156, no 21-24, pp. 1401-1407, 2006

66. K. Ogura and H. Shiigi, "Conducting-insulating polymer composites: Selectively sensing materials for humidity and CO_2", *Conducting Polymers and Polymer Electrolytes: from Biology to Photovoltaics - ACS Symposium Series*, vol. 832, pp. 88-102, 2003

67. M Matsuguchi, A Okamoto, and Y Sakai, "Effect of humidity on NH_3 gas sensitivity of polyaniline blend films", *Sensors and Actuators B-Chemical*, vol. 94, no. 1, pp. 46-52, 2003

68. H. Tai, Y. Jiang , G. Xie, J. Yu, and X. Chen, "Fabrication and gas sensitivity of polyaniline–titanium dioxide nanocomposite thin film", *Sensors and Actuators B,* vol. 125, pp. 644-650, 2007

69. A.Z. Sadek, W. Wlodarski, K. Shin, W.B. Kaner, and K. Kalantar-Zadeh, "A layered surface acoustic wave gas sensor based on polyaniline/ In_2O_3 nanofiber composite", *Nanotechnology*, vol. 17, pp. 4488 -4492, 2006

70. V. Dixit, S.C.K. Misra, and B.S. Sharma, "Carbon monoxide sensitivity of vacuum deposited polyaniline semiconducting thin films", *Sensors and Actuators B*, vol. 104, pp. 90-93, 2005

71. S.A Krutovertsev, S.I. Sorokin, A.V. Zorin, Y.A. Letuchy, and O.Y. Antonova, "Polymer film-based sensors for ammonia detection", *Sensors and Actuators B-Chemical*, vol. 7, no. 1-3, pp. 492-494, 1992

72. J. Do and W-B Chang, "Amperometric nitrogen dioxide gas sensor based on PAn/Au/Nafion® prepared by constant current and cyclic voltammetry methods", *Sensors and Actuators B*, vol. 101, pp. 97-106, 2004

73. D. Li, Y Jiang, Z. WU, X. Chen, and Y. Li, "Self-assembly of polyaniline ultrathin films based on doping-induced deposition effect and applications for chemical sensors", *Sensors and Actuators B*, vol. 66, no. 1-3, pp. 125-127, 2000

74. M.P Regaco, E.A.T Dirani, F.J Fonseca, and A.M. de Andrade, "Organic material as gas sensor for farm application", *12th International Symposium on Electrets*,. ISE-12, no 11-14, pp 441-444, 2005

75. A. Monkman, M.C. Petty, N. Agbor, and M. Scully, "Polyaniline gas sensors", U.S. Patent no. 5,536,473, 1996

76. N.E. Agbor, M.C. Petty, and A.P. Monkman, "Polyaniline thin films for gas sensing", *Sensors and Actuators B*, vol. 28,pp 173-179,1995

77. X.B. Yan, Z.J. Han, Y. Yang, and B.K. Tay, "NO_2 gas sensing with polyaniline nanofibers synthesized by a facile aqueous/organic interfacial polymerization", *Sensors and Actuators B*, vol. 123,pp 107-113, 2007

78. H. Shiigi, T. Oho, T. Tonosaki, and K. Ogura, "CO_2 Sensitive Characteristics of Base-type Polyaniline/poly(vinyl alcohol) Composites at Room Temperature and Effects of Coexisting Gases", *Electrochemistry*, vol. 69, no 12,pp 997-1001, 2001

79. G. Li, "Effect of Morphology on response of polyaniline based conductimetric gas sensors: Nanofibers vs. Thin films", *Electrochemical and Solid State Letter,* vol. 7, no 10, pp H44-H47, 2004

CHAPTER 2

2. Materials Synthesis and Characterization

2.1. ELECTROSPINNING

Electrospinning, patented by Formahls [1] in 1934, operates on the notion that the surface tension of a polymer based liquid precursor may be altered via the application of a high voltage yielding the formation of polymer based fibrous structures. The potential applied to the pre-spinning solution induces an accumulation of charges on the surface of droplets formed at the end of the electrospinning needle causing the surface of the liquid to break [2]. Jets of charged fibers are formed that collectively materialize into a charged active matrix [3]. Stability and directionality of the jet is dependent on the electrostatic fields formed between the collector and the needle.

The electrospinning setup is operated in air under a fume hood and consists of a DC high voltage power supply (Gamma High Voltage Research, Model ES 30P-6W), a programmable syringe pump (KD Scientific, model 200), and an aluminum collector plate. Substrates are affixed to the collector plate with conducting tape. A glass syringe is filled with the precursor solution, figure 2.1.1, and the metallic needle at the end of the syringe is connected to a cathodic clamp from the power supply while the anodic clamp is connected to the collector. During jet flight the solvent used in the precursor solution evaporates (due to low vapor pressure) and a dry non-woven mat of fibers can be collected. Several processing conditions can be varied to change the dimensions of these fibers. Table 2.1 outlines the processing parameters that affect the fiber morphology.

An advantage of this technique is that within this polymer based matrix, dissimilar materials (i.e. polymers, biologicals, etc.,) may be encapsulated. Polyaniline is insoluble in most solvents and thus cannot be electrospun by itself. Electrospun polyaniline composites have been explored in the past several years [4-6]. The advantage of the non-woven matrix is its high surface - to - area ratio and high porosity allowing an increase in gas surface interactions. The diameter of the fibers also plays a role in electrical conductivity of the mat. Zhou et. al showed that if the diameter of the fibers falls below 15 nm, the electrical conductivity of the matrix transitions from conducting to insulating.

The choice of matrix polymer depends on stability of the polymer in varying gas atmospheres, its vapor transport ability, and the affinity of the polymer to the encapsulated material. Electrospun composites have excellent transport properties, as outlined by Gibson et. al. The fibrous mat can be used to increase gas - surface interactions between polyaniline particles encapsulated within the electrospun matrix and the analyte.

Table 2.1: Electrospinning Processing Conditions

Precursor Parameters	Polymer concentration
	Precursor viscosity
	Ionic strength
	Temperature
	Solvent
Electrospinning Process Parameters	Needle to collector distance
	Voltage
	Flow rate

Several popularly used matrix polymers employed in electrospinning polyaniline are poly ethylene oxide (PEO), polyvinyl acetate (PVA), and poly-methyl-methacrylate (PMMA). Poly-vinyl pyrrolidone (PVP) is also a well known steric stabilizer for polyaniline. And cellulose acetate (CA) has also been shown to enhance the electrical properties of polyaniline. Neither however has been explored for processing polyaniline using the electrospinning technique.
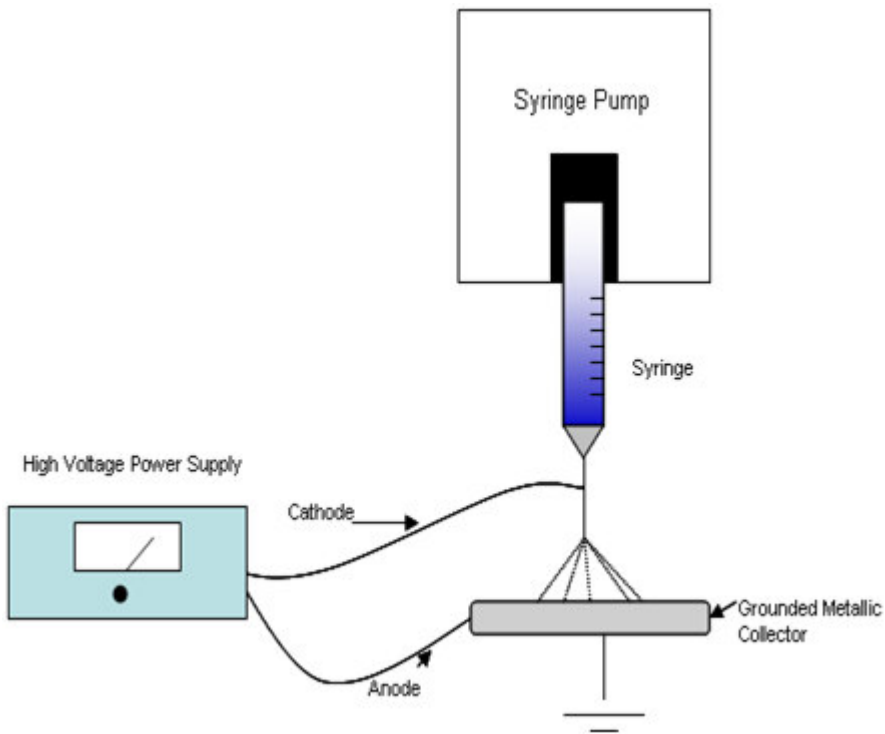
Figure 2.1.1 The Electrospinning Setup

2.2. MATERIALS

2.2.1. *Leucoemeraldine Base Polyaniline*

LEB-PANI powders were purchased through Sigma Aldrich from two vendors: Fluka (Selectophore®) and Sigma Aldrich. The certificate of analysis (CoA) for each powder can be found in Appendix A. The only difference between the two powders is that the chemical composition is slightly varied from one powder to the other. Table 2.2 shows the chemical composition of each system. The Sigma Aldrich powders have higher nitrogen content than the Fluka powders. It is qualitatively assumed this reflects the imine content. The color of the commercially available LEB-PANI powders imparts that there is some low level imine formation associated with partially crystalline regions within the polymer matrix, as evidenced by [15-16].

Table 2.2.Chemical composition of LEB-PANI from CoA

Content %	Fluka	Sigma Aldrich
Carbon	63.9	78.64
Hydrogen	6.13	5.57
Nitrogen	6.98	14.77

2.2.2. *LEB-PANI Composites*

2.2.2.a. PVP LEB-PANI Hybrids

Leucoemeraldine Base Polyaniline was mixed with 5.0 x10^{-5}M poly vinyl-pyrrolidone (PVP- Sigma-Aldrich) with a molecular weight of 1,300,000 in ethanol solution. While the molar concentration of PVP remained constant, the LEB-PANI

concentration varied between 20%w/w - 80%w/w. Samples were prepared and deposited onto 1cm x 1cm alumina substrates with gold interdigitated electrodes, figure 2.2.1, using the electrospinning technique under an applied voltage of 10-15 kV with 22 gauge needles and a flow rate of 20μl/min. The collector to needle distance was 55mm.
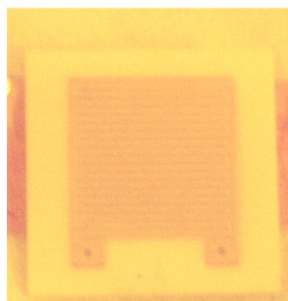
Figure 2.2.1 1 cm x 1 cm Al_2O_3 with Au electrodes transducer

2.2.2.b. CA LEB-PANI hybrids

LEB-PANI was mixed with cellulose acetate (CA- Fluka, Mr 29,000) in acetone. The composition consisted of 80%wt/wt CA and 20% wt/wt LEB-PANI. Samples were prepared and deposited onto 1 cm x 1cm alumina substrates with gold interdigitated electrodes, using the electrospinning technique under an applied voltage of 7-10 kV with a 20 gauge needle and a flow rate of 100-200μl/min. The collector to needle distance was 75-80 mm.

2.3. SENSING SETUP

Sensing tests were carried out for the PVP LEB-PANI and CA LEB-PANI electrospun mats under varying gas atmospheres in the sensor testing facility at the University of Brescia, Italy, where under a small applied voltage (1-2V) changes in

sample current were measured in wet synthetic air and at a constant temperature of 20°C. A flow-through technique was used for sensing experiments in which the synthetic air was the carrier gas for several gases outlined in Table 2.3. The sensing setup is illustrated in Appendix B.

Table 2.3: Target Analytes for Chemical Sensing Experimentation

Agent	Concentration (ppm)
NO_2	0.5 to 7
CO	2 to 500
Ethanol	500
Methanol	50 to 100
Benzene	10 to 25
NH_3	1-20
Isoprene	200
Humidity	0 to 60%

2.4. MORPHOLOGICAL CHARACTERIZATION

2.4.1. *SEM*

Scanning Electron Microscopy (SEM) characterization for these studies was conducted using a LEO-1550 FEG (Field Emission Gun) SEM. A high tension of 15kV

was used with the back scattering detector and a working distance between 7mm and 10mm. The samples were sputter coated with gold prior to analysis.

2.4.2. *TGA*

Thermo-gravimetric analysis was used to quantify the amount of volatiles absorbed by the air processed LEB-PANI. LEB-PANI powders were analyzed at U.S. Army Research Development and Engineering Command (RDECOM) Benet Laboratories using a Perkin-Elmer TGA 7 under argon atmosphere. The samples were weighed and heated at a rate of 5°C/min from 50° to 250°C.

2.5. SURFACE ANALYSES

2.5.1. *In-Situ Ultraviolet-Visible Spectroscopy*

Ultraviolet visible spectroscopy (UV-Vis) was used to identify the electronic transitions ($\pi \rightarrow \pi^*$, $n \rightarrow \pi^*$, $\pi \rightarrow$ polaron, polaron $\rightarrow \pi^*$, $\pi_Q \rightarrow$ bipolaron, bipolaron $\rightarrow$ polaron, etc.,), the oxidation level, and possible defect formations (polarons vs. bipolarons), determine the band gap of the conjugated system and the conformational structure (expanded versus compact coil configuration) of the polyaniline. Because the polyaniline varies in color in the visible spectrum by means of the transformations between the base and oxidized and protonated forms it can be characterized using photochemical spectroscopy. A gas sensing setup was specially designed for in-situ UV-

Vis spectroscopy of the composite films under varying NO_2 and humidity atmospheres using an Ocean Optics HR4000 UV-Vis Spectrometer with a composite grating and 50 micron slit width, a DH-2000 deuterium-tungsten halogen source (wavelength range: 215-2000nm), a R600-7-SR/125 reflection probe, and a modified gas chamber made of quartz glass fabricated with a 0.25 inch through depth window. Figure 2.5.1 depicts the modified gas sensor setup. N_2 was bubbled through a Kontes 24/40 100ml glass bubbler and humidity was controlled by varying the ratio of wet N_2 to dry N_2. An Extech 44550 pocket humidity temperature pen was used to calibrate the humidity setup for the humidity range 20-70%, the calibration data is in appendix C.
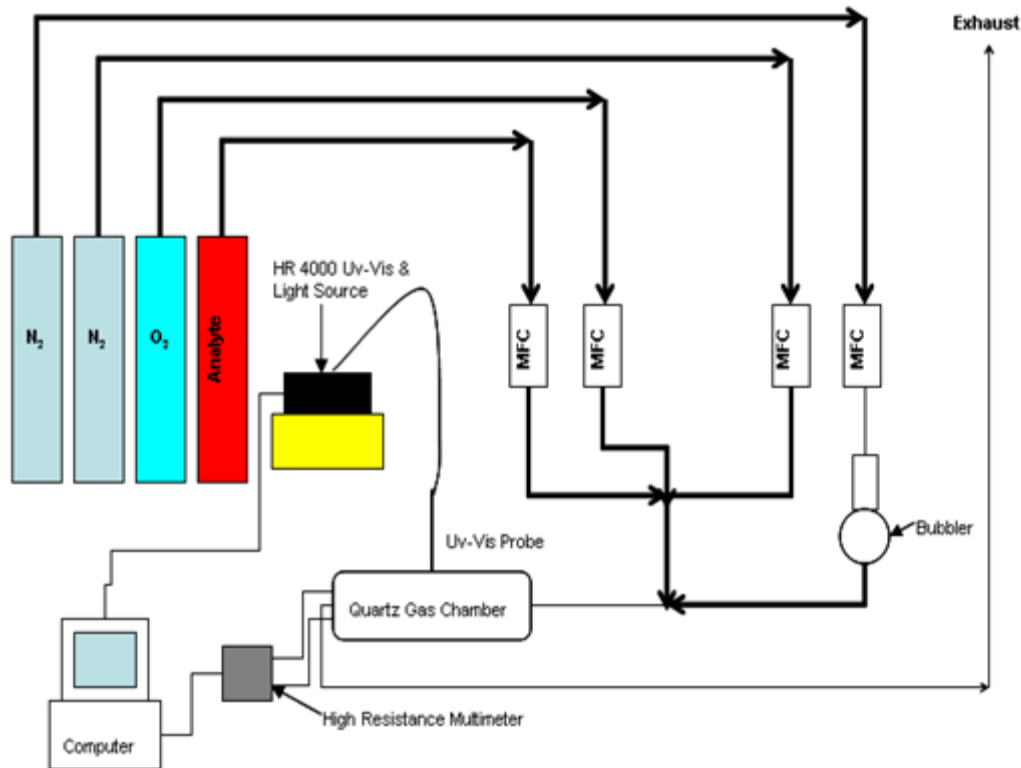
Figure 2.5.1 Modified gas sensing setup for In-situ UV-Vis absorption spectroscopy

LEB-PANI was analyzed in acetone and ethanol solutions in a 10cm glass and plastic cuvette respectively. For the in-situ gas analysis thin films of PVP LEB-PANI and CA LEB-PANI were prepared by drop coating onto silicon wafers. Thin films were used because the effect of the secondary component, gas, and water vapor on LEB-PANI was the main focus of this study and once CA and PVP are electrospun they are no longer transparent and the films are very porous lending the alteration of the incident beam and thus a decrease in intensity and possibly loss of information in the acquired spectrum.

The UV-Vis spectrums were recorded in reflectance using Spectrasuite ®. They were then analyzed using Omnic® V. 6.1, where they were converted to absorption spectra for band gap evaluation.

2.5.2. *Photo Acoustic FTIR*

Infrared spectroscopy can be employed to assess oxidation structure, molecular transformations (i.e. amine to imine), and the interactions between the dopant and the polymer matrix.

Photo Acoustic Fourier-Transform Infrared (PA-FT-IR) Spectroscopy of the 20% wt/wt LEB-PANI PVP and CA composites was performed in the lab of Dr. Namita Choudhury at the Ian Wark Research Institute, ARC Special Research Center, University of South Australia, Australia, using a Nicolet Magna-IR Spectrometer 750 equipped with an MTEC model 300 photo acoustic cell under helium atmosphere. Each run consisted of 120 scans at 8 cm^{-1} resolution, with a mirror velocity of 0.1581cm min^{-1} and purge gas

rate of 20ml min^{-1}. The samples were referenced against a background spectrum of carbon black.

The 50% wt/wt PVP LEB-PANI composite was however analyzed using a Bruker Vector 22 FTIR. The infrared spectra are recorded from 4000 to 500cm^{-1} with a resolution of 2cm^{-1}. This work was carried out in Dr. S. Pratsinis' Lab in ETH Zurich, Switzerland.

The polymers were prepared similarly to the samples for UV-Vis except the coatings were drop coated onto aluminum foil coated with teflon so that they could easily be removed.

2.5.3. *XPS*

X-Ray Photoelectron Spectroscopy was employed to measure the binding energy of core electrons (nitrogen, oxygen, and carbon) in polyaniline to identify the intrinsic structure, estimate the amount of amines and imines, and for differentiating between the neutral and protonated nitrogen centers. XPS was carried out under the supervision of Dr. Robert Bartynski of the ESCA facility operated by the Laboratory for Surface Modification at Rutgers University, USA, using a Kratos XSAM 800 spectrometer with an unmonochromatized Al Kα radiation, and a hemispherical electron energy analyzer equipped with a multichannel detection system.

The XPS data was analyzed using Spectral Data Processor (SDP ® V4.3) which decomposed the spectrums into individual peaks assuming a linear background fit which is optimum for materials with large band gaps such of polymers.

The composite samples were electrospun onto silicon wafers.   LEB-PANI powders were deposited onto carbon tape for analysis.

2.5.4. *Zeta Potential*

In order to assess the effects of the solvents used in processing the electrospun nanocomposites on LEB-PANI, a Brookhaven Zeta Potential with Phase Analysis Light Scattering (ZetaPALS) was employed to measure the zeta potential of LEB-PANI in acetone and ethanol solutions.

REFERENCES

1. Formahls, US Patent no. 1,975,504, "Process and Apparatus for Preparing Artificial Threads", 1934

2. S.A. Theron, E .Zuessman and A.L Yarin, "Experimental Investigation of the Governing Parameters in the Electrospinning of Polymer Solutions", *Polymer*, vol. 45, no. 6, pp. 2017 -2030, 2004

3. H. Schreuder-Gibson, P. Gibson, P. Tsai, P. Gupta, and G. Wilkes, "Cooperative Charging Effects of Fibers from Electrospinning of Electrically Dissimilar Polymers", *Inter. Nonwovens Journal*, pp.39-45, 2004,

4. I.D. Norris, M.M. Shaker, F.K. Ko, and A.G. MacDiarmid, "Electrostatic

5. Fabrication of Ultrafine Conducting Fibers: Polyaniline/Polyethylene Oxide Blends", *Synthetic Metals*, vol. 114, no. 2, pp. 109 -114, 2000

6. Y. Zhou, M. Freitag, J. Hone, and C. Stali, "Fabrication and Electrical Characterization of Polyaniline-Based Nanofibers with Diameter Below 30 nm", *Applied Physics Letters*, vol. 83, no. 18, pp. 3800 - 3802, 2003

7. K. Desai and C. Sung, "DOE Optimization and Phase Morphology of Electrospun Nanofibers of PANI/PMMA Blends", *NSTI Nanotech 4* , vol. 3, pp. 429-432, 2004

8. P. Gibson, H. Schreuder-Gibson, and D. Rivin, "Transport Properties of Porous Membranes Based on Electrospun Nanofibers", *Colloids and Surfaces A: Physiochemical and Engineering Aspects*, vol. 187-188, pp. 469 – 481, 2001

CHAPTER 3

3. Leucoemeraldine Base Polyaniline – Effects of Solvent on the Conformational Structure

Electrospinning of LEB-PANI employs a base polymer dissolved in an organic solvent. For this work, the two powders (LEB-PANI and the base polymer) are placed in a 7 ml glass bottle and then the solvent is added. The solution is then ultrasonicated for 1 hour to optimize mixing. Effects of solvents on LEB-PANI will be discussed further in this chapter. The solvents used are polar solvents. Hydrogen bonding between the solvent and LEB-PANI facilitates conformational changes (same structural formula, $C_6H_8N_2$, different molecular arrangements, i.e. torsion and relaxation of the molecular structure of the polymer chain) along the polymer chain [1] enhancing overall conductivity through chain ordering and secondary doping mechanisms.

Because these are commercial LEB-PANI powders, it is important to assess the chemical and molecular nature of this material in order to detail the effects of processing and the sensoric character of this polymer.

3.1. STRUCTURAL EVALUATION OF LEB-PANI

3.1.1. *SEM &TGA of As Received LEB-PANI Powders*

SEM was performed on dry LEB-PANI powders affixed to carbon tape to assess the initial morphology of LEB-PANI prior to electrospinning. Figure 3.1.1 reveals that the LEB-PANI particles have agglomerated into large configurations ranging from 10 – 50 μm in dimension. One source may be the long range Van der Waals forces created between like charged particles yielding assimilation into larger aggregates, the other is related to Angelopoulos' observation that interchain interactions between reduced and oxidized sites along the polymer chain induces aggregation in polyaniline (studies were carried out on the emeraldine base form) [2]. In his study he concluded that hydrogen bonds formed along the backbone of polyaniline, at nitrogen sites, supported the interchain reactions and promoted assimilation of particles into larger agglomerates. Moreover as the oxidation level moved towards the reduced polymer state the aggregation yield also diminished. LEB-PANI is the reduced form of polyaniline, amorphous, and insulating. In theory, due to lack of imine centers it is not supposed to endure aggregation because H-bonding between the amine centers is not energetically favorable [2].
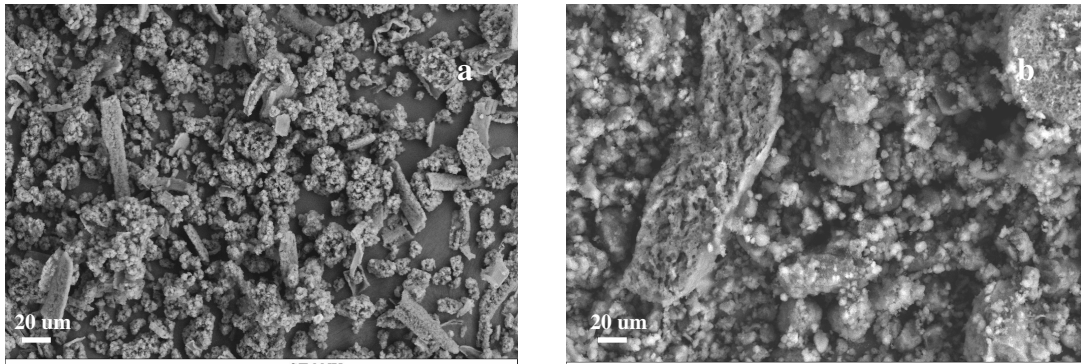
Figure 3.1.1 SEM of as received LEB-PANI particles from (a) Fluka and (b) Sigma Aldrich.

The above figures are representative of LEB-PANI particles from the two vendors mentioned in section 2.2, (a) Fluka and (b) Sigma Aldrich. As evidenced by SEM, they are morphologically comparable.

The most probable cause for aggregation in the as-received LEB-PANI powders is that on exposure to air, adsorption of water vapor and other volatile species may induce some low level transformation of amines to imines by the oxidation of amine centers, consequently yielding interchain reactions between imine and amine sites (through hydrogen bonding). TGA analysis of the as received LEB-PANI particles after exposure to air, figure 3.1.2, suggests the material adsorbs volatiles on exposure to lab air. About 5 wt% of the material mass removed during the thermal cycle consists of adsorbed water vapor and other volatile species; this is also consistent with the work of Matveeva [3].

The disadvantage of these self-assembled microstructures is that they may inhibit molecular conformation and retard charge transport between conducting sites along the structure of polyaniline resulting in decreased charge mobility and increased electronic

instability [2]. The agglomerated structures formed may also hinder interactions between the gas molecules and reaction sites along the polymer chain.
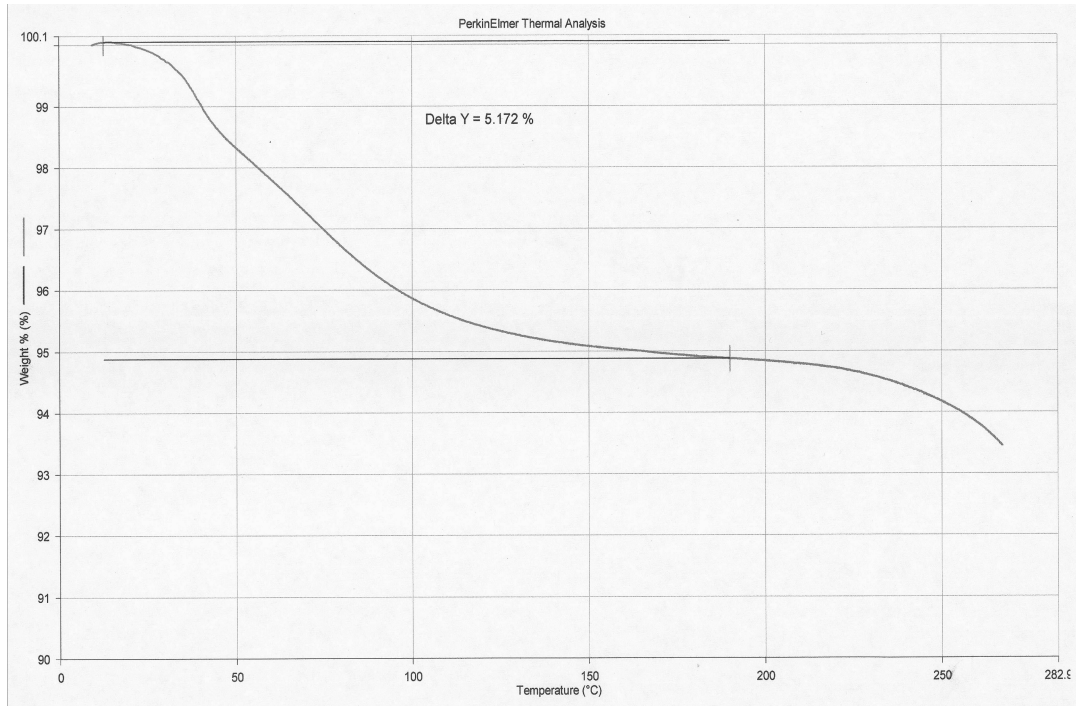
Figure 3.1.2 TGA analysis of as received LEB-PANI powders after exposure to laboratory air

3.2. CHEMICAL EVALUATION OF LEB-PANI

3.2.1. *Effects of Processing LEB-PANI*

The sensoric nature of leucoemeraldine base polyaniline may be directed by the processing conditions employed. Miejerink et. al, [4] showed that post processing conditions of a commercially available polyaniline powder can affect the electron

exchange between the processed polymer and select analytes yielding a possible increase in selectivity and sensitivity of the polyaniline film to target gases. If the films were post-processed using acetone, they would become insensitive to acetone. Similarly, the same reaction occurs for post processing treatments in ethanol and water. The theory is that the solvent molecules occupy sites along the polymer chain blocking reactions between similar groups of other molecular species. The advantage of these post processed films is the decrease in response to common interferents found in ambient air.

Processing using the aforementioned yields changes within the polymer chain analogous to oxidation and possibly light doping. Post treatment of polyaniline with acetone (CH_3COCH_3) and ethanol (C_2H_5OH) may induce oxidation at the amine centers transforming them into imines due to reactions between the amine and carbonyl groups of acetone [5] and between the amine and the hydroxide groups in ethanol. Post processing of polyaniline with such polar molecules may induce chain ordering and facilitate conformational changes along the polymer chain enhancing charge transport and electrical conductivity [6]. In this study acetone and ethanol were employed for processing the LEB-PANI composites. The effects of these solvents on the conformational structure of LEB-PANI will be discussed further in this chapter.

To detail the effect of these solvents on as received LEB-PANI, the constituents of the base structure must be first analyzed. XPS analysis of the as received LEB-PANI powders was carried out to detail the initial structure a priori processing in the selected solvents.

Figure 3.2.1 displays the N1s XPS spectra for the as received LEB-PANI powders. The peaks at 398.2 eV, 401.7 eV, and 399.9 eV correspond to the imine (=N-), protonated N (N$^+$), and amine (-NH-) peaks, respectively and are in agreement with the literature values [7-10].   If we compare the relative intensity of the =N-, -NH- and N$^+$ to the original N concentration (14.77 atomic %) then the percentage of each molecular structure in the original LEB-PANI system is calculated to be 10.17% for -NH-, 3.69% for N$^+$, and 0.9% for =N-.   XPS data, table 3.1, suggests that a significant amount of protonated nitrogen centers exist on the LEB-PANI backbone. These charged species can exist as polarons, bipolarons, or protonated amines.   The protonation of amine centers however, is typically carried out under strong acidic conditions, i.e. pH < 4 [11].

Figure 3.2.2 shows the C1s core energy spectra for the as received LEB-PANI powders. According to [7] the peak at 288.6 eV can be attributed to protonated imines (>C=N$^+$H) and the peak at 287.6 eV can be attributed to the protonated amine structures (>C-N$^+$H$_2$). If we compare the composition of the C1s peak to the concentration of carbon (78.6 atomic %) in the original structure the amount of protonated imines bonded to carbon is estimated to be ~4% and ~0.31% for protonated amines bonded to carbon. The C1s spectrum reveals that the material may be contaminated with adsorbed water vapor and/or some other oxygen containing species. This adsorption facilitates bond formation between the aromatic ring and O and OH groups of the adsorbate as well as oxidation of the benzenoid amine structure into the quinoid imine structure. According to [12] in the presence of laboratory or atmospheric air the stoichiometry of LEB-PANI should not change. On removal of the polymer from the contaminant and via slight thermal treatment (>100 °C to dehydrate the polymer and remove any contaminants) the

polymer will return to its original state.   Figure 3.2.3 depicts the O1s core energy

spectrum for adsorbed O on the polymer chain. There is only 1 peak at 531.8 eV which

is attributed to C-O, C=O and –OH groups.

Table 3.1 N1s, C1s, and O1s core energy spectra for as received LEB-PANI powders

Spectrum	Peak	B.E. (eV)	Compound	Rel. Area	% of N
N1s	A	399.9	-NH-, possibly a mix of polarons and neutral -NH-	68.9%	10.17653
	B	401.7	N+	25.0%	3.6925
	C	398.2	=N-	6.0%	0.8862
C1s	A	284.8	CH, C-C, C=C	58.0%	----
	B	285.9	C=N, C-N, possibly associated protonated species	36.5%	----
	C	288.6	C=O, C=N$^+$H	5.1%	4.0086
	D	287.6	C=N$^+$H, C-N$^+$H$_2$, C-O	0.4%	0.3144
O1s	A	531.8	C-O, CH-OH, C=O	100%	----
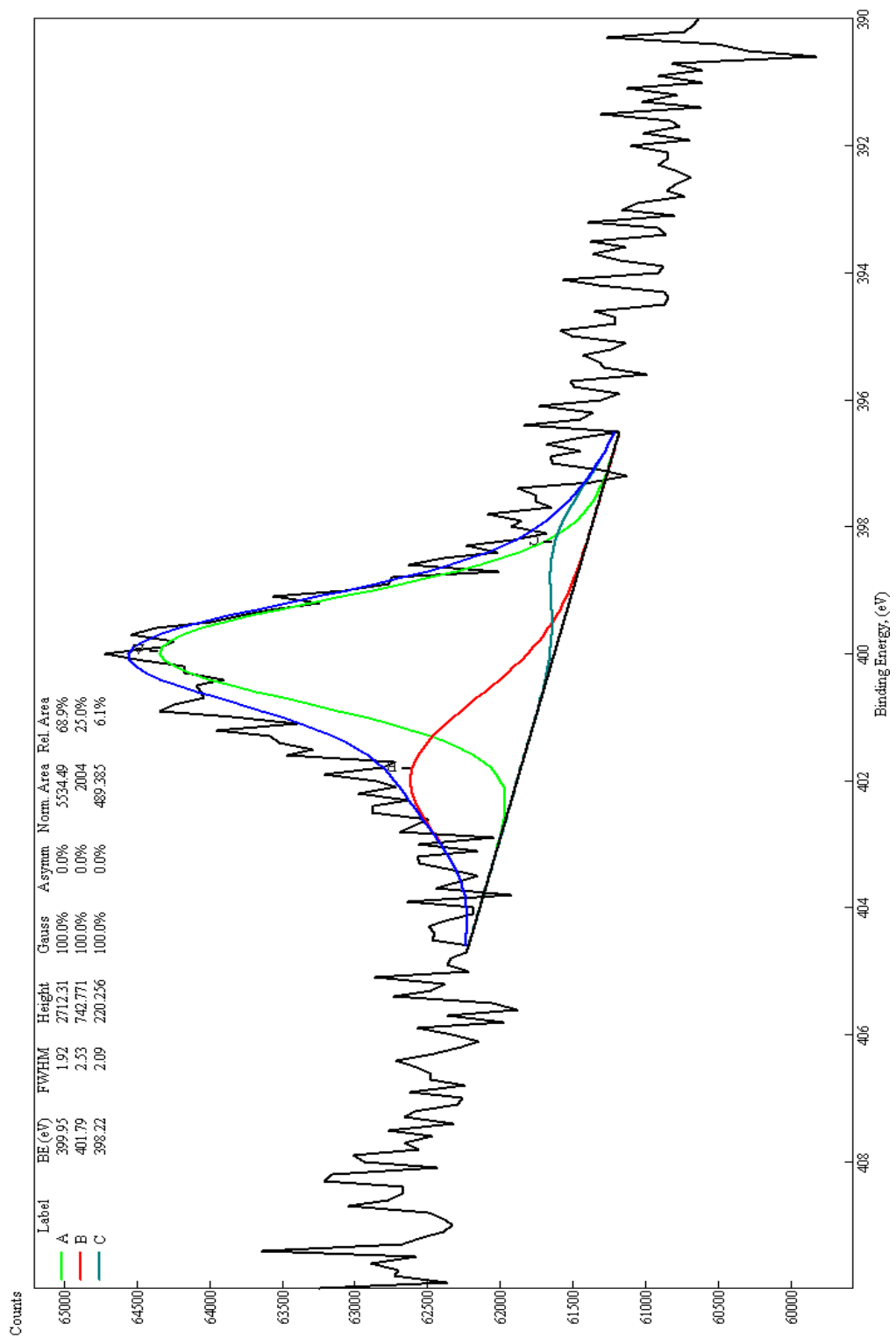
Figure 3.2.1 N1s core energy XPS Spectra of as received LEB-PANI Powders
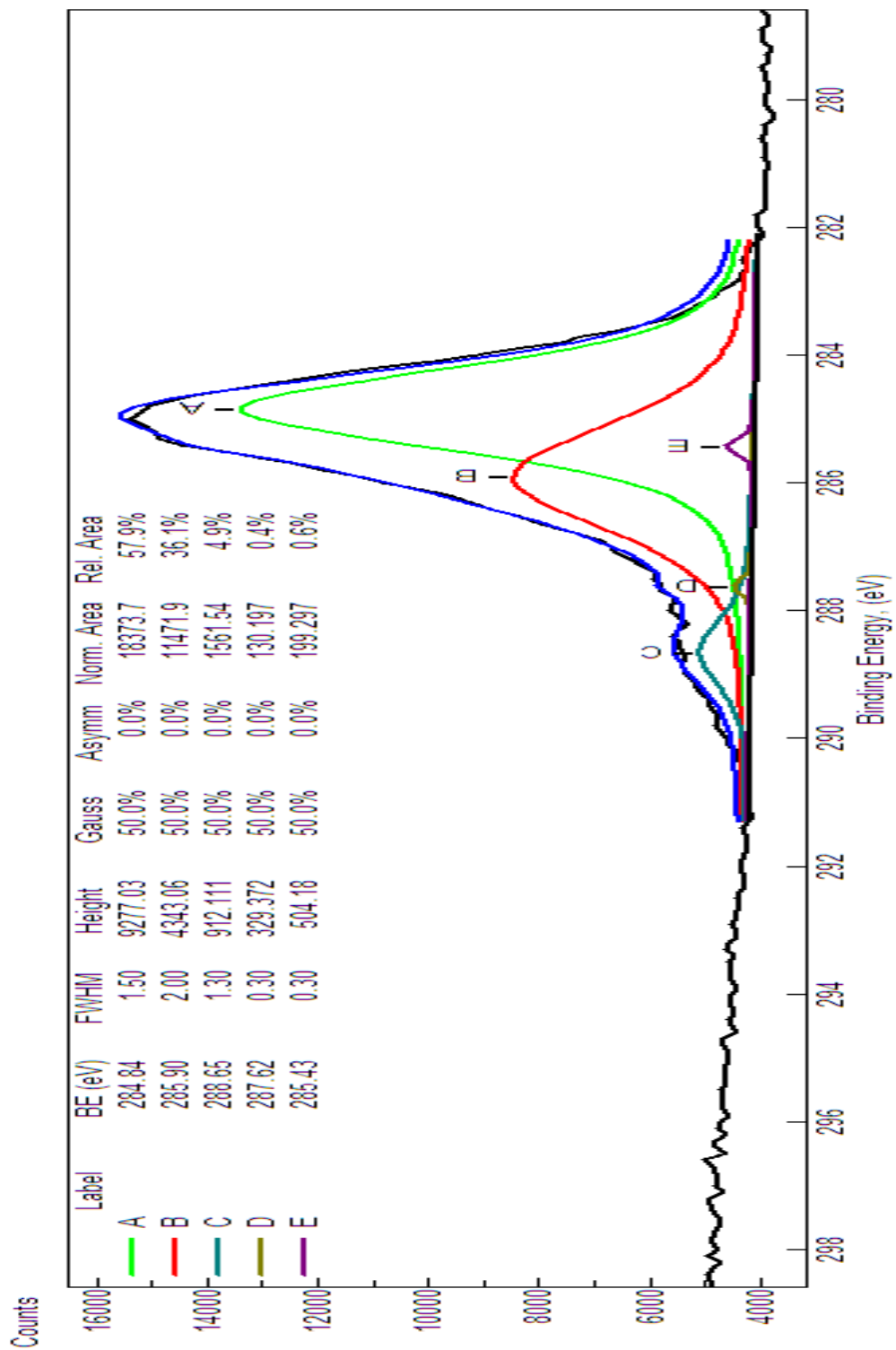
Figure 3.2.2 C1s core energy XPS Spectra of as received LEB-PANI Powders
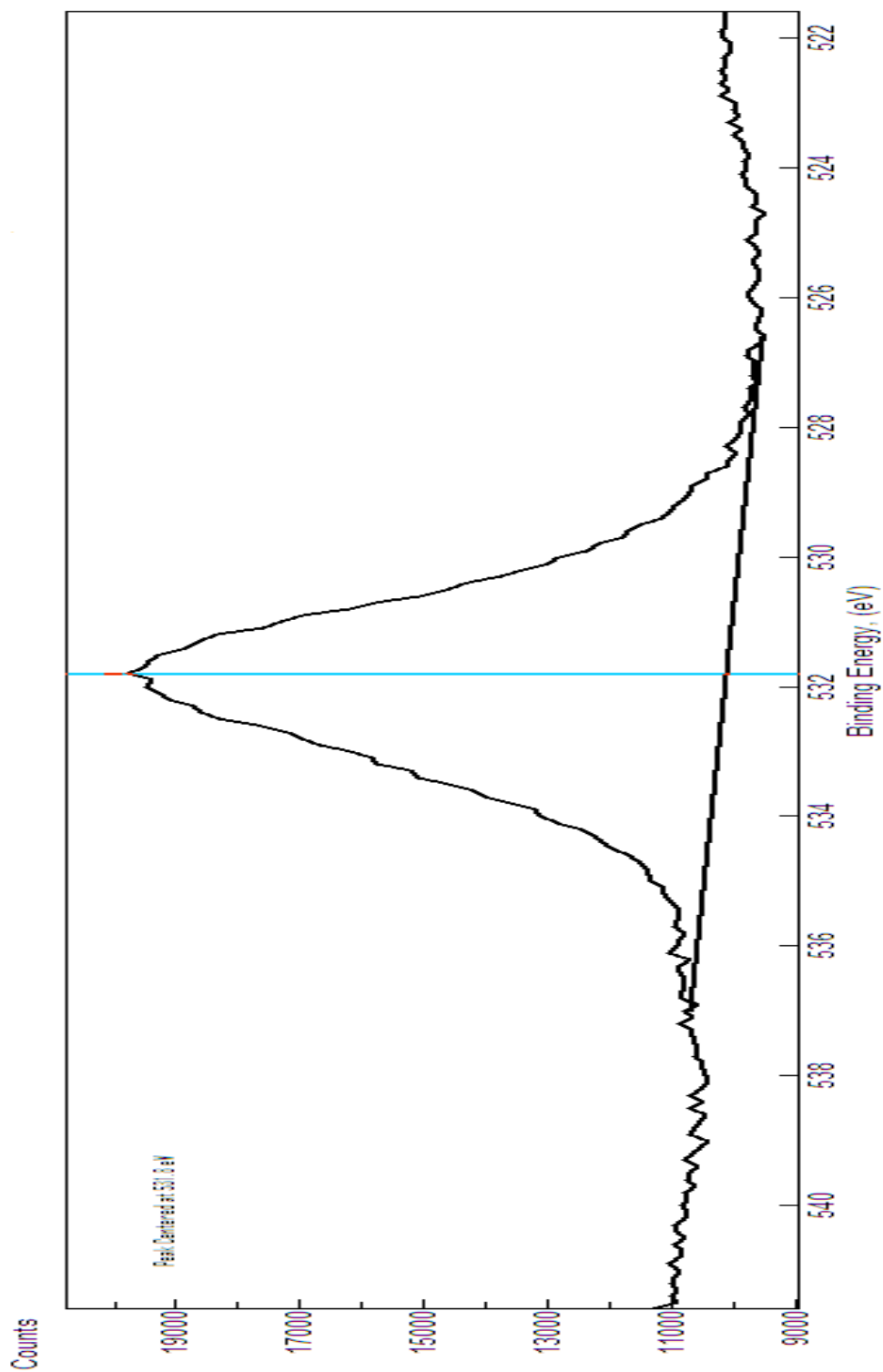
Figure 3.2.3 O1s core energy XPS Spectra of as received LEB-PANI Powders

3.2.2. *UV-Visible Spectroscopy*

UV-Vis spectroscopy was used to analyze the effects of solvents ethanol and acetone, used in processing the proposed composites, on the conformational structure of LEB-PANI. This technique provides valuable information regarding the evolution of the electronic and conformational structure of the polymer. Electronic transitions $\pi \rightarrow \pi^*$ (bonding to anti-bonding), $\pi_B \rightarrow \pi_Q$ (benzenoid to quinoid), n $\rightarrow \pi^*$ (unbonded N electrons to anti-bonding band), and $\pi \rightarrow$ polaron/bipolaron can be photochemically induced (by light radiation) and are observable in the ultraviolet-visible (UV-Vis) near infrared (NIR) spectrum. Figure 3.2.4 displays the UV-Vis spectra of LEB-PANI powders dispersed in aqueous solutions of ethanol and acetone. It is reported that the peak which reflects the $\pi \rightarrow \pi^*$ transition of the benzenoid ring ranges from 280 – 340 nm (depending of solvent effects), exciton transitions (i.e. $\pi_B \rightarrow \pi_Q$) of the quinoid ring range from 540 - 660 nm (depending on chain - conjugation - length and number of quinoid rings), and if protonation occurs an appearance of a peak ~410-490 nm (bipolaron and polaron) can be observed. The latter of which is usually associated with a free carrier tail (broad - delocalized polaron, sharp - localized polaron) in the NIR region (780-2000 nm) which reflects the structural conformation of the polymer [13-16]. Red shifts (longer wavelength -bathochromic) from these wavelengths reflect oxidation and H bonding while blue shifts (shorter wavelength – hypsochromic) represent protonation and reduction.

It has been shown from XPS analysis of the as received powders that several
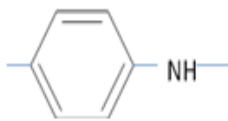
structures aside from the expected may exist. These may be reflected

in UV-Vis spectroscopy as shifts from the wavelength associated with the base structure

of LEB-PANI to wavelengths associated with an oxidized or doped structure. Possible

observable structures include polarons, bipolarons, protonated amines, imine structures,

C-O, C=O, and CH-OH (in this case, OH groups of a dopant/oxidant/contaminant may

bond to the aromatic rings in polyaniline). The absorption peak at 341 nm in the LEB-

PANI acetone system reflects $\pi \rightarrow \pi^*$ transition of the benzenoid peak, this however is

red shifted from the expected band (280-300 nm) due to bonding between the aromatic

ring and the carbonyl group in acetone (either via substitution or H bonding) as well as

oxidation of the amine N. This peak is red shifted by 57 nm in the LEB-PANI ethanol

system. This can be attributed to oxidation and bonding between the OH group of

ethanol and the aromatic ring (either via substitution or H bonding). The low absorption

peak in the LEB-PANI ethanol solution ~230 nm is associated with high energy

transitions of ethanol [17].
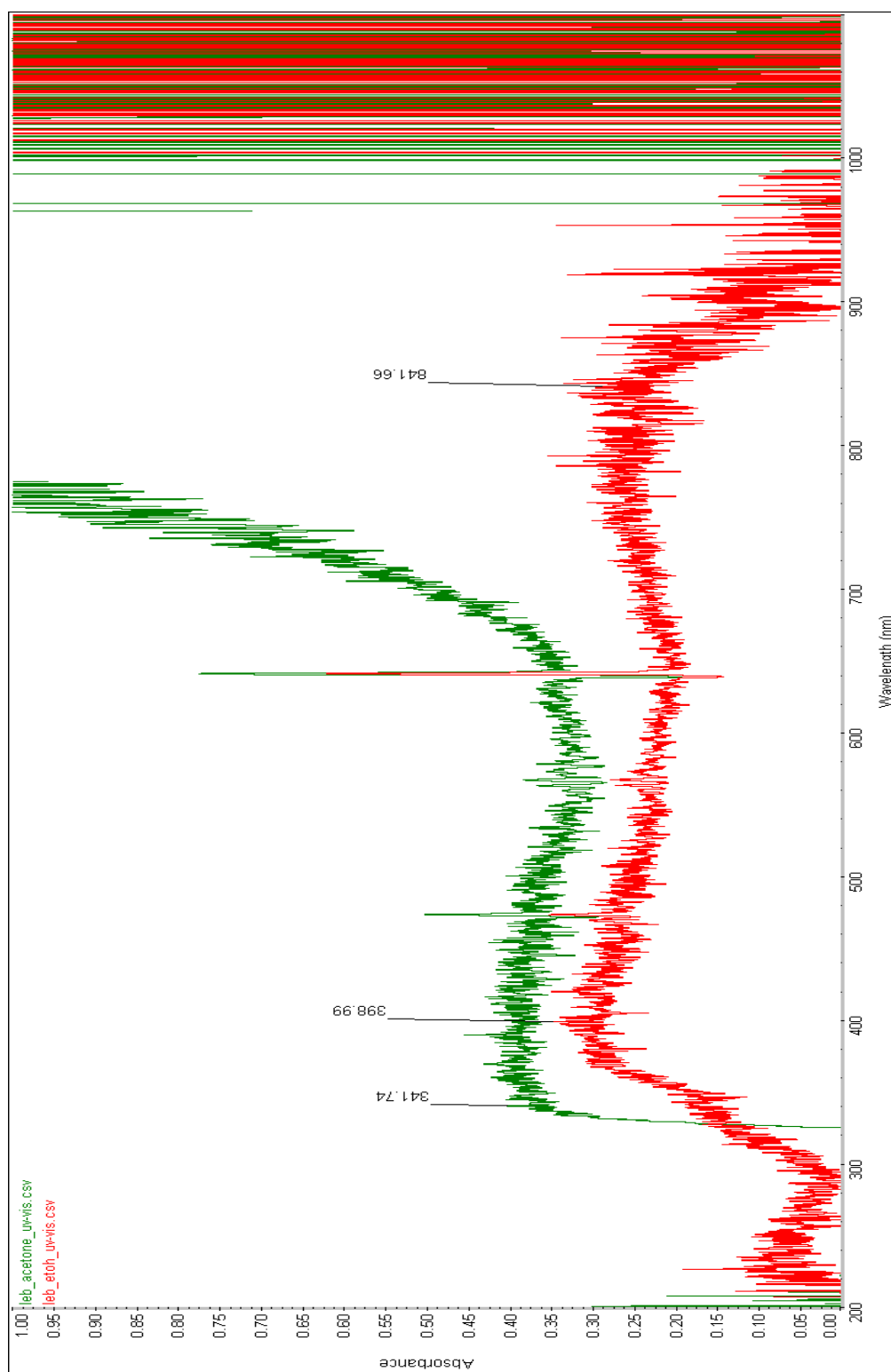
Figure 3.2.4 UV-Vis Absorption spectra for LEB-PANI in acetone and ethanol

65

The LEB-PANI acetone system exhibits a carrier tail around 700 nm. This carrier tail is representative of the polymer conformational structure. The polymer in its reduced form will most probably retain a compact configuration. Upon oxidation and reactions with oxygen (through covalent – substitution - or hydrogen bonding) transformation to an expanded configuration may occur. The electronic properties of polyaniline are dependent on the conformational structure of the polymer chain. The more expanded the polymer chain the easier charge transport between conducting sites becomes. The LEB-PANI ethanol structure however does not exhibit such a carrier tail. Instead a broad energy peak around 841 nm emerges. This peak reflects a red shift in the exciton transition of the quinoid structure, as supported by the lack of a polaron peak around 400 nm. The red shift is likely a result of bonding between the OH group in ethanol with the imine N and substitution or H bonding between the hydroxide and quinoid ring of LEB-PANI. Because this peak is so broad it may contain some low level 'localized' polaron bands created from volatile/water adsorption in the as received state. This is presumed because results from XPS analysis suggests that roughly 4% of the N centers along the LEB-PANI structure are protonated (of which may consist of both protonated imines or protonated amine structures). As described in chapter 1, through charge delocalization and internal redox processes bipolaronic structures in the polymer chain can transform into polaronic structures. Although typically delocalized, the existence of protonated amines can retard π conjugation resulting in confinement of polarons to localized sites along the polymer chain [13]. It is also possible that if an amine structure is protonated the $\pi - \pi^*$ transition may occur at higher energies (lower wavelengths) [13].

It can also be inferred from the UV-Vis spectra of LEB-PANI acetone and LEB-PANI ethanol that LEB-PANI in the pure solvent solution oxidizes to a higher state. According to [18-19] we can estimate the oxidation state of polyaniline using the acquired UV-Vis spectra. This is done by comparing the absorption intensity of the benzenoid band to the absorption intensity of the quinoid band (A_B/A_Q). For the LEB-PANI ethanol solution the ratio of the energy band at 398 nm (intensity = 0.347) to the energy band at 841 nm (intensity = 0.317) is 1.09.   After comparing this ratio to MacDiarmid's plots (please refer to reference) in [18] it can be deduced that LEB-PANI in 100% ethanol solution is transformed to the emeraldine oxidation state. The oxidation state of the LEB-PANI acetone solution cannot be estimated because the intensity of the quinoid peak is not distinguishable.

3.2.3. *Zeta Potential and Surface Charge*

As shown in figure 3.1.1, the LEB-PANI particles have aggregated into larger microstructures which inhibit electrical transport of charges between active sites. The presence of these aggregated structures diminishes in a colloidal solution of polyaniline in select solvents. When the polymer interacts with a solvent in solution, an active layer along the surface of individual polymer particles is formed yielding charge neutrality between the particle surface and the solvent. This active layer is termed a diffuse double layer which allows for charge from the solvent to interact with the charges on the surface layer of the particle. The surface of the double layer is sheathed with a single charge. This allows for electro-neutrality between the particle and the solution. Each particle has the

same charge and thus repulsive forces between like charged particles inhibit agglomeration. The zeta potential is the electric potential beneath this double layer and is calculated as the difference in potential between the solvent and the double layer. The higher the zeta potential (positive or negative) the more stable the colloidal solutions. Zeta potentials below ±30 mV are associated with an unstable colloidal solution. Since LEB-PANI is insoluble in most organic solvents as well as in water, a zeta potential analyzer has been employed to assess the effects of ethanol and acetone on the colloidal stability of LEB-PANI. The zeta potentials of acetone and ethanol were measured to be -31.31 mV and +68.86 mV respectively. This suggests that the colloidal solutions are stable (with the latter having a higher stability) and that the LEB-PANI particles become positively charged in ethanol and negatively charged in acetone. The surface charge is related to the acidic or basic strength of the solvent. This information can be correlated to the UV-Vis data in the previous section. The zeta potential analyses suggest that ethanol may act as a basic solvent for LEB-PANI. This is in agreement with the increase in oxidation level of LEB-PANI as shown in figure 3.2.4. The basicity of the solvent can dictate the degree of oxidation. The acetone, conversely, from the zeta potential analysis may act as an acidic solvent. The sharp absorption edge around 700 nm in the UV-Vis spectrum of LEB-PANI in acetone in figure 3.2.4 may be attributed to the effects of the acidic properties of acetone giving rise to the formation of charged species, such as polarons and bipolarons, and chain expansion.

LEB-PANI films constructed using the electrospinning technique may also inhibit particle agglomeration. The intensity of the induced charges within the electric field and within the electrospun mat may be high enough to break hydrogen bonds formed along

the polymer chain (from exposure to water and other volatiles that trigger self assembly and amine to imine transformations) as well as bonds between the polymer and the contaminant. The appropriate selection of a base polymer will also promote de-aggregation. Polymer blends of polyaniline with insulating polymers such as PVP and CA have been studied for their effectiveness as dispersion agents and as electron transports. The effects of electrospinning and the base polymer employed on dispersion, structure, and sensing properties of LEB-PANI will be discussed in the oncoming chapters.

REFERENCES

1. E. Segal, R. Tchoudakov, I Mironi-Harpaz, M. Narkis, and A. Siegmann, "Chemical sensing materials based on electrically conductive immiscible polymer blends, *Polymer International,* vol. 54, no 7, pp. 1065-1075, 2005

2. M. Angelopoulous, R. Dipietro, W. Zheng, A.G. MacDiarmid, and A.J. Epstein, "Effect of selected processing paratments on solution properties and morphology of polyaniline and impact on conductivity", *Synthetic. Metals*, vol. 84, no 1-3, pp. 35-39, 1997

3. E.S. Matveeva, R.D. Calleja, and V.P. Parkhutik, "Thermogravimetric and calorimetric studies of water absorbed in polyaniline", *Synthetic Metals*, vol. 72, no. 2, pp. 105-110, 1995

4. M.G.H. Meijerink, D.J. Strike, N.F. de Rooij, and M. Koudelka-Hep, "Reproducible fabrication of an array of gas sensitive chemoresistors with commercially available polyaniline, *Sensors and Actuators B- Chemical*, vol. 68, no 1-3, pp. 331-334, 2000

5. W. Brown and C.S. Foote, *Organic Chemistry 3rd Ed.*, Thomas Learning Inc., p. 574, 2002

6. E. Segal, R. Tchoudakov, I. Mironi-Harpaz, M. Narkis, and A. Siegmann, " Chemical sensing materials based on electrically-conductive immiscible polymer blends", *Polymer International,* vol 54, no. 7, pp. 1065-1075, 2005

7. V. Jousseame, M. Morsi, A. Bennet, and S. Lefrant, "X-ray photoelectron spectroscopy of conducting polyaniline and polyaniline polystyrene blends", *J. Applied Polymer Science*, vol. 67, pp. 1209-1214, 1998

8. K.L. Tan, BTG Tan, ET Kang, and KL Neoh, "X ray photoelectron spectroscopy studies of the chemical structure of polyaniline", *Physical Review B*, vol. 39, no. 11, pp 8070-8073, 1989

9. ET Kang, KG Neoh, and KL Tan , "Protonation and deprotonation of polyaniline films and powders revisited" , *Synthetic Metals*, vol. 68, pp 141-144, 1995

10. MG Han and SS Im, "X-ray Photoelectron study of electrically conducting polyaniline/polyamide blends" , *Polymer*, vol 41, pp. 3253-3262, 2000

11. K. G. Neoh, E. T. Kang , K. L. Tan, " Protonation of leucoemeraldine in the solid state and in solution", J. *of Polymer Science Part B: Polymer Physics*, vol . 31 no 4, pp 395-401, 1992

12. D. Rodrigue, O. Snauwaert, C. Demaret, J. Riga, and JJ Verbist, "Thermal Treatment and oxygen exposure dependence of the electronic structure of polyaniline – an X-ray photoelectron spectroscopy approach", *Synthetic Metals*, vol. 41, no. 1-2, pp 769- 773, 1991

13. W.S. Huang and A.G. MacDiarmid, "Optical properties of polyaniline", *Polymer*, vol 34, no 9, pp 1833-1845, 1993

14. K.G Neoh, E.T. Kang, and K.L. Tan, "Spectroscopic studies of protonation, oxidation and light irradiation of polyaniline solutions", *Polymer*, vol. 33 no. 11, pp2292-2298, 1992

15. S. Quillard, S. Louarn, S. Lefrant, A.G. MacDiarmid, "Vibrational analysis of polyaniline- A comparativity study of leucoemeraldine, emeraldine, and pernigraniline bases", *Physical Review B* , vol. 50, no. 17, pp. 12496-12508, 1994

16. D. Yang, P.N. Adams, L. Brown, and BR Mattes, "Impact of H bonds in polyaniline AMPSA/acid solutions", *Synthetic Metals*, vol. 156, no 18-20, pp 1225-1235, 2006

17. C.N.R. Rao, Ultraviolet and visible spectroscopy Chemical applications, 3rd edition, , Butterworth and Co., 1975

18. J.E Albuquerque, L.H.C. Mattoso, D.T. Balogh, R. M Faria, J.G. Masters, and A.G. MacDiarmid, " A simple method to estimate the oxidation state of polyaniline", *Synthetic Metals*, vol. 113, pp 19-22, 2000

19. L.H.C. Mattoso, D.T. Balogh, R. M Faria, J.G. Masters, and A.G. MacDiarmid, "Study of the interconversion of polyaniline oxidation states by optical absorption spectroscopy" , *Synthetic Metals*, vol. 146, pp 1-10, 2004

CHAPTER 4

4. Leucoemeraldine Base Polyaniline - Poly vinyl pyrrolidone Composites

Poly vinyl-pyrrolidone (PVP), C_6H_9NO, has been employed for various applications. As a binding agent for drug delivery [1-2], as membranes for dialysis and molecular sieving [3], and for sensors [4-6]. With the latter it has been most popularly employed for humidity sensing, [7], as a carrier polymer for electrochemical and biological sensing [8] and for piezoelectric sensing applications [9-10].

PVP is a water soluble polymer and thus the films can be easily processed in polar solvents and deposited using various techniques. Researchers have employed the electrospinning technique to develop novel composite membranes with PVP as a base polymer [11-13]. In all sensing applications it has been employed as part of a composite system either with an organic, inorganic, or biological component. For polyaniline, PVP is well known steric stabilizer, it can be chemisorbed on the surface of polyaniline, form a solvated barrier coating between the particle and its surrounding environment [14-15], and can stabilize chain conformational changes (i.e. ring torsion). Researchers have employed it as base component for in-situ precipitation, dispersion [14], and oxidative polymerization of polyaniline [16]. [16] have observed enhanced particle dispersion and retention of the polymer electronic properties in the presence of PVP.

The aim of the work presented in this chapter is to employ the electrospinning process to develop PVP LEB-PANI composites for chemical sensing applications. It is anticipated that the composite solution will provide an enhancement in dispersion and

colloidal stability of polyaniline by obstructing possible Van der Waal's forces between individual particles and hydrogen bonding between amine and imine nitrogen sites within the polymer chain. Moreover, these polymers may also perform as co-dopants for polyaniline [16-17] by increasing the oxidation level via hydrogen bonding between PVP and LEB-PANI [18].

4.1. STRUCTURAL CHARACTERIZATION

PVP dissolved in ethanol was employed as a carrier polymer for electrospinning polyaniline. It plays the role of the nonreactive component in the PVP LEB-PANI composite. While pure PVP matrices are inherently insulating they exhibit a high affinity to water, and thus can be used to amplify the sensitivity of polyaniline to humidity [19]. In the presence of gases, PVP may exhibit physical changes such as swelling as a result of gas absorption and thus can be used as a standalone sensor in surface acoustic wave or quartz microbalance sensor technologies [20]. This reaction can also be observed in the PVP matrix developed here where LEB-PANI acts as the reactive component. Coupled with the electrospinning technique, dispersed polyaniline matrices can be acquired with high porosity and high surface to area ratios.

The concentration of PVP chosen for this research is 0.5mM. This provides fiber diameters roughly on the order of 1-2µm. Several PVP LEB-PANI composites were developed ranging from 20% to 80% wt/wt LEB-PANI in the hybrid matrix to discern effects of concentration of LEB-PANI on the electronic and sensoric nature of the

composite film (with LEB-PANI being the sensing element). This was feasible because of the concentration of PVP employed (0.05 mM) allowing for variability in matrix composition; the drawback however, is the increase in bead formation within the microstructure due to the low molar concentration. Figure 4.1.1 shows that as the concentration of LEB-PANI increases the conductivity of the film increases exponentially.
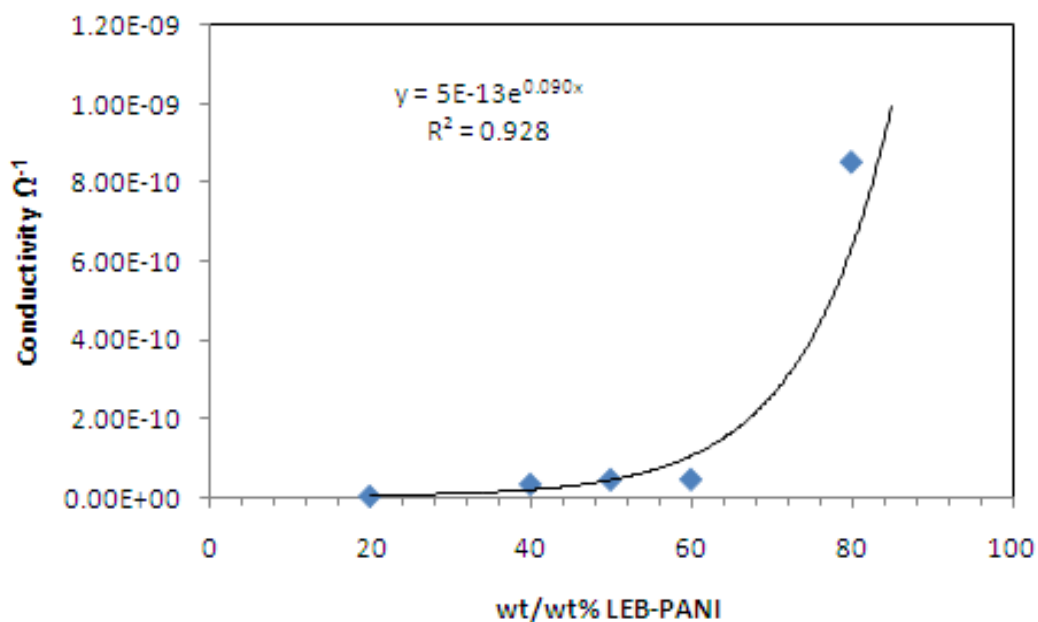
Figure 4.1.1 PVP LEB-PANI composite conductivity as a function of LEB-PANI concentration

The rise in conductivity is due to the lack of surface coverage by PVP which leads to an increased level of contaminant (i.e. water vapor, volatiles) poisoning of LEB-PANI. In this chapter the effects of 20% wt/wt, 50% wt/wt and 80%wt/wt LEB-PANI compositions on the morphology, structure, and composite sensitivity to NO_2 will be

determined. These three composites are most representative of the high, mid, and low concentration hybrids and their effects on the microstructure and response of LEB-PANI to NO_2.

4.1.1. *SEM*

The morphology of electrospun composites containing 20% wt/wt, 50% wt/wt, and 80%wt/wt LEB-PANI with PVP as a base polymer was observed using SEM. Complementary to the increased colloidal stability of LEB-PANI particles due to PVP, charges accumulated within the electrospun matrix (consequently a result of the electrospinning process) may assist in ion separation - breaking inter- and intrachain bonds formed between and at the amine and imine nitrogen sites further promoting the de-aggregation of the agglomerated structures described in chapter 3. Figure 4.1.2 reveals the morphology of the electrospun PVP LEB-PANI composite matrix at varying LEB-PANI concentrations: (a) 100% wt/wt LEB-PANI, (b) 20%wt/wt LEB-PANI, (c) 50% wt/wt LEB-PANI, and (d) 80% wt/wt LEB-PANI.

As compared to the micrograph of the as received LEB-PANI powders, the electrospun matrix contains very few to none of the self assembled structures at low LEB-PANI concentrations in the electrospun matrix. However as the concentration of LEB-PANI increases to 80%wt/wt, as expected, there is an increase in degree of aggregation in the electrospun matrix (about 90% of the matrix has agglomerated). This is attributed to the decrease in PVP shielding which allows for higher adsorption of atmospheric contaminants that can induce conformational changes in the structure

resulting in increased aggregation and increased conductivity due to contaminant doping effects, as evidenced by figure 4.1.1. The 'globs' in the SEM pictures (figures 4.1.2 b and c) are consequences of the concentration of PVP in the pre-spinning solution.
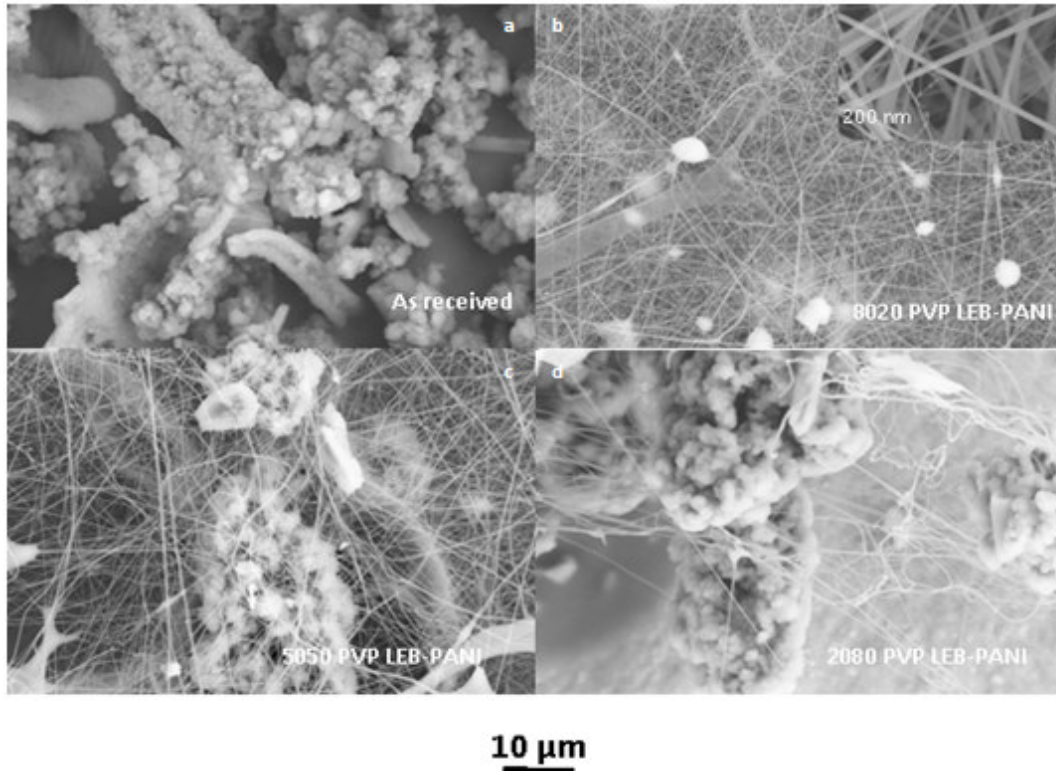
Figure 4.1.2 – SEM of a) as received LEB-PANI powders, b) electrospun 20% wt/wt LEB-PANI, c) electrospun 50% wt/wt LEB-PANI, and d) electrospun 80% LEB-PANI

4.2. CHEMICAL EVALUATION OF PVP LEB-PANI COMPOSITES

4.2.1. *FTIR*

FTIR was employed to determine the interactions between PVP and LEB-PANI. Thin films were solution casted onto aluminum foil for both photo acoustic and transmission FTIR analyses. Figure 4.2.1 depicts the photo acoustic spectra of 20%wt/wt

and 80% wt/wt LEB-PANI composites and the transmission spectrum for the 50% wt/wt LEB-PANI composite.

According to the absorption spectra of PVP, appendix E [21], the characteristic peaks are 3439 cm^{-1}, 2872 cm^{-1}, 2944 cm^{-1}, 1671 cm^{-1}, 1489 cm^{-1}, 1367 cm^{-1}, and 1286 cm^{-1}. Literature states that the characteristic bands for LEB-PANI are 1555 cm^{-1}, 1491 cm^{-1}, 1312 cm^{-1}, 1167 cm^{-1}, and 843 cm^{-1} [22-25]. In comparing these peaks in all three samples, Table 4.1, it is observed that the peak around 1555 cm^{-1} is strongest in the 80% wt/wt LEB-PANI composite and weakens with decreasing LEB-PANI concentration. The peak around 1490 cm^{-1} is strongest for the 20% wt/wt LEB-PANI and the 50% LEB-PANI composite but as the concentration increases to 80% wt/wt the peak becomes very weak. This peak also reflects the adsorption of PVP at the amine N center of LEB-PANI and the concentration of amines in the polymer structure. As expected the intensity of the peak is highest for the 20% wt/wt LEB-PANI composite suggesting maximum adsorption, maximum coverage by PVP, and the structure is composed of mostly amines. The adsorption of PVP is also evidenced by the distinct carbonyl peak ~1670 cm^{-1}. According to [18] this is from intermolecular H-bonding at the NH sites on LEB-PANI and >C=O groups of PVP.

The shoulder peak around 1312 cm^{-1} reflects the benzenoid ring vibrations and C-N stretching in LEB-PANI and exhibits relatively the same intensity for each composite. The peaks at 1167 cm^{-1} 843 cm^{-1} are associated with ring distortions of reduced polyaniline and are strongest and sharpest for the 20% LEB-PANI composite and broad and weak for the 50% LEB-PANI and 80% LEB-PANI composites.

Synonymous within the three PVP LEB-PANI composites is a broad peak around ~3400 – 3500 cm^{-1} which reflects N-H stretching of polyaniline and OH stretching of adsorbed water. The peaks ~2920 cm^{-1} and 2880 cm^{-1} and 2870 cm^{-1} reflect CH_2/ CH_3 stretching of residual ethanol.

Evaluation of the peaks in ~1600cm^{-1} suggest low level protonation and formation of quinoid rings and imine N in all composites, however these peaks are well defined for the 80% LEB-PANI composite. This broad peak is also characteristic of the PVP structure. The wavelengths between 1370 cm^{-1} and 1440 cm^{-1} reflects adsorbed water into the polymer matrix. For all three composites this occurs via H bonding or substitution (of H for OH) on the benzenoid ring, for the other two composites this may occur also at the imine N centers. These peaks are strongest for the 80% wt/wt LEB-PANI composite suggesting that there are more sites for bonding available. This in part is due to the lack of PVP shielding. Presorbed ethanol is evidenced from the CH-OH bonds formed between the alcohol and the carbon rings at ~1289 cm^{-1}, ~1266 cm^{-1}, and ~1227 cm^{-1} in all composites. Table 4.2 in appendix D provides a detailed analysis of each IR peak for each composite system.
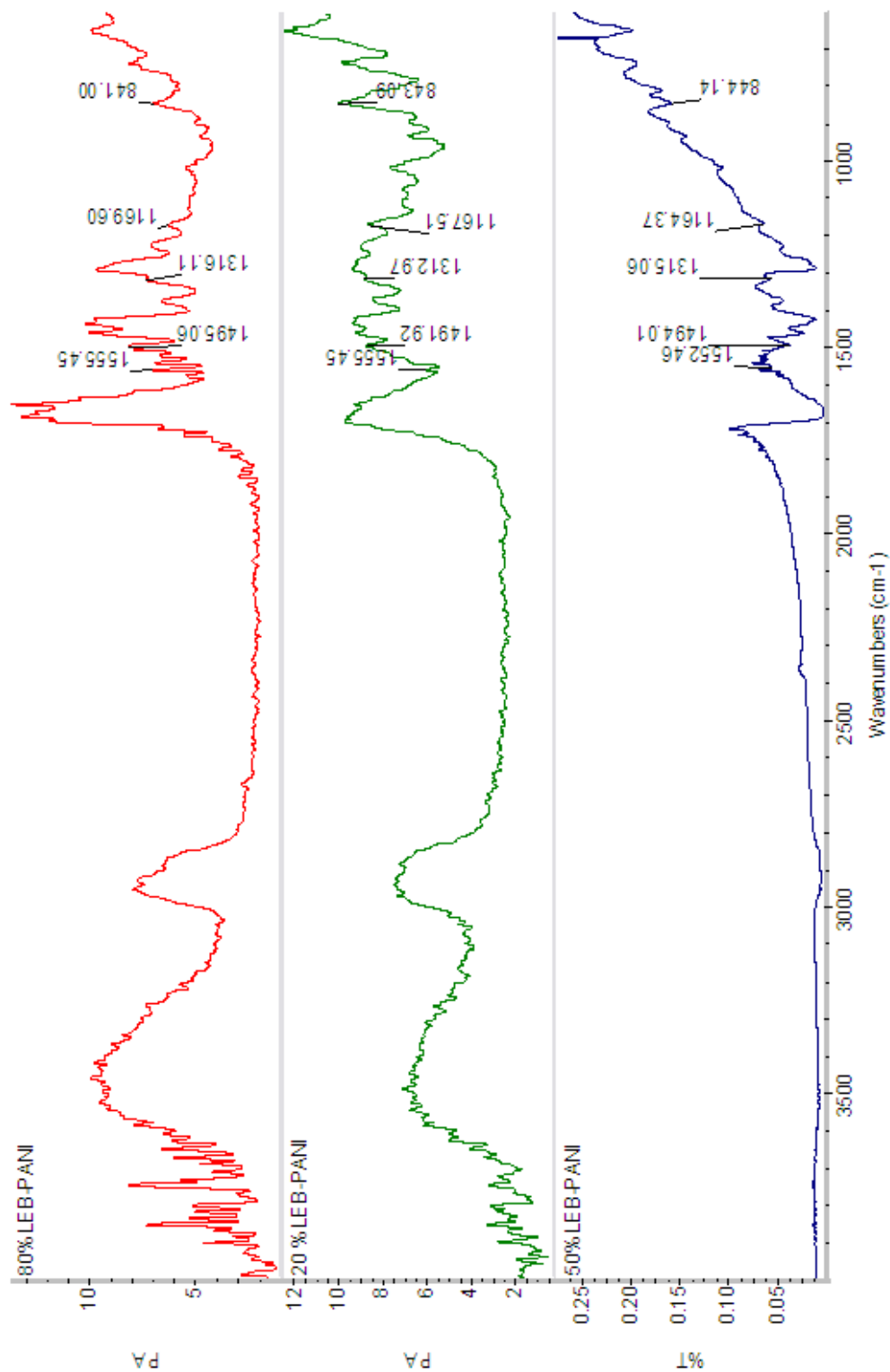
Figure 4.2.1 Photo acoustic and transmission FTIR spectrums for the three LEB-PANI hybrid systems.

Table 4.1 FTIR analyses of LEB-PANI characteristic peaks in 8020, 5050, and 2080 PVP LEB-PANI composites

LEB-PANI Characteristic Peaks	Vibration	8020 PVP LEB-PANI	5050 PVP LEB-PANI	2080 PVP LEB-PANI
1555 cm^{-1}	C=N stretching; CH in plane bend of quinoid	Weak intensity	Medium intensity	Strong intensity
1491 cm^{-1}	C-N stretching, CH bending in benzenoid	Strong intensity	Medium intensity	Very weak intensity
1312 cm^{-1}	Benzenoid ring vibrations; C-N stretching	Medium intensity shoulder	Medium intensity shoulder	Medium intensity shoulder
1167 cm^{-1}	CH in plane bending of benzenoid	Medium strong broad shoulder intensity	Weak broad intensity	Medium strong sharp intensity
843 cm^{-1}	CH out of plane deformation of benzenoid	Very strong intensity	Weak intensity	Medium Intensity

4.2.2. *UV-Vis Absorption Spectroscopy*

Figure 4.2.2 depicts the UV-Vis spectrums of the 20%, 50% and 80% wt/wt LEB-PANI composite films. The band at 282 nm in the 20% LEB-PANI composite reflects the π–π^* transition of the benzenoid ring (as discussed in chapter 3). The shoulder peak at 268 nm can be attributed protonated amine structures as evidenced by the LEB-PANI XPS studies in the previous chapter. Analysis of the UV-Vis absorption spectra of the

PVP LEB-PANI composites, Table 4.3, show the emergence of a peak ~350 nm also representative of the π–π* transition in LEB-PANI which is commonly referred to in the literature. Realistically it is representative of the π–π* transition in processed LEB-PANI (either in solvent or in a composite). This peak emerges at 350 nm in the 8020 PVP LEB-PANI composite and is red shifted to 355 nm for 5050 PVP LEB-PANI and 357 nm for 2080 PVP LEB-PANI composites as a result of oxidation and hydrogen bonding between PVP, LEB-PANI, and residual ethanol. Exciton transitions of the quinoid structure is expected to occur in the region 550-620nm [18]. Figure 4.2.2 suggests that quinoid di-imines exist within all the LEB-PANI matrices this is also supported by the infrared spectra in figure 4.2.1. This complements the blue color of the commercial LEB-PANI powders as discussed in chapters 1 and 3. With increasing oxidation level, electronic transitions occur at longer wavelengths which are associated with a myriad of colors in the ultraviolet visible spectrum. The absorption band for the quinoid exciton transition undergoes a bathochromic shift in wavelength with increasing LEB-PANI concentration from 577 nm for the 8020 PVP LEB-PANI composite to 649 nm for the 5050 PVP LEB-PANI composite to 652 nm in the 2080 PVP LEB-PANI composite. Associated with this shift is an increase in absorption intensity due to increased chain expansion. The shift in wavelength reflects increased oxidation and hydrogen bonding possibly between adsorbed water/volatiles from the atmosphere and the imine N as evidenced by [28].

To determine the nature of the electronic transitions reflected by the 546 nm peak in the 5050 PVP LEB-PANI composite and the 544 nm and 514 nm peaks for the 2080 PVP LEB-PANI composite, this data can be correlated with the FTIR data to determine

which chromophores (the part of the conjugated structure, i.e. C=C, in polyaniline, responsible for its color) are best represented by these peaks. FTIR of the 5050 PVP LEB-PANI composite suggests that the vibrations at 1572 cm^{-1}, 1565 cm^{-1}, and 1555 cm^{-1} belong to C=N$^+$O$^-$ group. This suggests that bipolarons exist on the lattice and the absorption band at 546 nm best reflects this. FTIR of the 2080 PVP LEB-PANI composite also reflects similar vibrations and additional >C=N$^+$H, >C-N$^+$H, and >C-N$^+$H$_2$ vibrations in the 1800-2600 cm^{-1} region. The polaronic vibrations in FTIR (>C-N$^+$H and >C-N$^+$H$_2$) can be translated to a polaron band at 514 nm. Subsequently the band at 546 nm similarly reflects the bipolaron band in the oxidized PVP LEB-PANI composite. Any discrepancy between these peaks and the peaks reported in the literature (410-490 nm) is related to the effects of processing on the conformational structure of LEB-PANI.
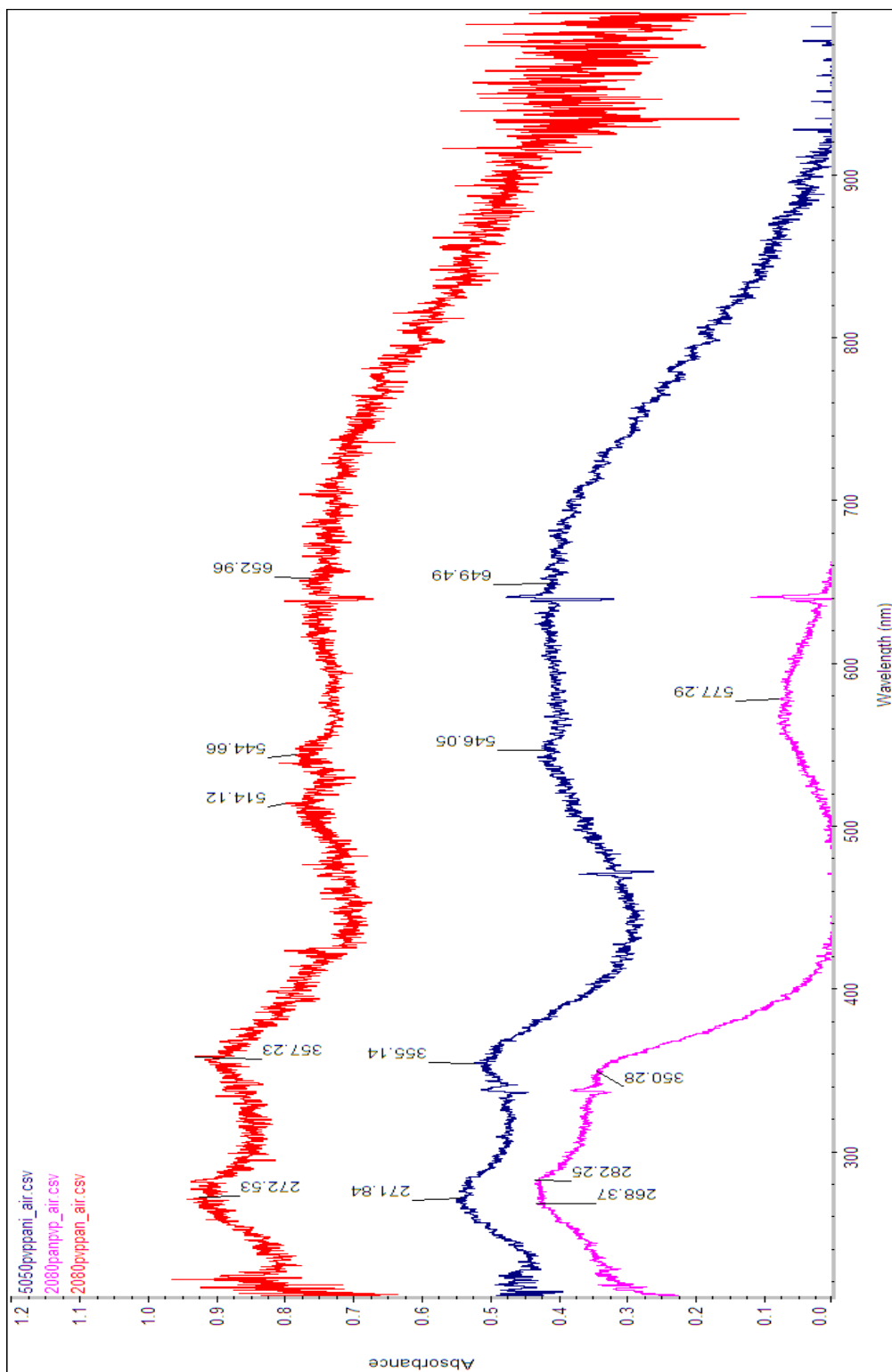
Figure 4.2.2 UV-Vis absorption spectra for 8020 PVP LEB-PANI, 5050 PVP LEB-PANI, and 2080 PVP LEB-PANI composites

Table 4.3 Electronic transitions in PVP-LEB-PANI

Transition	8020 PVP LEB-PANI	5050 PVP LEB-PANI	2080 PVP LEB-PANI
$\pi \rightarrow \pi^*$ of Benzenoid structure	350nm, 282nm (3.5eV, 4.3eV)	355nm (3.4 eV)	357 nm (3.4eV)
$\pi_B \rightarrow \pi_Q$, exciton transition of Quinoid	577nm (2.1eV)	649 nm (1.9eV)	652 nm (1.9eV)
Polaron	----	----	514 nm (2.4eV)
Bipolaron	----	546 nm (2.2eV)	544 nm (2.2eV)
Protonated Amine	268 nm(4.6eV)	271nm (4.5eV)	272 nm (4.5eV)

The broadening of the quinoid imine peak into the 800 – 900 nm region for 5050 and 2080 PVP LEB-PANI composites is associated with delocalized polaron formation and accompanies the emerging polaron/bipolaron peaks ~500 nm. This typically extends into the near IR region and also reflects the chain conformation of LEB-PANI. The broadness and increased intensity of this peak suggests transformation of the polymer from a compact configuration to an expanded chain configuration (this may also correlate to an increase in chain length as well).

PVP exhibits a high energy absorption peak around 225 nm. However, because it appears transparent in the UV-Visible range it does not absorb light at higher wavelengths.

4.2.3. *Energy Gap in PVP LEB-PANI Composites*

According to literature the band gap for leucoemeraldine is 3.8 eV for emeraldine is 1.4 eV and for pernigraniline is 1.8eV [25]. The absorption band edge of the $\pi \rightarrow \pi*$ transition for each LEB-PANI composite can be used to estimate the evolution of LEB-PANI's band gap as a function of composition using the Tauc relation [27-29]. This transition reflects the energy necessary for an electron to be excited from the π - bonding molecular orbital to the $\pi*$- antibonding molecular orbital and the absorption edge associated with this transition is the estimated length of its energy gap.

Using the relation:

$$A = \alpha c l \tag{4.1}$$

where A is absorbance measured from the UV-Vis spectrum, α is the molar absorption coefficient, c is concentration (usually in mol/L), and l is the path length of light through the sample (usually in cm), the absorption coefficient can be calculated. This can then in turn be used in the Tauc relation to determine the material's energy gap.

The Tauc relation states that the absorption coefficient, α (which is proportional to the intensity of the $\pi \rightarrow \pi*$ band absorption edge), is related to the material's band gap via the relation:

$$\alpha = \frac{\left(\dfrac{hc}{\lambda} - E_g\right)^n}{\dfrac{hc}{\lambda}} \tag{4.2}$$

where λ is the corresponding wavelength, h is Planck's constant, c is the speed of light, E_g is the band gap of the material, and n is an index which reflects the nature of the electronic transition in polyaniline. 'n' can vary from ½ for a direct allowed transition, to 3/2 for a direct forbidden transition, to 2 for an indirect allowed transition, and 3 for an indirect forbidden transition. The $\pi \rightarrow \pi^*$ transition for polyaniline has shown to be direct and allowed according to [29-30]. Thus the band gap can be calculated (for direct transitions) using the relation $\left(\alpha \bullet \dfrac{hc}{\lambda} \right)^2$ vs $\dfrac{hc}{\lambda}$ where the intercept of the linear portion of the curve with $\dfrac{hc}{\lambda}$ gives E_g.

Figures 4.2.3, 4.2.4, and 4.2.5 depict the estimated band gaps for the 20% wt/wt LEB-PANI, 50% wt/wt LEB-PANI, and 80% wt/wt LEB-PANI composites, respectively. The LEB-PANI concentration is known from the solutions used to cast the thin films and the path length l is taken as a finite number but was not measured and thus the plots are of $(\alpha lE)^2$ vs. E (energy) where E is $\dfrac{hc}{\lambda}$.
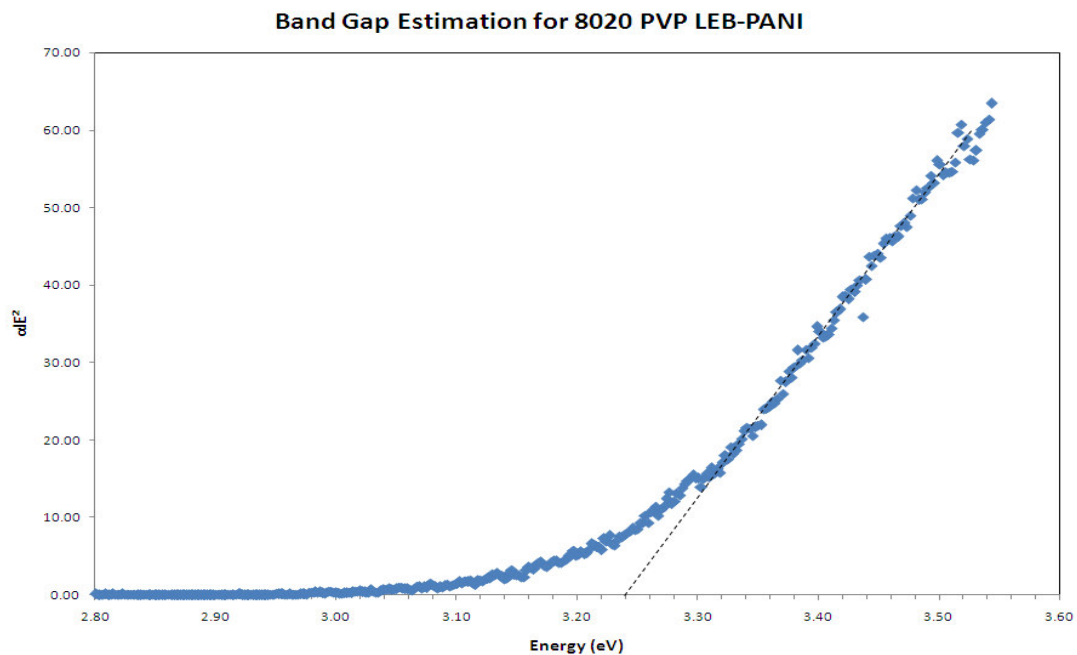
Figure 4.2.3 Band gap estimation for 8020 PVP LEB-PANI
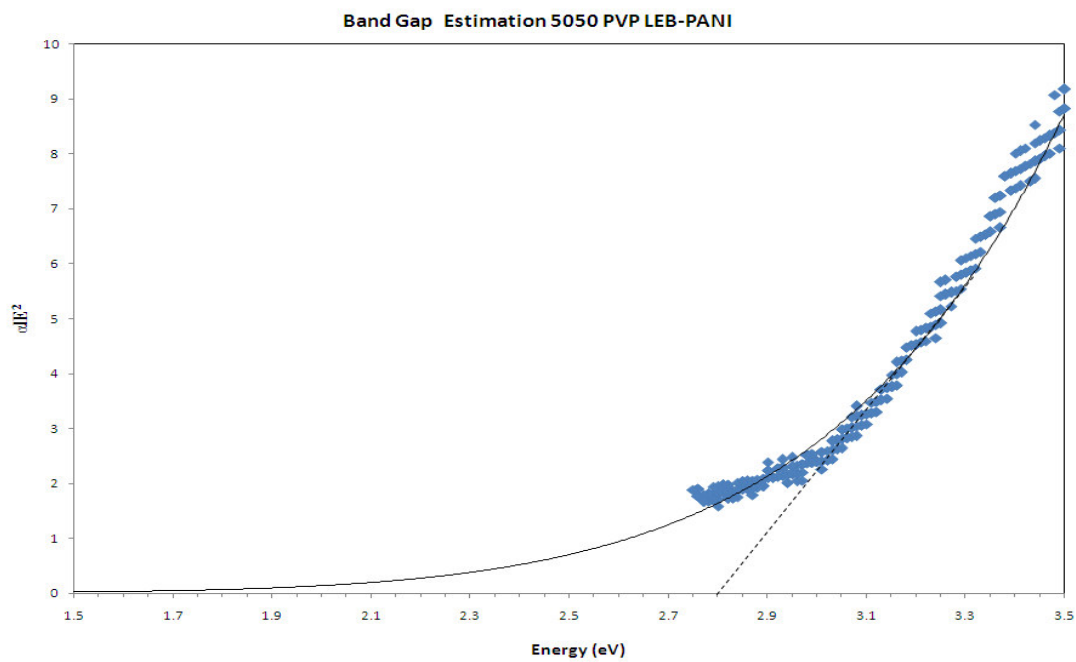
Figure 4.2.4 Band gap estimation for 5050 PVP LEB-PANI
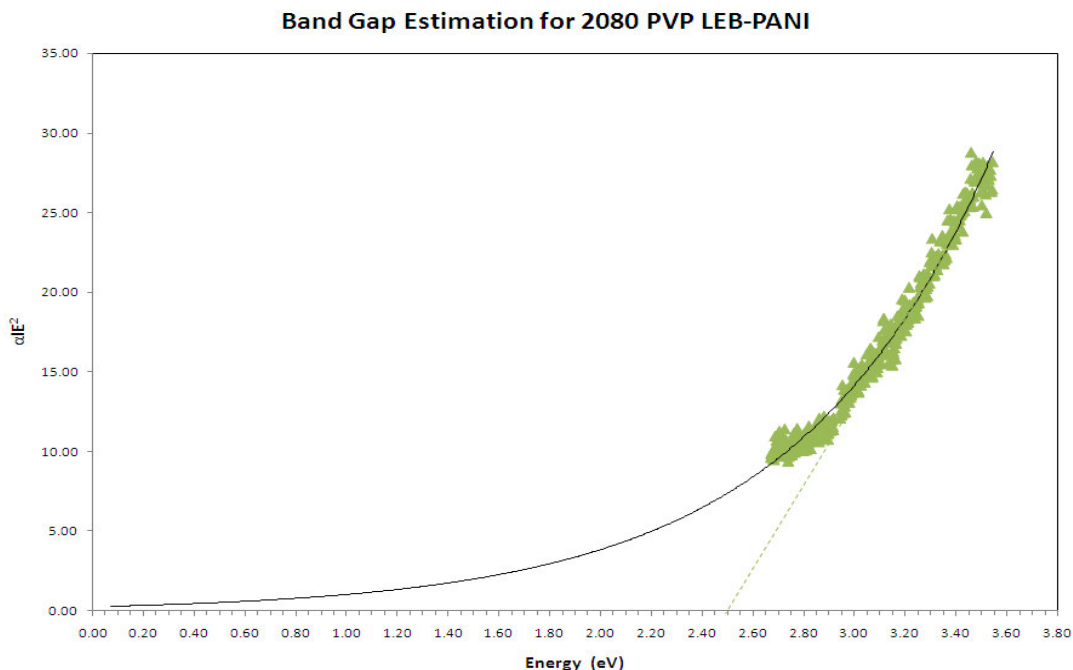
Figure 4.2.5 Band Gap estimation for 2080 PVP LEB-PANI

The band gap for the LEB-PANI composite decreases with increasing concentration from 3.24 eV for 20% wt/wt LEB-PANI, to 2.8 eV for the 50% wt/wt LEB-PANI composite, and to 2.5 eV for the 80% wt/wt LEB-PANI composite. These calculations suggest the formation of mid gap states (polarons and bipolarons) within the material's band gap which supports the evidence of polaronic and bipolaronic bands and structures in the preceding UV-Vis and FTIR data.

4.3. GAS SENSING BASED ON PVP LEB-PANI

4.3.1. *8020 PVP LEB PANI Electrospun Gas Sensing Matrix*

Figures 4.3.1 and 4.3.2 reflect the response of 8020 PVP LEB-PANI to NO_2 at 20% RH and 40% RH, respectively. The sensor response depicted in figure 4.3.1 suggests that the 20% wt/wt composite has no response to NO_2 at 20% RH. The sensor response in figure 4.3.2 shows a significant improvement in response to NO_2 at 40% RH. NO_2 is an oxidizing gas and during exposure electrons from the sites which the gas reacts with (typically the N centers) are transferred to the gas making the polymer positively charged. At the amine sites of LEB-PANI the following reaction may occur:

$$-NH- + NO_2 \rightarrow -N^+H- + NO_2^- \qquad (4.3)$$

The charged amine center can then translate into:

$$-N^+H- \rightarrow =N- + H^+ \qquad (4.4)$$

where on removal of the gas the polymer will try to energetically stabilize itself by forming an imine structure by liberating a H^+. It is observed that for NO_2 concentrations of 1, 5, and 10 ppm, the resistance of the film decreases with exposure to NO_2 suggesting that majority of charge carriers in the polymer are holes. However, at 0.5 ppm of NO_2 the resistance of the film increases. This may be a consequence of the dissolution of NO_2 at this level of humidity. Because of the low NO_2 concentration it is plausible that the gas becomes dissolved by the water vapor via the following reaction:

$$2NO_2 + H_2O \rightarrow HNO_3 + 3HNO_2 \qquad (4.5)$$
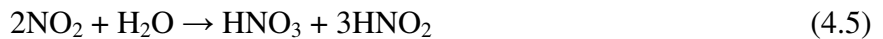
HNO_2 formed can then act as a reducing agent (this compound can donate electrons to protonated sites) while the HNO_3 formed can operate as an oxidizing agent for polyaniline; however the latter when reacted with water can further decompose into

$$HNO_3 + H_2O \rightarrow H_3O^+ + NO_3^- \quad\quad\quad (4.6)$$
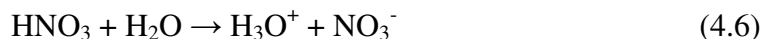
With the byproducts of this reaction also acting as reducing agents, an increase in resistance of LEB-PANI can be observed on exposure to low NO_2 concentrations. The magnitude of the sensor response can be attributed to the adsorption of the acidic byproducts which can act as secondary dopants for LEB-PANI. Moreover because of the volatility of these agents (which can poison the sensor), the polymer will take a longer time to recover and may not recover fully. This is evidenced by the baseline drift in the sensor response after exposure to 0.5 ppm NO_2. Table 4.3 shows the sensitivity, response, and recovery times of the 20%wt/wt LEB-PANI composite to 40% RH. Figure 4.3.3 shows the effect of NO_2 concentration on sensitivity of the LEB-PANI composite.

As shown in Table 4.3 the sensors response time decreases with increasing concentration and its recovery time increases with increasing concentration. This can be explained by basic kinetics. At higher concentrations there is an increase in diffusion of NO_2 into the sensor matrix yielding faster reactivity rates and a higher level of ion exchange between the gas molecule and the sensor film. The drawback is that with the higher concentration, as with many sensors, a catalyst is sometimes needed for full extinction of the analyte from the sensor film. The constant flow of humidity performs as such.
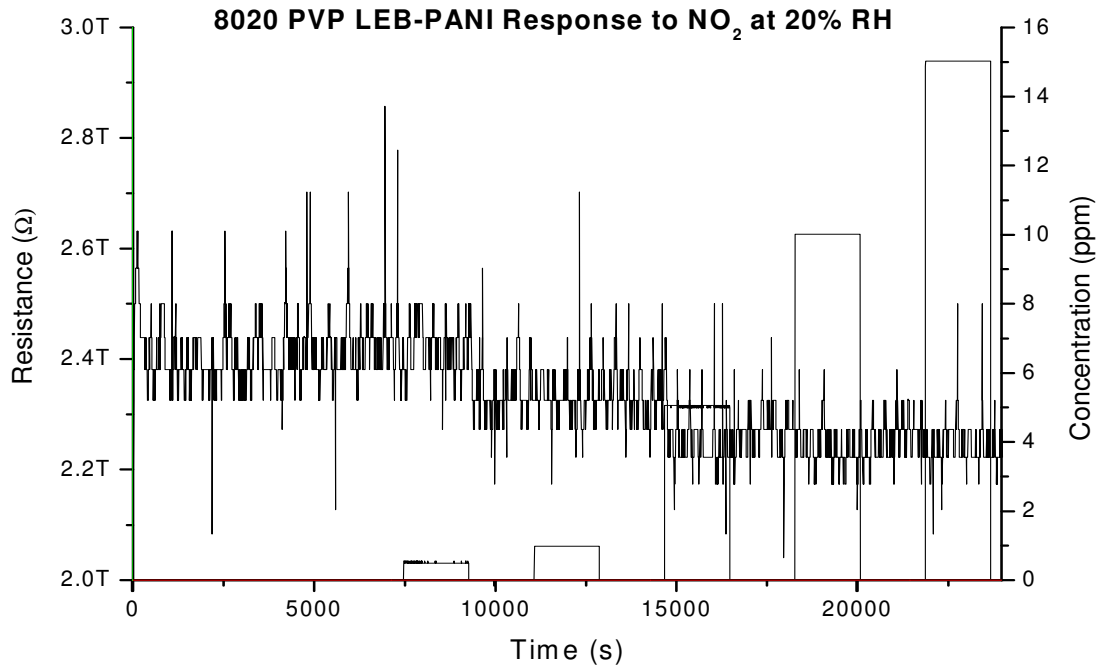
Figure 4.3.1 Response of 8020 PVP LEB-PANI to NO$_2$ at 20% RH
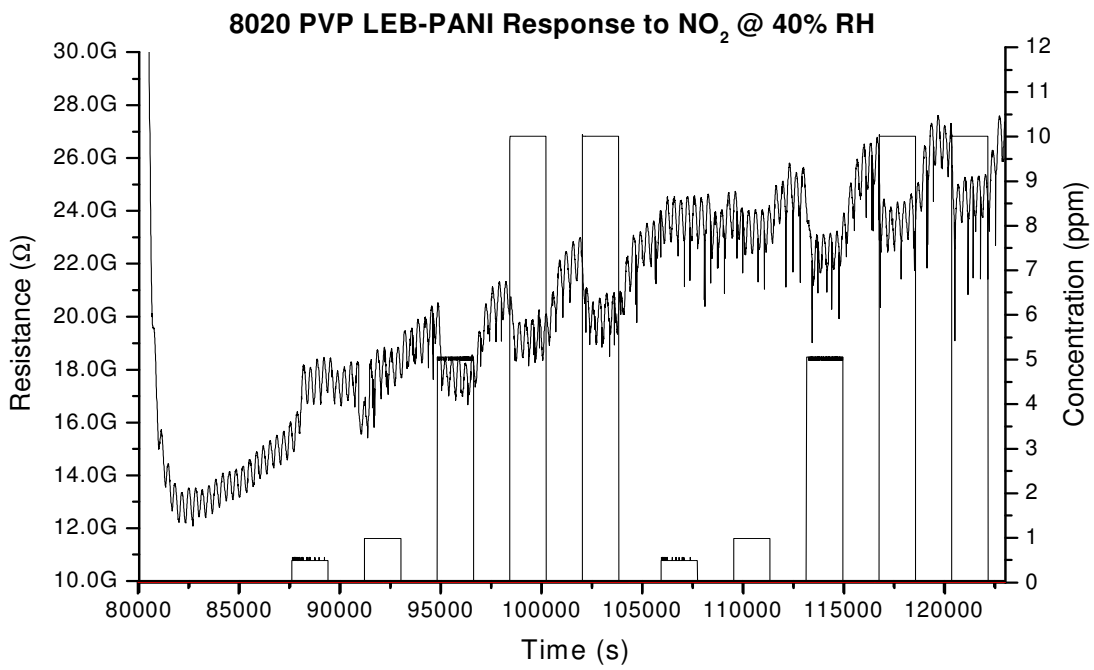
Figure 4.3.2 Response of 8020 PVP LEB-PANI to NO$_2$ at 40% RH

Table 4.3 Sensitivity, Response, and Recovery times of 20%wt/wt LEB-PANI at 40% RH

Concentration (ppm)	Sensitivity	Response Time (s)	Recovery Time (s)
0.5	0.20	520	1585
1	-0.12	1230	200
5	-0.13	355	340
10	-0.15	40	455
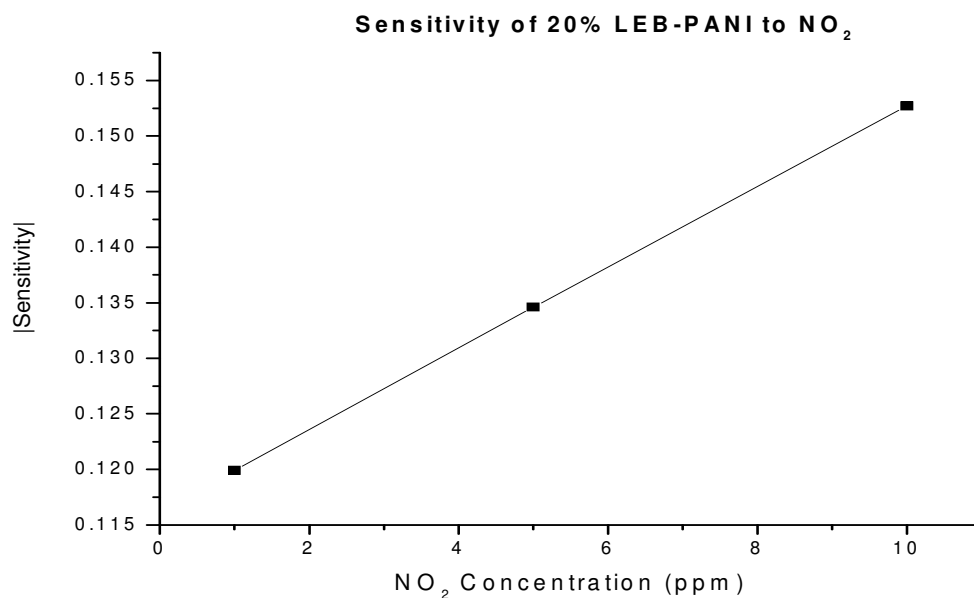
Figure 4.3.3 NO$_2$ sensitivity of 8020 PVP LEB-PANI at 40% RH

4.3.1.a.   Effects of Humidity

Figures 4.3.4 and 4.3.5 depict the response of 8020 PVP LEB-PANI to humidity and its associated sensitivity to RH, respectively. The resistance of the film decreases exponentially with increasing levels of humidity. The sensitivity of the film increases slowly to 40% and then becomes saturated. This phenomenon was also observed by Mcgovern [30] and Ogura [31] and is attributable to the water soluble PVP matrix. As the water vapor concentration increases, the PVP fibers will transform into a thin hydrated film that may affect the structural properties of LEB-PANI and inhibit or hinder reactions between LEB-PANI, NO_2, and humidity.
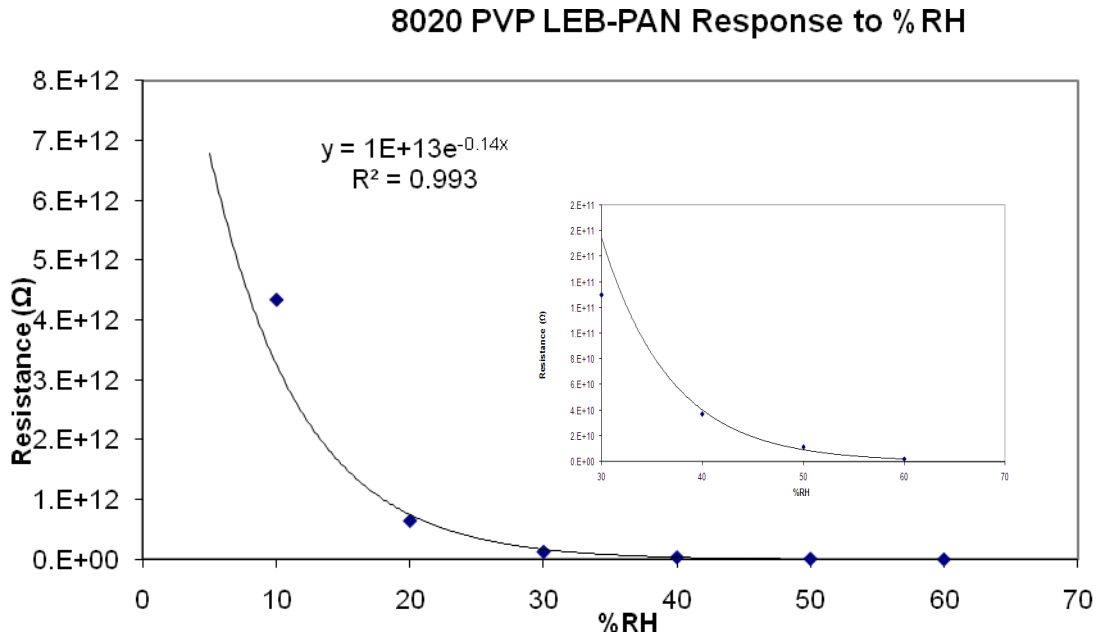
Figure 4.3.4 Response of 8020 PVP LEB-PANI to humidity
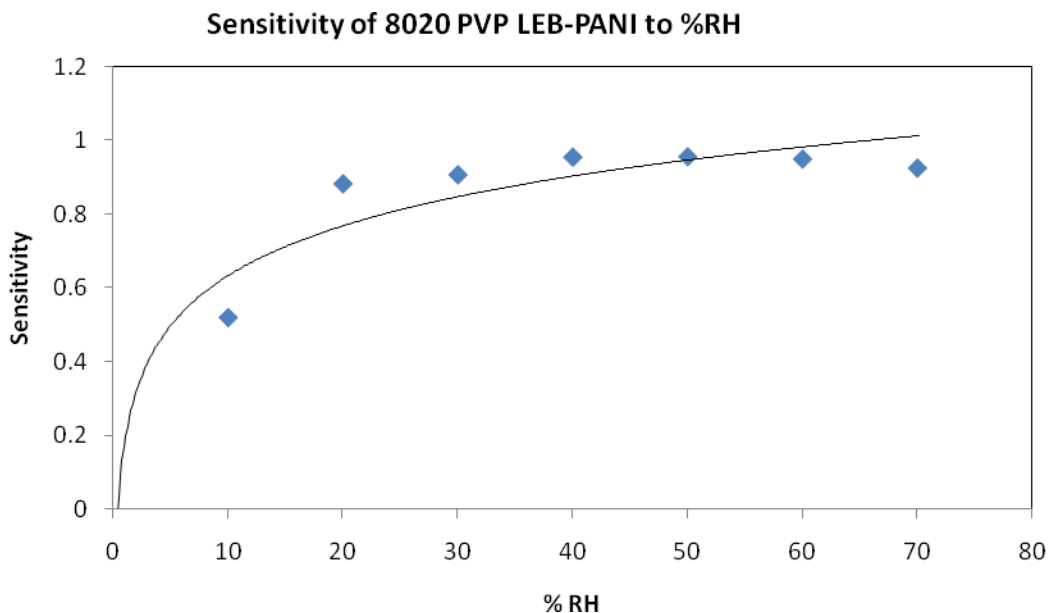
Figure 4.3.5 Sensitivity of 8020 PVP LEB-PANI to varying humidity levels

4.3.1.b. In – Situ UV-Vis Spectroscopy of 8020 PVP LEB-PANI

In-situ UV-Vis spectroscopy was employed to analyze the effects of humidity on the conformational structure of the 20% wt/wt LEB-PANI composite. Figure 4.3.6 depicts the UV-Vis spectra of the 8020 PVP LEB-PANI composite at 46% RH, 59%RH, and 68% RH, as calibrated for 20 ppm NO_2.

The peak at 350 nm for 8020 PVP LEB-PANI is shifted to 351 nm when exposed to 46% RH, 354 nm when exposed to 59% RH, and 355 nm when the humidity is increased to 68%. The peak at 577 nm for the dry film reduces to 575 nm at 46% RH. This suggests protonation of imine N resulting in decrease in absorption intensity and the blue shift. At higher levels of humidity this peak completely disappears. This suggests a

complete reduction of imine structures due to protonation by the water vapor.   It must be noted here that the 59% RH and 68% RH exposures were taken subsequently after exposure to NO_2. Thus with the increase in protonation no new peaks emerge in these two samples reflecting polaron/bipolaron formation. However shifts in both intensity and wavelength of the doublet peak at 268 nm and 282 nm are observed. As the humidity level increases these two peaks begin to converge into one peak.   With increasing humidity the peak at 282 nm goes through a hypsochromic shift till it disappears and becomes a part of the peak at 268 nm suggesting protonation of the amine centers, likely due to formation of HNO_2, H_3O^+, and NO_3^- after intermittent exposures to NO_2. Through disassociation of NO_2 into HNO_2, H_3O^+, and NO_3^-, protonic acid doping of amine sites becomes plausible.

Figures 4.3.7, 4.3.8, and 4.3.9 show the effects of NO_2 exposure on the LEB-PANI composite at 46% RH, 59% RH, and 68% RH. Figure 4.3.7 shows that on exposure to NO_2 the peaks at 282 nm and 350 nm undergo a bathochromic shift to 283 nm and 352 nm respectively due to oxidation by NO_2. With the onset of NO_2, at 46% RH, the intensity of the band at 577 nm decreases significantly. This is attributed to the liberation of OH^- from the imine N (OH groups from dissociated water can attach themselves to the imine N centers during water adsorption; this will be discussed in detail in the oncoming chapters). Figures 4.3.8 and 4.3.9 show no significant difference in the spectrum with the exception of a slight red shift of the peak from 280 nm back to 282 nm with the onset of the analyte.

According to [32] the ratio of the peak absorption intensity of the band at 350 nm (0.355) to the peak absorption intensity of the band at 577 nm (0.077) is 4.6. This suggests that the composite retains its leucoemeraldine structure.

PVP is represented by the peak at 225 nm. As the %RH increases this peak decreases in intensity suggesting that the structure is breaking down with respect to the increasing humidity levels.
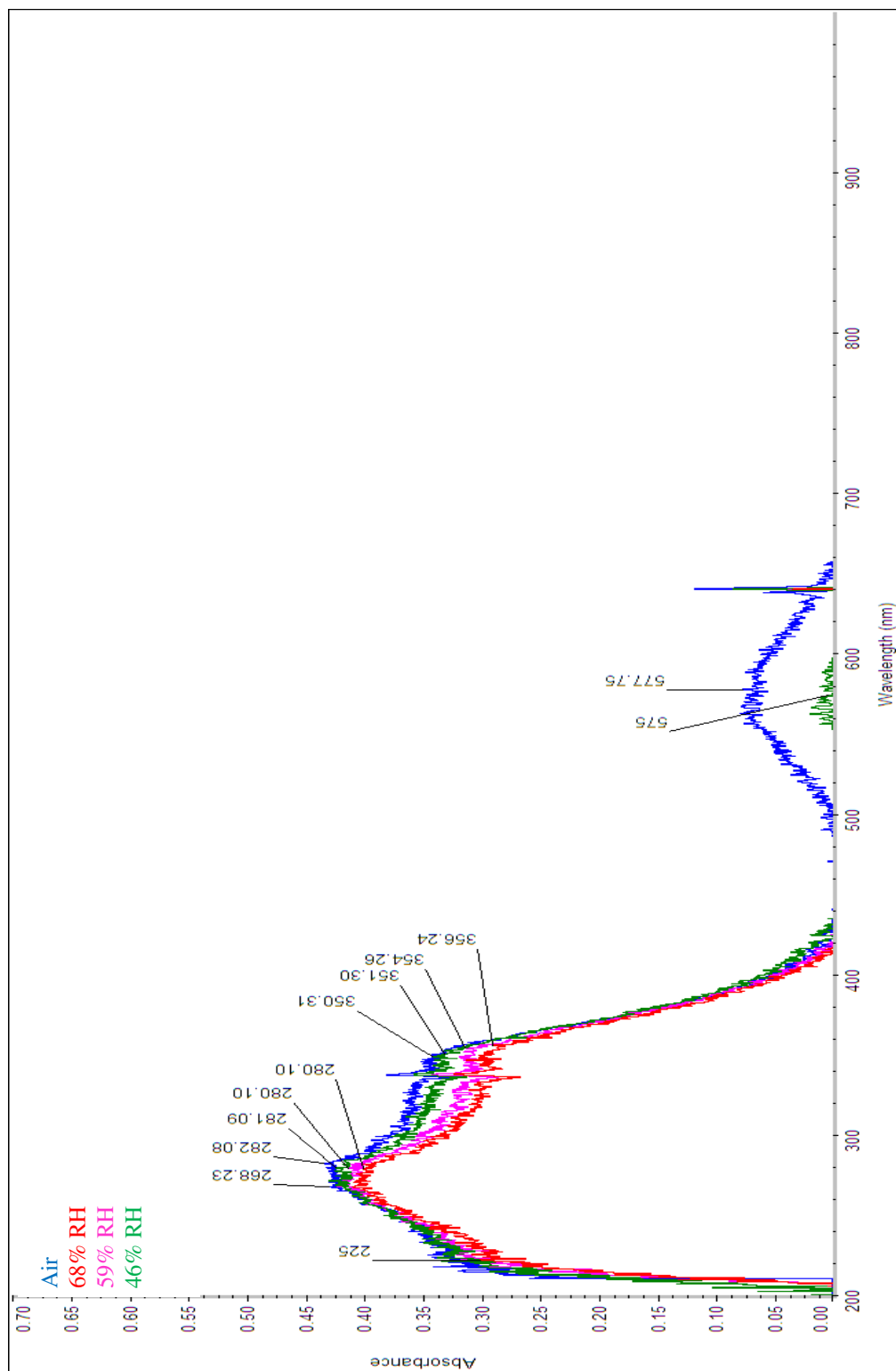
Figure 4.3.6 In-Situ UV-Vis of 8020 PVP LEB-PANI at 46% RH , 59% RH, and 68% RH
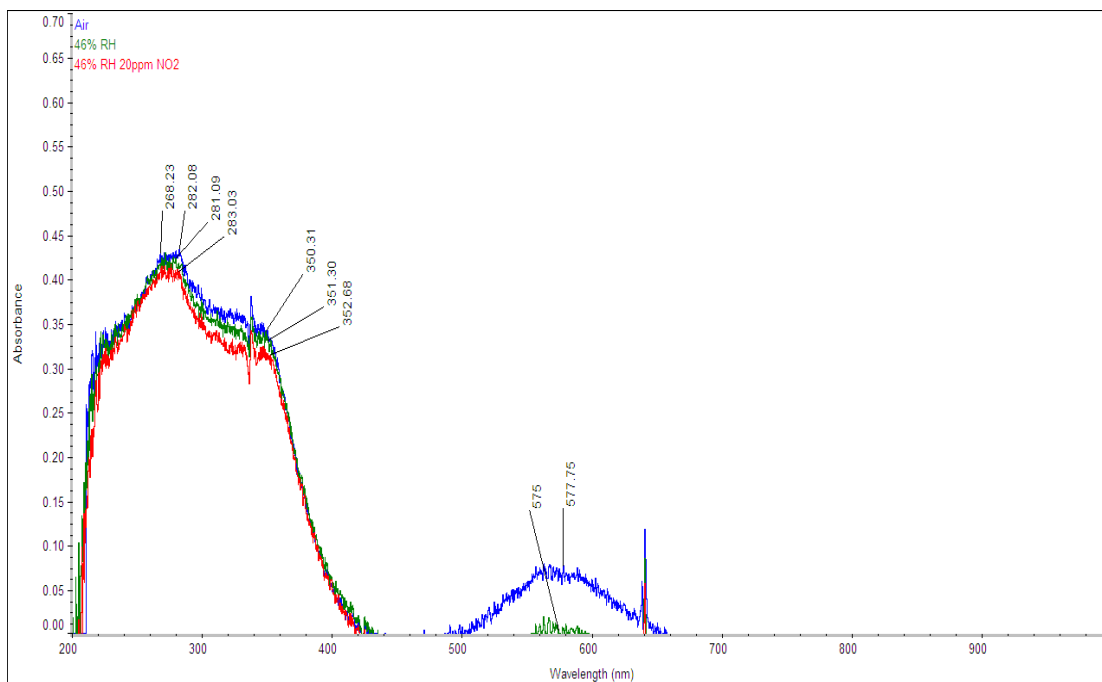
Figure 4.3.7 Effect of NO$_2$ adsorption on 8020 PVP LEB-PANI at 46% RH and 46% RH with 20 ppm NO$_2$
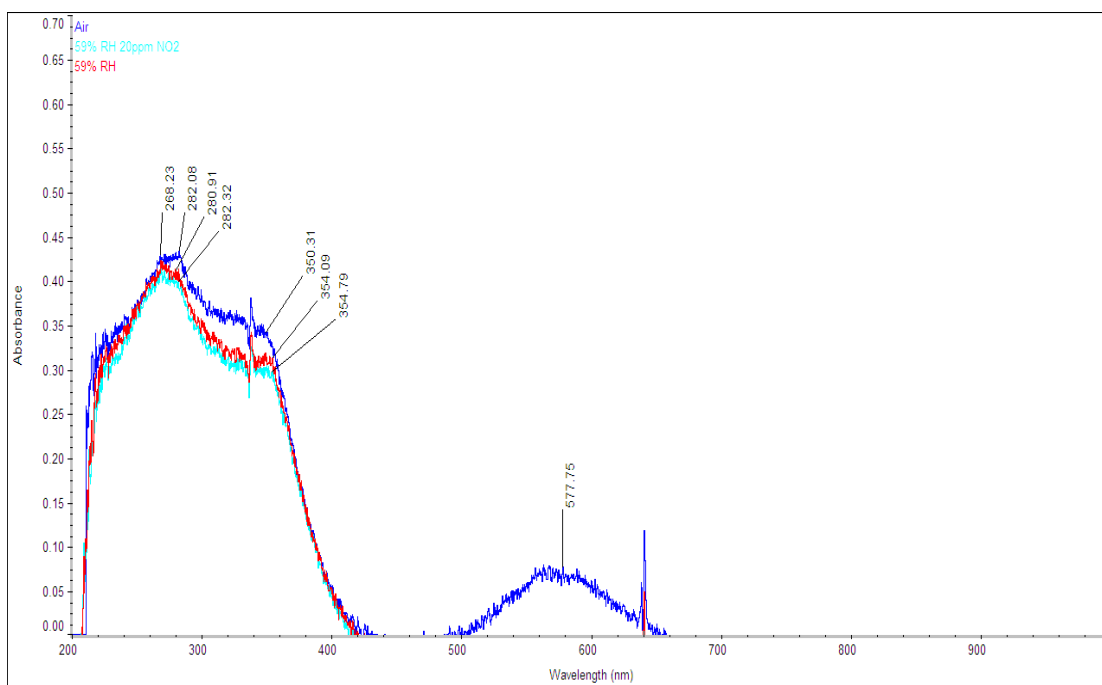
Figure 4.3.8 Effect of NO$_2$ adsorption on 8020 PVP LEB-PANI at 59% RH and 59% RH with 20 ppm NO$_2$
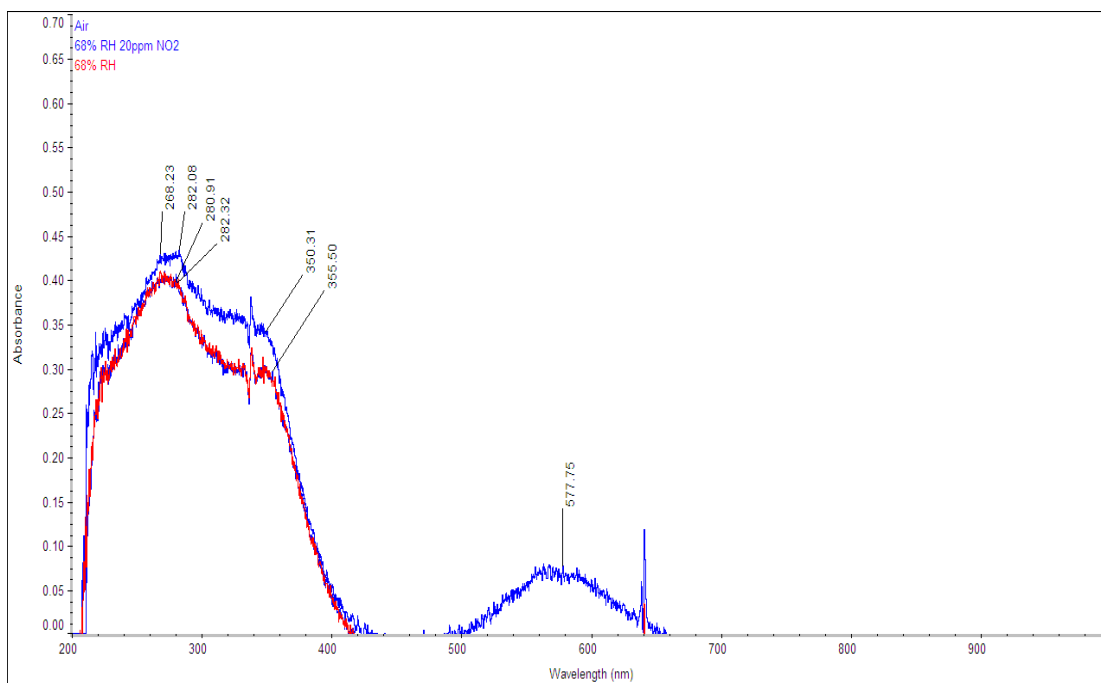
Figure 4.3.9 Effect of NO$_2$ adsorption on 8020 PVP LEB-PANI at 68% RH and 68% RH with 20 ppm NO$_2$

4.3.1.c. Stability

PVP is a hygroscopic material. As evidenced by UV-Vis it begins to degrade with increasing levels of humidity. Sensor stability testing was carried out on the same sensor to discern whether these sensors can be employed for single use of multiple use sensing applications. These studies revealed that the matrix exhibits a strong drift in the baseline and little to no response to NO$_2$. Moreover, the morphology of the structure has transformed from a fibrous mat to a thin 'gluey' film. The latter is a direct consequence of the solubility of PVP in water.

Figure 4.3.10 shows the effect of NO_2 on the 50% wt/wt LEB-PANI composite. This data reveals that the sensor exhibits no response to NO_2.
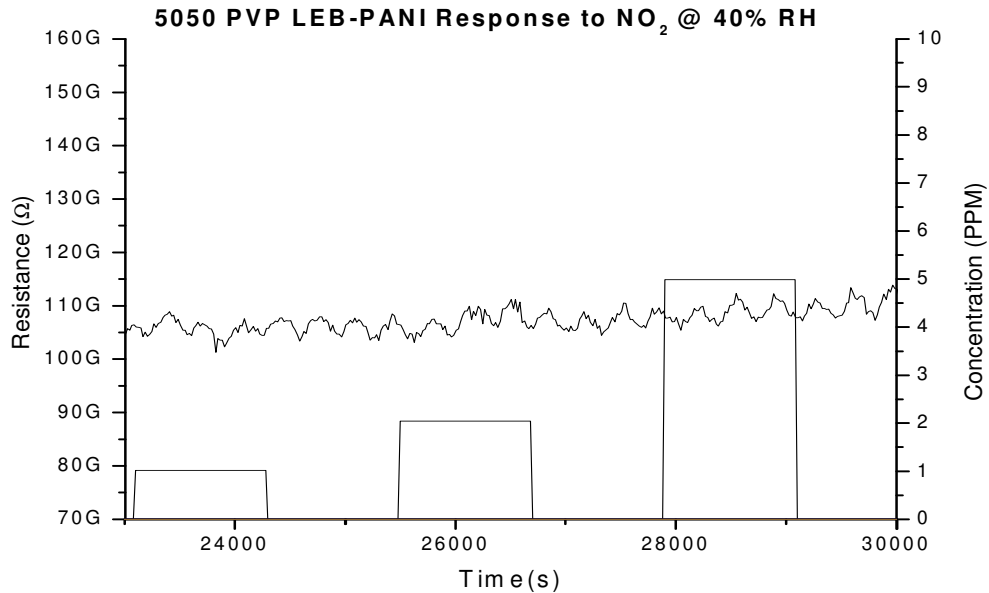
Figure 4.3.10 Sensor response of 5050 PVP LEB-PANI to NO_2

4.3.2.a. Effects of Humidity

Figure 4.3.11 shows the response of 5050 PVP LEB-PANI to humidity. Figure 4.3.12 shows the sensitivity of this sensor as a function of RH. Similar to the 8020 PVP LEB-PANI composite, the resistance of the film exponentially decreases to saturation which occurs around 40% RH. The sensitivity of the film however is observed to decrease slowly with increasing levels of humidity. This is due in part to the effect of humidity on PVP. There is less surface coverage by PVP as the concentration of LEB-

PANI in the composites increases. At high humidity the PVP fibers will converge into thin films and altering the reactivity and response of the composite to humidity.
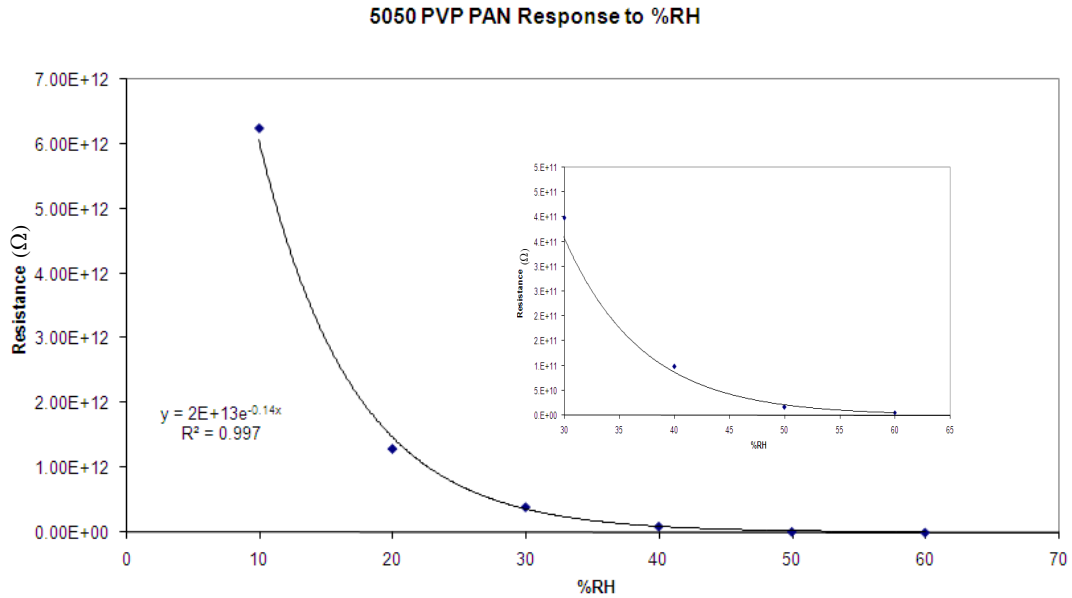
Figure 4.3.11 Response of 5050 PVP LEB-PANI to humidity
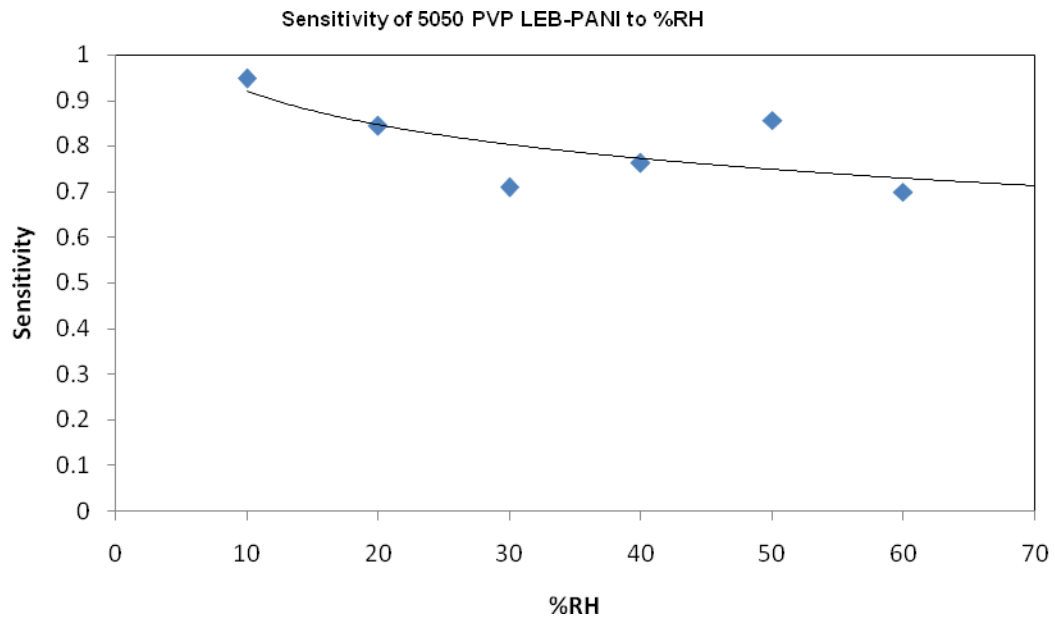
Figure 4.3.12 Sensitivity of 5050 PVP LEB-PANI to humidity

4.3.2.b. In situ UV-Vis Spectroscopy of 5050 PVP LEB-PANI

Figure 4.3.13 is UV-Vis spectrum of the 5050 LEB-PANI PVP composite during exposure to varying levels of humidity. Observed is the disappearance of the peak around 546 nm as the humidity level increases from 46% RH to 59% RH to 68% RH. This may be a direct consequence of the intermittent gas exposures (to be discussed further in chapter 6).   Also observed is an increase in the intensity of the protonated amine peak at 271 nm. The absorption intensity is proportional to concentration and governed by the size of the irradiated molecules. Increase in intensity at 649 nm and 355 nm may reflect changes in the size of individual LEB-PANI grains induced by water adsorption that may cause swelling in LEB-PANI. This adsorption may also stimulate assimilation of smaller particles into larger microstructures through H bonding between amine and imine sites, by way of disassociated water molecules.

As discussed earlier, the oxidation level can be estimated according to [32] by taking the ratio of the absorption intensity of the band at 355 nm (0.522) to the absorption intensity of the exciton band at 649 nm (0.429). The ratio yields a value of 1.21 which according to MacDiarmid's group reflects the emeraldine oxidation state.
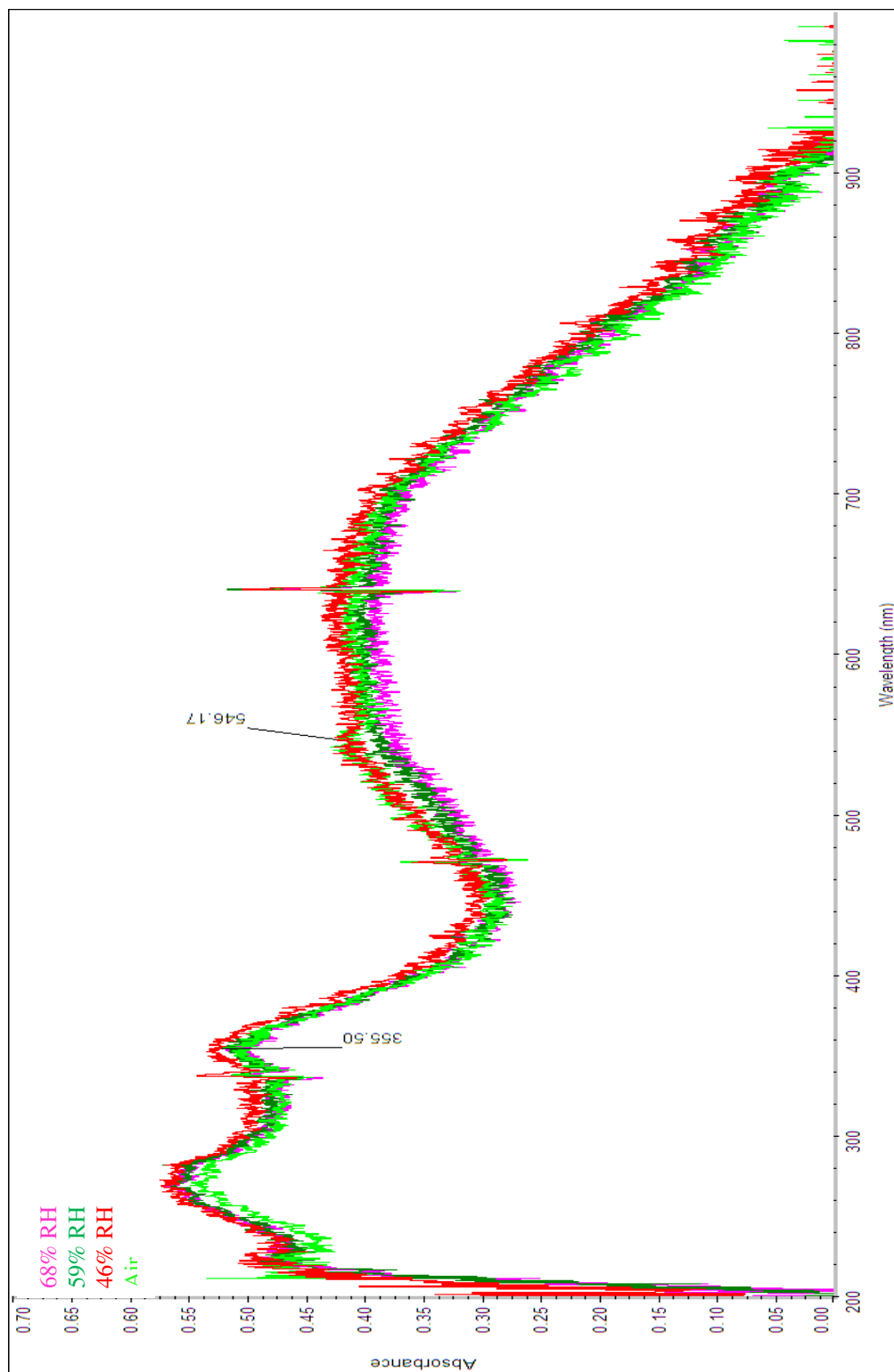
Figure 4.3.13 In-situ UV-Vis of 5050 PVP LEB-PANI at 46% RH, 59% RH and 68% RH

4.3.3. *2080 PVP LEB-PANI*

Figures 4.3.14 and 4.3.15 depict the response of the 80% wt/wt LEB-PANI composite to NO_2 at 20% RH and 40% RH. Table 4.3 lists the sensitivity, response and recovery times of the sensor.
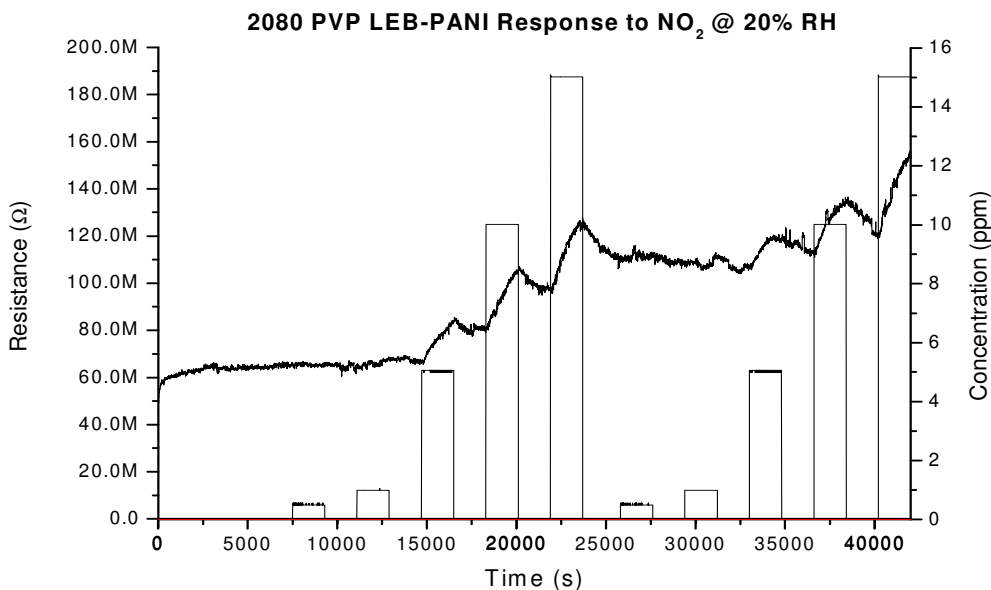
Figure 4.3.14 Response of 2080 PVP LEB-PANI to NO_2 at 20% RH

The data presented in these figures reveals that the 80% wt/wt LEB-PANI sensor exhibits an increase in DC electrical resistance on exposure to NO_2. This has been explained by [33] to be a consequence of the increased oxidation level in polyaniline. The UV-Vis data depicted in figure 4.2.2 suggests that the 2080 PVP LEB-PANI composite has been oxidized through processing to the emeraldine oxidation state (where according to MacDiarmid's relation [32], the ratio of the absorption intensity of the band at 357 nm

(0.931) to the absorption intensity of the band at 652 nm (0.777) yields 1.19 suggesting

the polyaniline in the composite film exists in the emeraldine oxidation state).
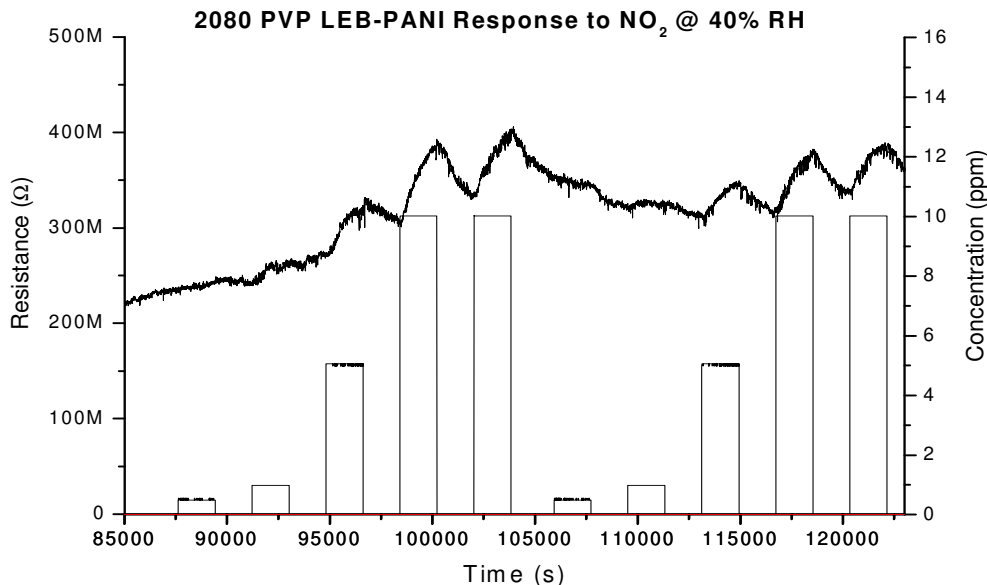
Figure 4.3.14 Response of 2080 PVP LEB-PANI to NO_2 at 40% RH

Table 4.3 Sensitivity, Response, and Recovery times of 80%wt/wt LEB-PANI at 20% RH and 40% RH - DNR= Does not recover back to baseline

Concentration (ppm)	% RH	Sensitivity	Response Time (s)	Recovery Time (s)
5	20	0.14	970	DNR
10	20	0.21	1420	DNR
15	20	0.27	1305	DNR
5	40	0.10	1315	DNR
10	40	0.19	1345	DNR

The theory behind the change in the response mechanism of these films is that on exposure to NO_2 the gas will begin to oxidize to a higher state (PB-PANI) and on continued exposure the polymer will degrade and reduce in oxidation level, imine structures will reduce to amines structure in the presence of water vapor. This can be depicted by the following reaction:

$$=N- + NO_2 \rightarrow =N^+- + NO_2^- \qquad (4.7)$$
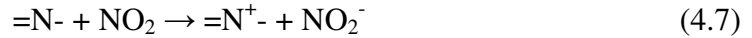
Charge resonation can transform $=N^+-$ into $-N^+-$, which when reacted with water can form

$$-N^+- + H_2O \rightarrow -NH- + OH \qquad (4.8)$$
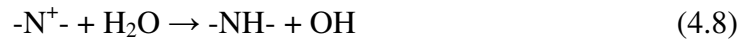
As discussed previously in section 4.3.1, NO_2 can also dissolve at high water vapor concentrations into H_3^+O, HNO_2, and NO_2^- which may also act as reducing agents for the polymer at higher oxidization levels. The results of sensing tests represented in table 4.3 suggests that the sensor's response time increases with concentration and that the sensor does not recover back to baseline, thus the recovery time could not be recorded. Moreover, the sensor only exhibits a response to NO_2 concentrations above 5 ppm at both 20% RH and 40% RH. The response mechanism of the 2080 PVP LEB-PANI sensor may be attributed the morphology of the composite.

As shown in figure 4.1.2 in the beginning of this chapter, the 2080 PVP LEB-PANI composite exhibits a high degree of aggregation. Gas molecules would then take longer to diffuse through the bulk of the LEB-PANI membrane and reactions would be hindered by blocked amine sites bound to imine N sites [23, 34]. The lack of recovery

can be explained by secondary doping effects between LEB-PANI and the acidic byproducts of NO_2 dissolution which may degrade the polymer even further. Moreover it has been shown that at higher oxidized states NO_2 adsorbed on the surface of this sensor may not desorb completely out at this oxidation level or of these self assimilated structures as explained by [35-36].

4.3.3.a. Effects of Humidity

As shown in figure 4.3.15 the films exhibit an increase in sensitivity to NO_2 at both 20% and 40% RH.
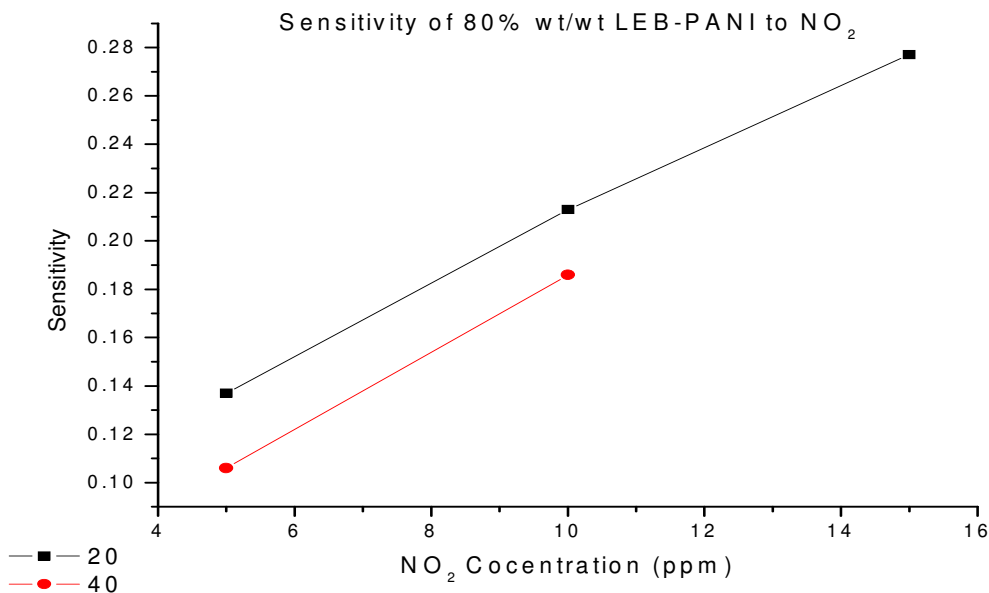
Figure 4.3.15 Sensitivity of the 2080 PVP LEB-PANI composite to NO_2 at 20% RH and 40% RH

As shown in the above figure the sensitivity of the film at 20% RH is roughly 20% higher as compared to the sensitivity of the film at 40% RH. When water adsorbs on the surface of the oxidized polyaniline powders as observed in the lower concentration composites it is likely to compete with NO_2 adsorption. At 40% RH, coupled with the blocked sites along the aggregated structure, the water molecules will adhere to available sites and may further inhibit some of the reactions between NO_2 and polyaniline. At 20% RH the polymer is less hydrated thus allowing for higher reactivity between NO_2 and available polyaniline sites.

Figures 4.3.16 and 4.3.17 show the response and sensitivity of the 80% wt/wt polyaniline composite to humidity, respectively. The resistance of the sensor follows a power law with increasing humidity. This suggests that the composite's resistance decreases by a factor of 4.87 with increasing humidity. Figure 4.3.17 shows that this is associated with a decrease in sensitivity to higher levels of humidity. This is attributed to the reformed structure of PVP (at high water vapor concentrations) coupled with the assimilated structure of polyaniline. In the next section in-situ UV-Vis spectroscopy will be employed to assess the reaction between NO_2, humidity, and the 80% wt/wt polyaniline composite.
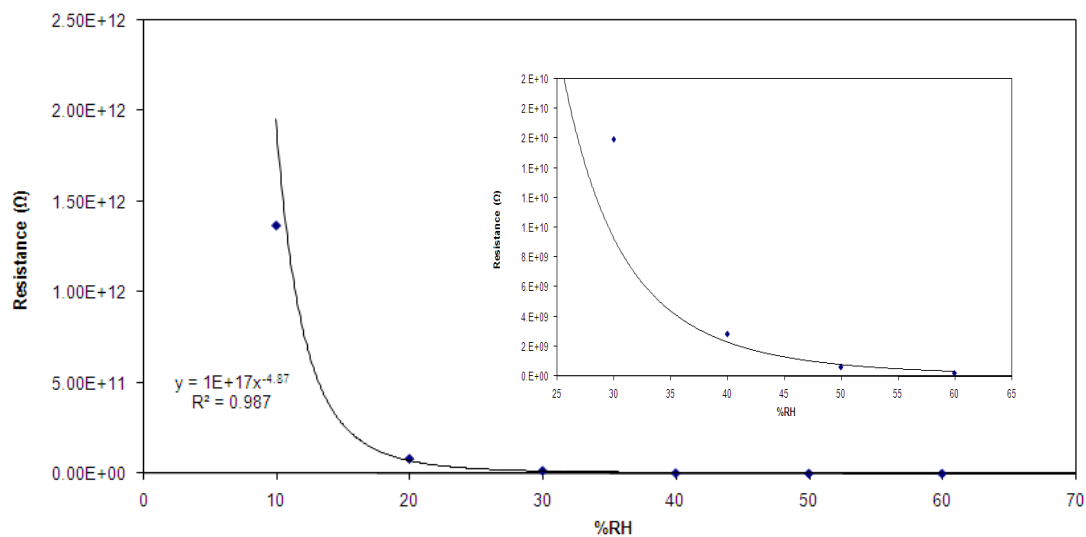
Figure 4.3.16 Response of 2080 PVP LEB-PANI to humidity
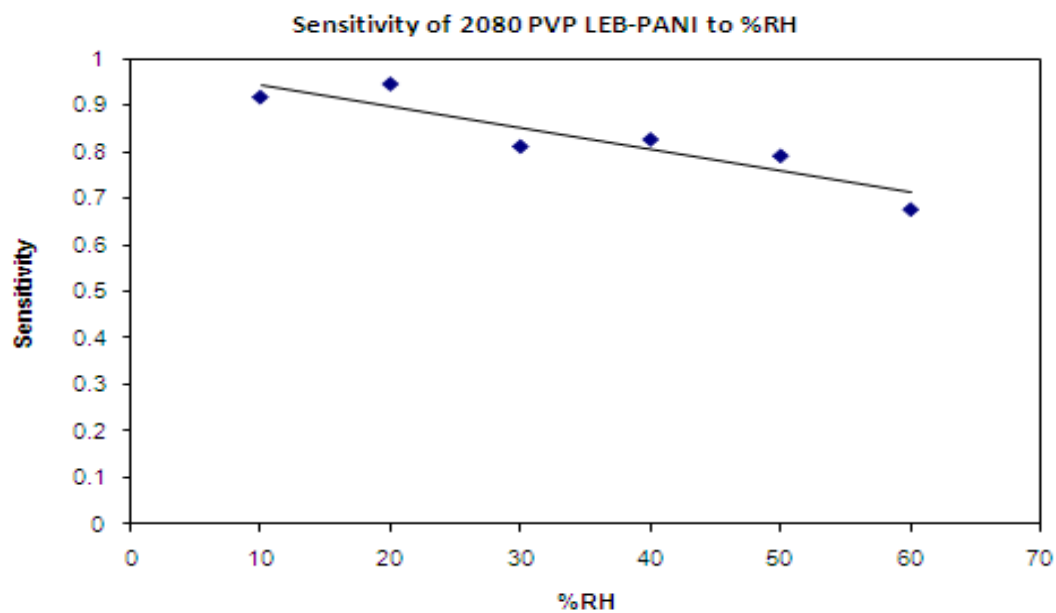
Figure 4.3.17 Sensitivity of 2080 PVP LEB-PANI to humidity

110

4.3.3.b. In-situ UV-Vis

In-situ UV-Vis was employed to assess the effects of humidity and NO_2 on the conformational structure of the 80%wt/wt polyaniline composite. Figure 4.3.18 depicts the effect of humidity on the 2080 PVP LEB-PANI composite. Similarly as with the observed effects of humidity on the 8020 PVP LEB-PANI composite, the absorption intensity decreases with exposure to humidity. The peak at 357 nm represents the $\pi\rightarrow\pi^*$ transition of the benzenoid ring. The peak at 652 nm represents exciton transitions of the quinoid ring, while the peaks at 546 nm and 514 nm represent polaron and bipolaron formations, respectively. With the increase in humidity from 46% to 59% and 68%, two new peaks emerge, one at 475 nm and one at 960 nm. The latter is attributed to localized polaron structures along the polymer chain. The former according to [37] is a sharp polaron peak associated with the salt form of polyaniline. The increase in the absorption intensity of the peak at 475 nm with the onset of NO_2 may be attributed to the reaction between dissolved NO_2 products, H_3^+O, HNO_2, and NO_2^-, and the oxidized LEB-PANI composite.

This peak is observed at the 59% RH and 68% RH exposures as a consequence of earlier reactions between NO_2 and the LEB-PANI composite prior to exposure. Associated with the increase in humidity is the disappearance of peaks at 546 nm and 514 nm. The latter is presumably blue shifted to the peak at 475 nm. This is in agreement with the optical studies of NO_2 on EB-PANI and ES-PANI by [32].

The peak ~225 nm, representative of PVP, disappears with increasing levels of humidity and gas adsorption. This suggests the degradation or transformation of PVP at

in this composition is more pronounced as compared to the other two composites PVP LEB-PANI composites.

Figures 4.3.19, 4.3.20, and 4.3.21 are UV-Vis spectrums which reflect the effects of NO_2 absorption on the 2080 PVP LEB-PANI composite at 46% RH, 59% RH, and 68% RH, respectively.
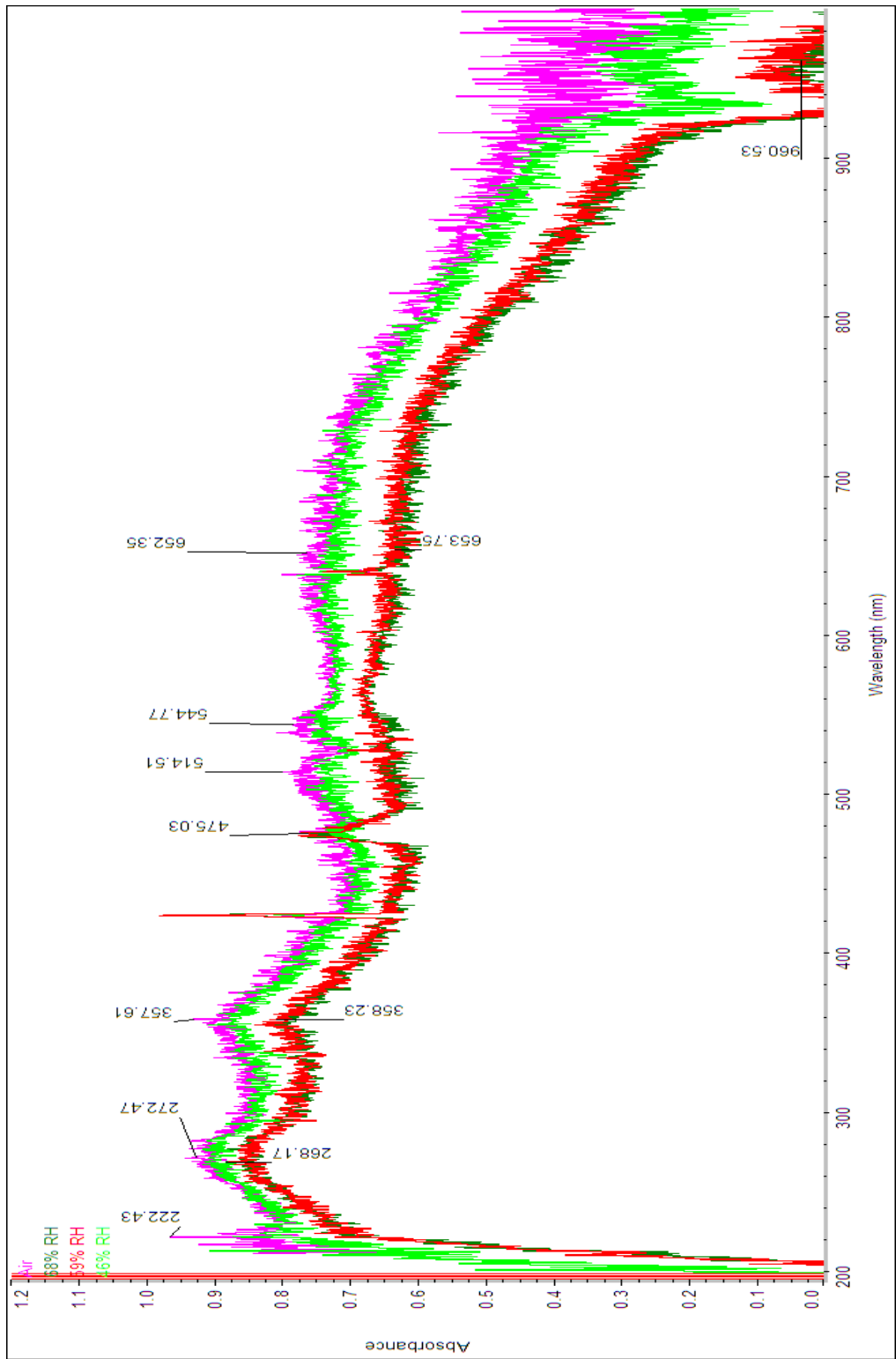
Figure 4.3.18 In-situ UV-Vis of 2080 PVP LEB-PANI at 46% RH, 59% RH and 68% RH
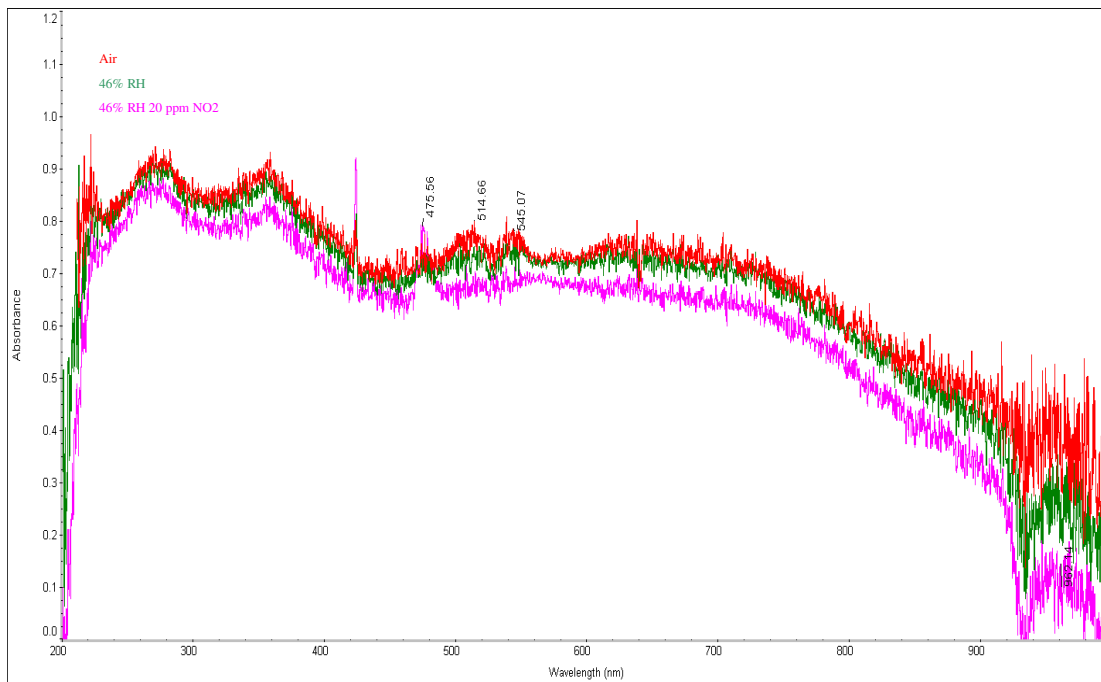
Fig 4.3.19 In-situ UV-Vis spectrum of 2080 PVP LEB-PANI at 46% RH and 46% RH
with 20 ppm NO$_2$

As mentioned earlier the emergence of a peak at 475 nm after exposure to NO$_2$ at

46% RH and the disappearance of the polaron/bipolaron peaks at 514 nm and 544 nm

were observed. The latter can be attributed to the reactions between NO$_2$ and the

bipolaron and polaron. When NO$_2$ reacts with a bipolaron, it is likely to react with its

anion (in this case OH$^-$ from H$_2$O doping or O$^-$ from PVP). An electron is transferred to

the gas which brings about internal redox processes such that electroneutrality can be

obtained at that site. This might lead to the reduction of the protonated imine structure

back to its neutral imine state upon liberation of a proton (the protonated imine is not as

energetically stable as the –N$^+$H- of the polaron [38]). As the gas reacts with the polaron

the reaction is similar, but now due to loss of the OH$^-$ or O$^-$ anion, the band is blue shifted

to a lower wavelength (loss of a hopping site for π electron means more energy is needed

114

to excite it to $\pi*$ [39]). The sharp polaron peak may also be attributed to a combination of NO_2 oxidation at the polaron sites, and reactions between the dissolved NO_2 acidic byproducts and the polymer, transforming the material into a light salt.

Figures 4.3.20 and 4.3.21 show the effects of NO_2 adsorption on the 2080 PVP LEB-PANI composite at 59% and 68% RH, respectively. Observed are no significant differences between the spectrums before and after exposure to NO_2. This suggests that adsorption of NO_2 does not affect the structure at these high levels of humidity. What can be observed however is the emergence of a weak broad peak at 562 nm. This is likely representative of the reduction of the bipolaronic structure to a neutral quinoid unit.
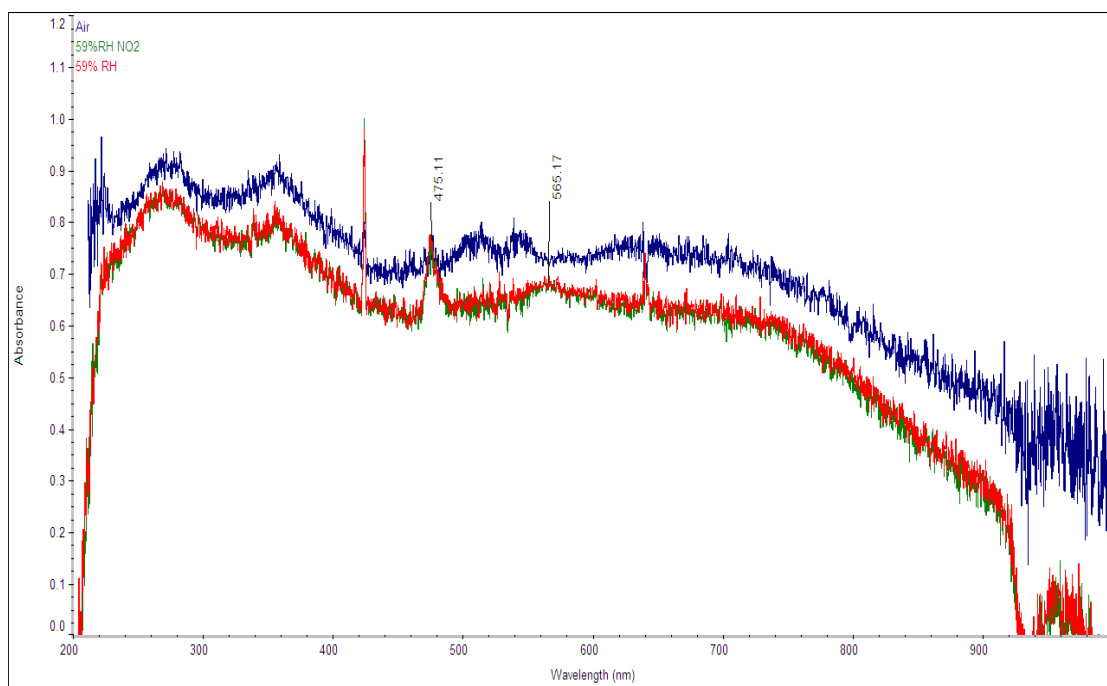
Figure 4.3.20 In-situ UV-Vis spectrum of 2080 PVP LEB-PANI at 59% RH and 59% RH with 20 ppm NO_2
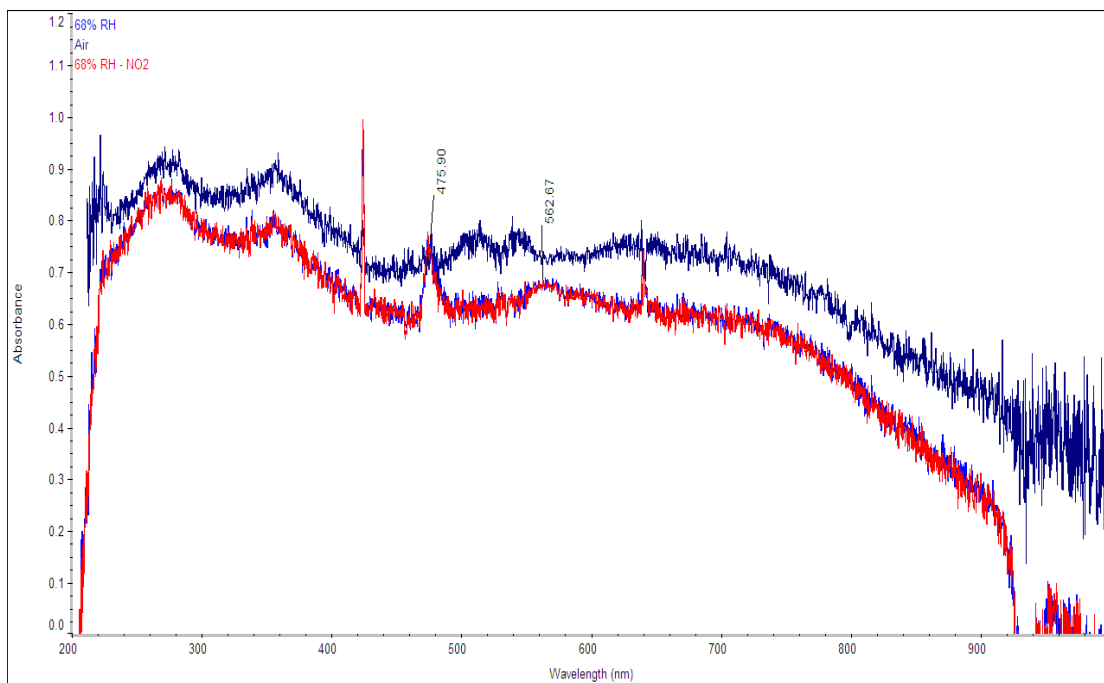
Figure 4.3.21 In-situ UV-Vis spectrum of 2080 PVP LEB-PANI at 68% RH and 68% RH with 20 ppm NO_2

4.3.3.c. Stability

Chemical analyses and sensor tests reveal that with increasing humidity and exposure to NO_2 the polymer becomes poisoned and degrades. The former is evidenced by the non-recovery of the film back to its baseline after exposure to NO_2. UV-Vis spectra of the films after NO_2 exposure and humidity conditioning provide proof of the latter - the formation of a polaronic band suggests that structure of LEB-PANI has been altered by the gas.

Table 4.4 summarizes the response mechanism of the three PVP LEB-PANI composites. These studies suggest that the 8020 PVP LEB-PANI is the best sensing device for NO_2 detection. As stated at the beginning of this dissertation, the aim of this work was to determine the applicability of **LEB-PANI** for selective NO_2 gas detection. It has been shown that the only composite that retains any resemblance of the reduced structure is the 8020 PVP LEB-PANI composite. In the next section XPS analyses of the film will be provided to detail the structure of this film to corroborate with the above information. Analysis of the response mechanism of the 8020 PVP LEB-PANI sensor to several interferents, as outlined in chapter 2, will also be discussed to discern the hybrid's selectivity.

Table 4.4 Sensing response of PVP LEB-PANI Composites

	8020 PVP LEB-PANI	**5050 PVP LEB-PANI**	**2080 PVP LEB-PANI**
Detection Limit	1 ppm	No response	5 ppm
Response Time	40 s for 10 ppm @ 40% RH	No response	1345 s for 10 ppm@ 40% RH
Recovery Time	200 s for 1 ppm	No response	Does not recovery

4.3.4. *XPS of LEB-PANI PVP for NO$_2$ Sensing*

The N1S, C1s, and O1s XPS spectra of the 20%wt/wt LEB-PANI composite were analyzed to identify the effects of processing as compared to the as received LEB-PANI powders. Figures 4.3.22, 4.3.23, and 4.3.24 depict the N1s, C1s and O1s spectrums, respectively, for the 8020 PVP LEB-PANI composite. Table 4.5 outlines the data from XPS analysis.

The data presented in table 4.5 reveals an increased level of water adsorption, O, and OH bonding through processing LEB-PANI with PVP and ethanol. This is evidenced by the O1s peak at 532.9 eV. Although LEB-PANI is vulnerable to oxygen containing species, these peaks were not distinguishable in the pure LEB-PANI XPS data. The effect of oxygen on the composite however is more distinct (this is likely due to the O of PVP and OH of ethanol binding to LEB-PANI). Also observed is a decrease in the amount of protonated N and an increase in the concentration of imine N. The latter may be a consequence bonds formed between LEB-PANI, PVP, and ethanol. Both act as oxidants for the polymer (this is supported by the LEB-PANI in ethanol UV-Vis data in chapter 3) and may stimulate transformations between amines and imines. Moreover, the protonated N species associated with imine Ns which were present in the as received powders (table 3.1) are likely to have been converted to neutral imines via internal redox processes that liberate H$^+$ as discussed earlier. This is also supported by the absence of the peak at 287 eV (C=N$^+$H, C-N$^+$H$_2$) in the C1s spectra.

Table 4.5 XPS analysis of 8020 PVP LEB-PANI Composite

Spectrum	Peak	B.E. (eV)	Compound	Rel. Area
N1s	A	399.7	—NH—	79.0%
	B	398.5	=N-	19.5%
	C	400.6	N+	1.6%
C1s	A	285.1	C=N, C-N, CH, C-C, C=C, possibly associated protonated species	50.9%
	B	286.4	C-O, C=O	37.5%
	C	284.3	CH, C-C, C=C	10.6%
	D	289.2	C=O	1.5%
O1s	A	531.5	C-O, CH-OH, C=O	76.9%
	B	532.9	OH, H_2O	23%
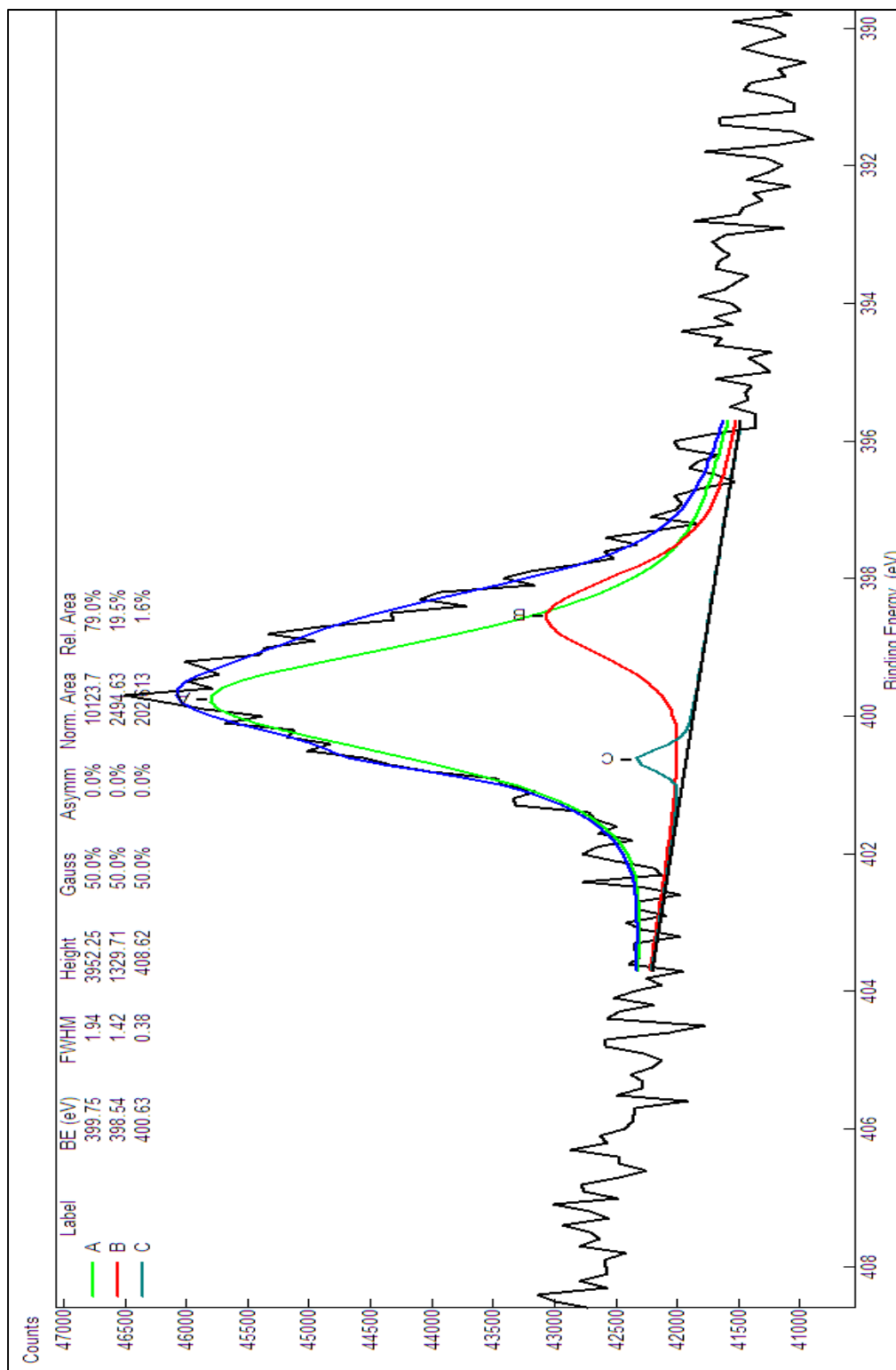
Figure 4.3.22 N1s core energy XPS spectra for 8020 PVP LEB-PANI

Label	BE (eV)	FWHM	Height	Gauss	Asymm	Norm. Area	Rel. Area
A	285.11	1.81	8450.66	100.0%	0.0%	16247.2	50.4%
B	286.46	4.16	2730.61	100.0%	0.0%	12087.1	37.5%
C	284.32	1.35	2383.09	100.0%	0.0%	3420.37	10.6%
D	289.20	1.70	261.687	100.0%	0.0%	472.31	1.5%
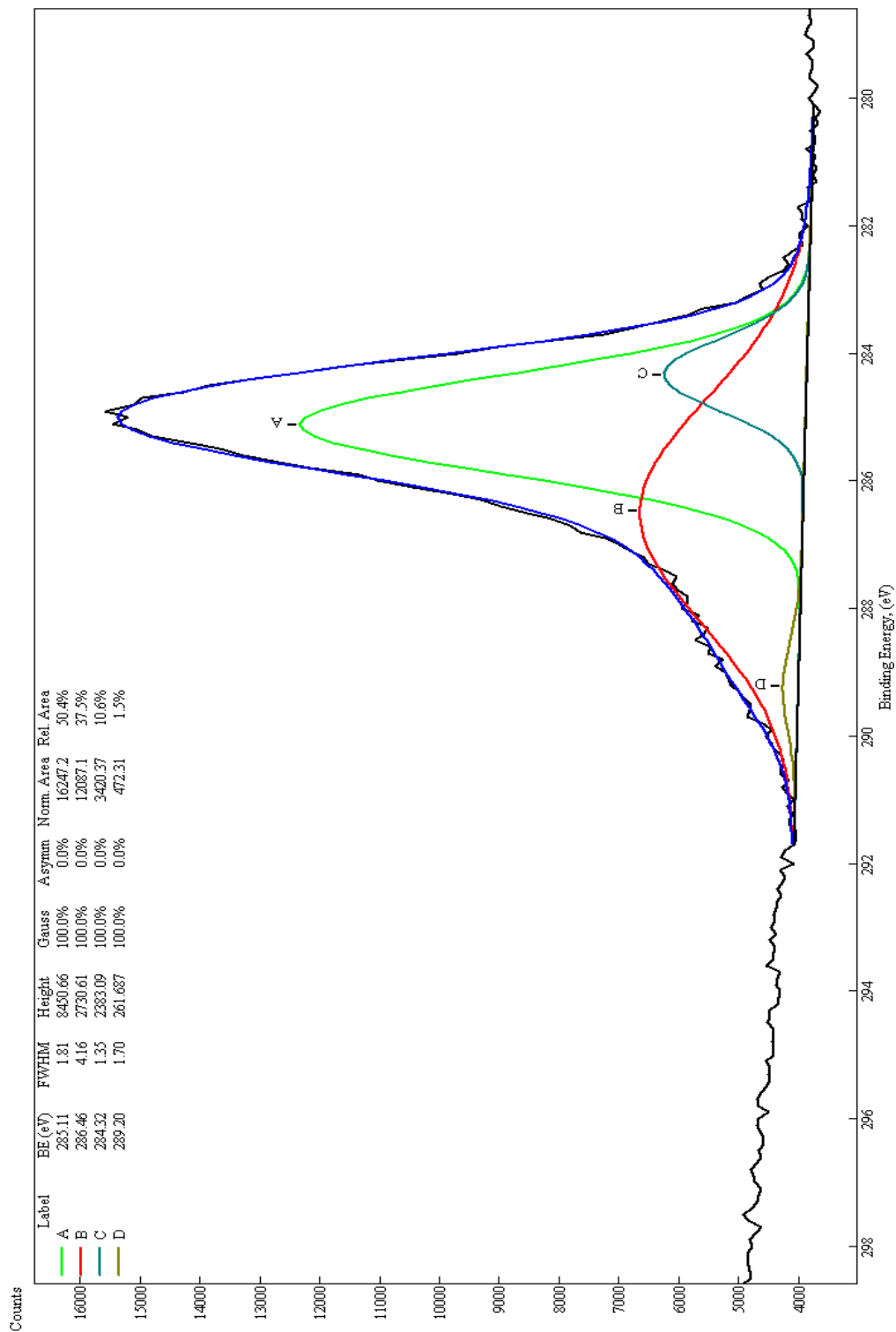
Figure 4.3.23 C1s core energy XPS spectra for 8020 PVP LEB-PANI

Label	BE (eV)	FWHM	Height	Gauss	Asymm	Norm. Area	Rel. Area
A	531.52	2.07	10361.8	50.0%	0.0%	28261.8	76.9%
B	532.97	1.88	3439	50.0%	0.0%	8496.25	23.1%
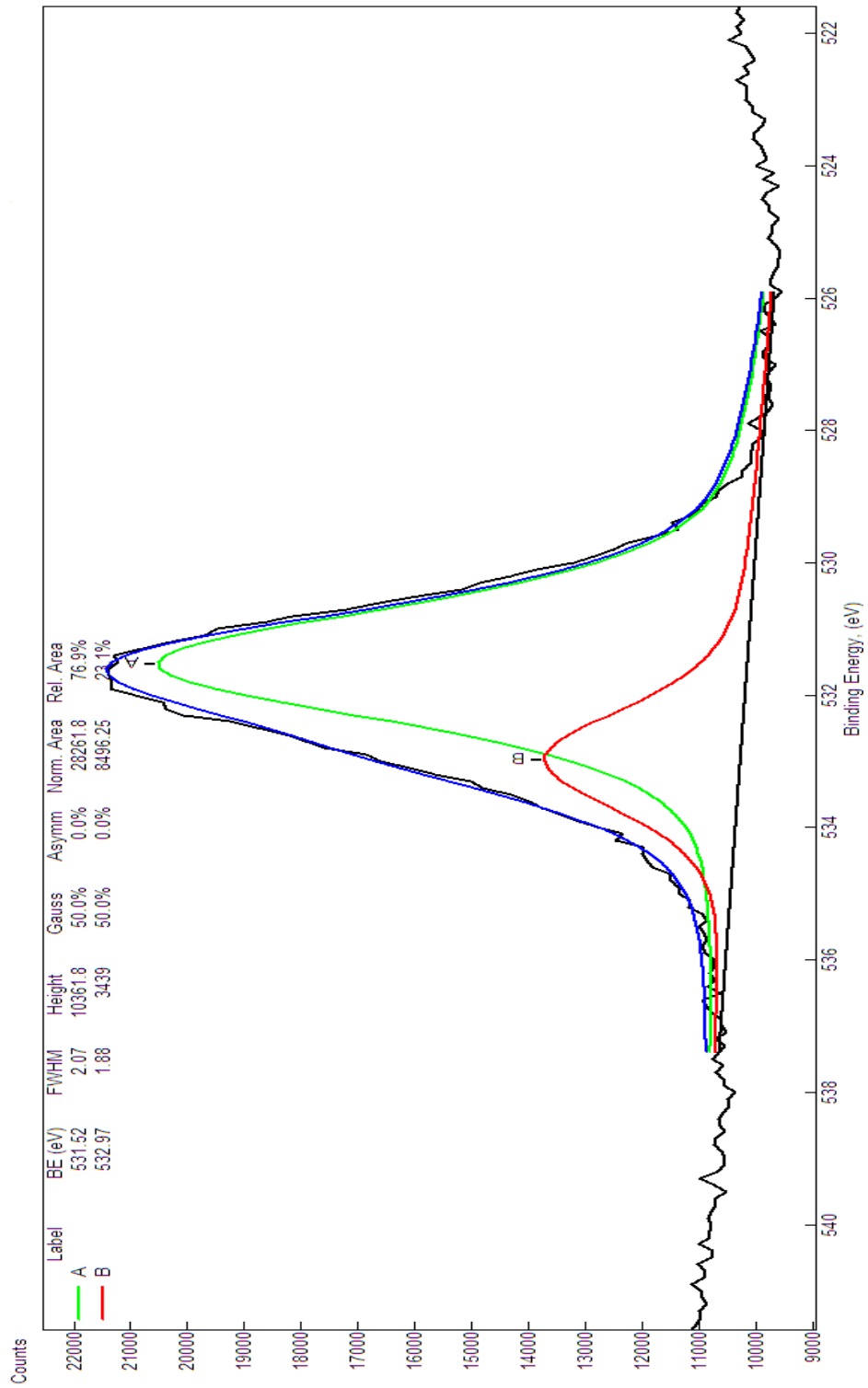
Figure 4.3.24 O1s core energy XPS spectra for 8020 PVP LEB-PANI

4.3.5. *Selectivity Studies of 8020 PVP LEB-PANI*

The following figures depict the response of the 20% wt/wt LEB-PANI composite to varying gas atmospheres. As observed the material exhibits little to no response to the gases in figures 4.3.25 to 4.3.30. Figure 4.3.30 shows that the material increases in resistance with NH_3 but doesn't recover. This mechanism is associated with deprotonation of the LEB-PANI matrix, forming NH_4^+. Table 4.6 summarizes the response mechanism of the 8020 PVP LEB-PANI composite to each of these gases.
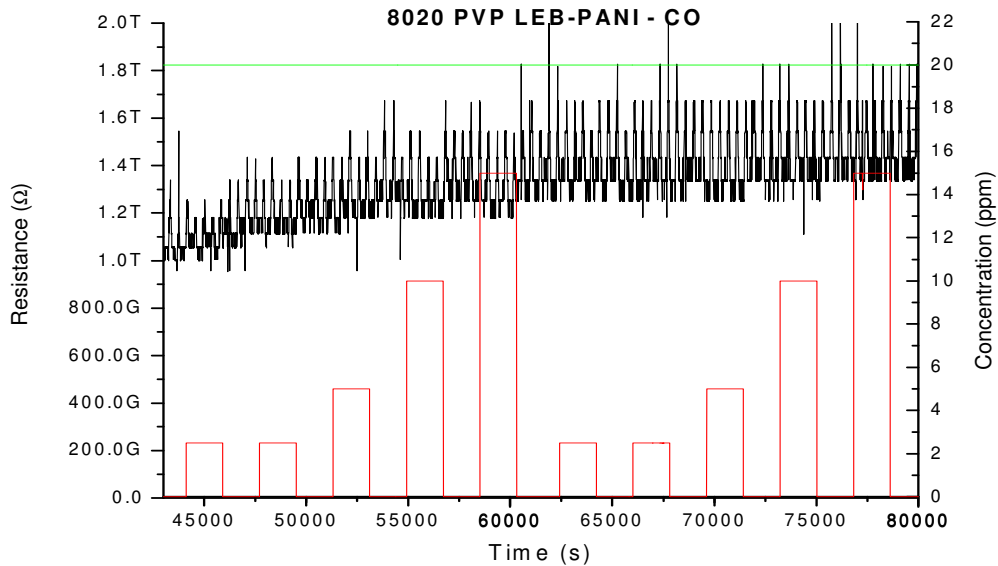
Figure 4.3.25 Response of 8020 PVP LEB-PANI to CO
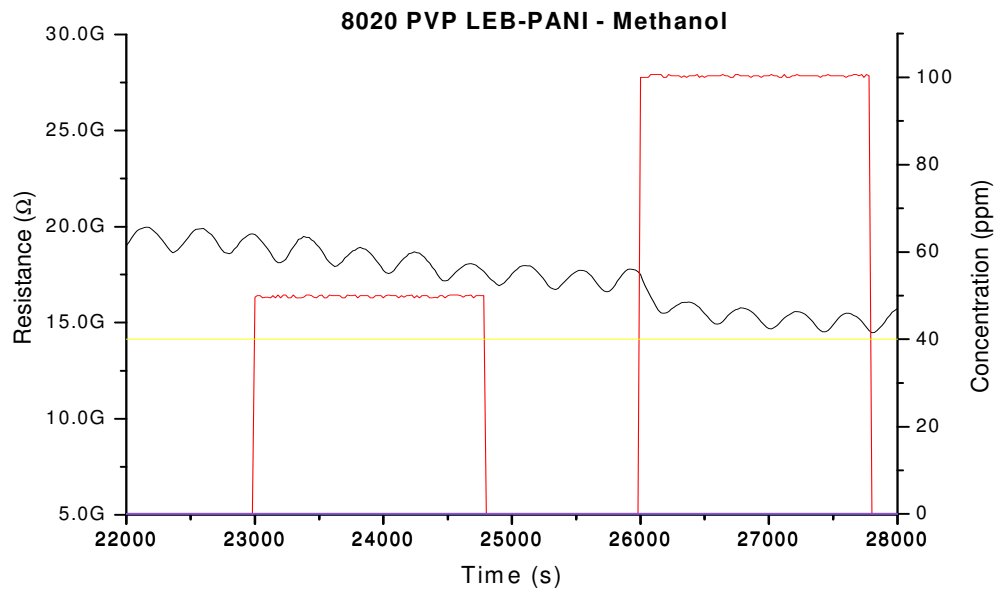
Figure 4.3.26 Response of 8020 PVP LEB-PANI to Methanol
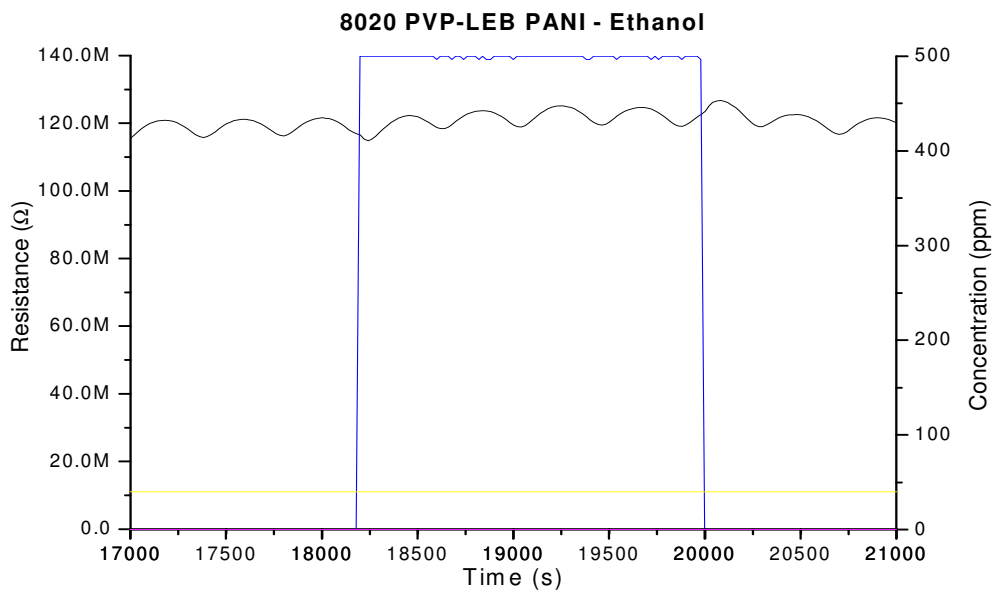
Figure 4.3.27 Response of 8020 PVP LEB-PANI to Ethanol
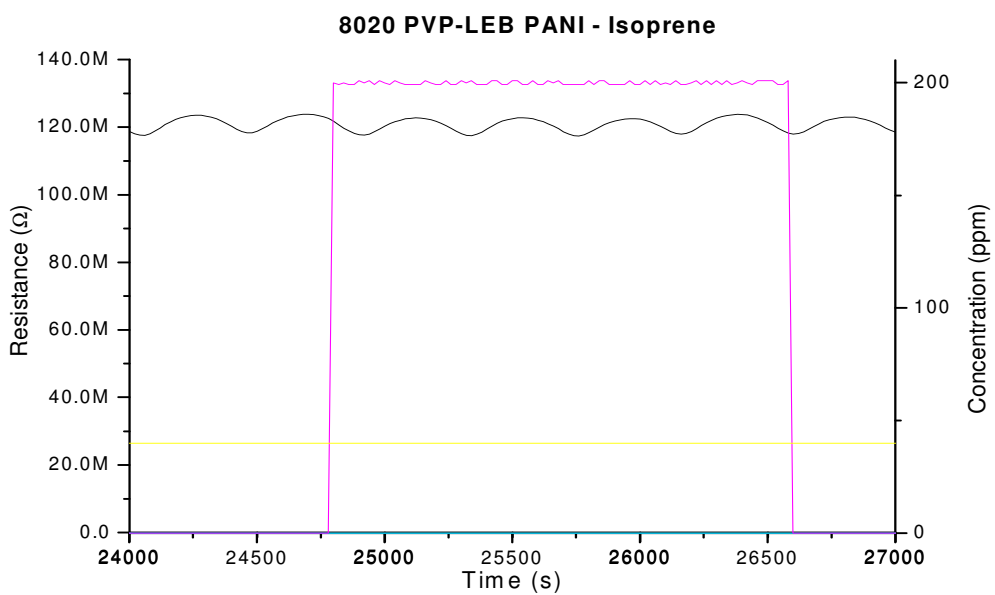
Figure 4.3.28 Response of 8020 PVP LEB-PANI to Isoprene
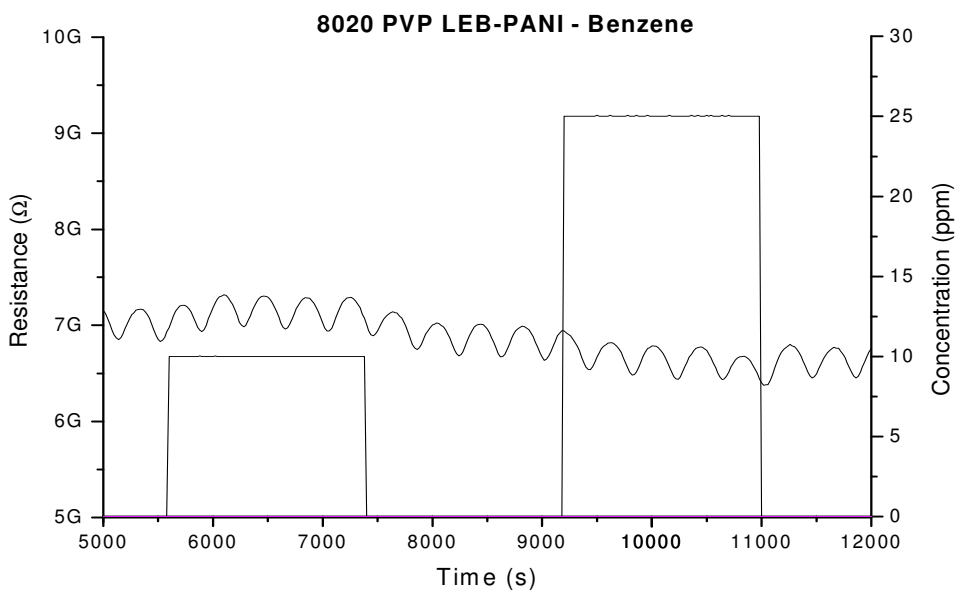
Figure 4.3.29 Response of 8020 PVP LEB-PANI to Benzene

125
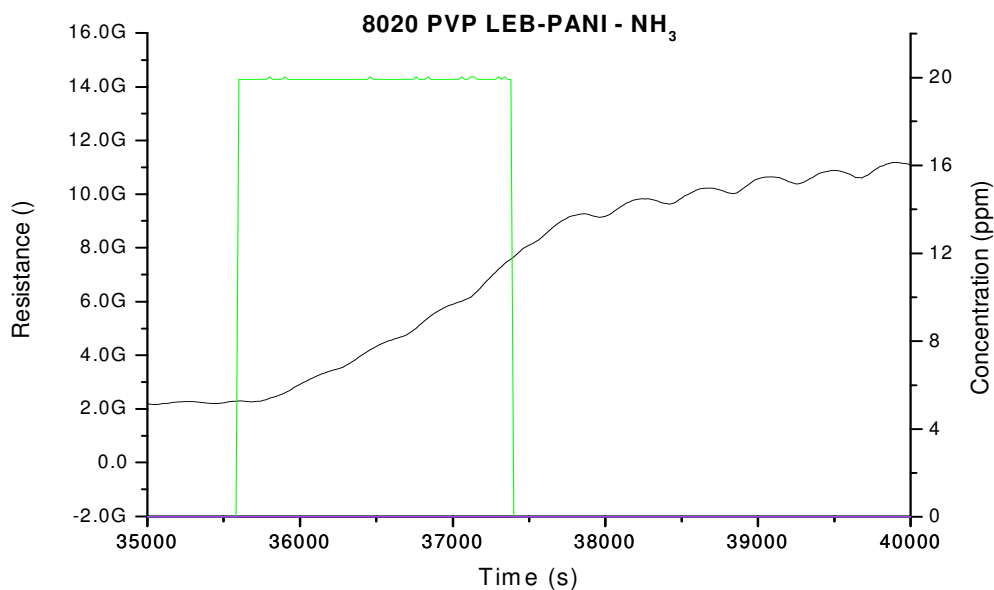
Figure 4.3.30 Response of 8020 PVP LEB-PANI to NH$_3$

Much of the effect of humidity on the sensitivity of LEB-PANI to NO$_2$ is due in part to the base polymer employed. Because PVP is a water soluble polymer, while it successfully facilitates the exchange of charge between LEB-PANI and water vapor and NO$_2$, the disadvantage is that the morphology of the composite breaks down with elevated humidity. In the next chapter the use of a less hydrophilic base polymer for high humidity applications and selective NO$_2$ detection will be explored

126

Table 4.6 Selectivity of 8020 PVP LEB-PANI

Gas	Response	Reason
Benzene	None	Analyte reflects structure of LEB-PANI
Methanol	None	Material treated in alcohol, thus will have no response to analyte
Ethanol	None	Material treated in alcohol, thus will have no response to analyte
Isoprene	None	Reducing agents will have limited effects on amine sites of LEB-PANI
CO	None	Reducing agents will have limited effects on amine sites of LEB-PANI
NH_3	Slight increase in R at 20 ppm, no recovery	Compensation effect with protonated imine structures; Reducing agents will have limited effects on amine sites of LEB-PANI

REFERENCES

1. S. Fitzpatrick, J.F. McCable, C.R. Petts, and S.W. Booth, "Effect of moisture on polyvinylpyrrolidone in accelerated stability testing", *International J. of Pharmaceutics*, vol. 246, no 1-2, pp 143-151, 2002

2. F. Kiekens, R. Zelko, and J.P. Remon, "Effect of the storage conditions on the tensile strength of tablets in relation to the enthalpy relaxation of the binder", *Pharmaceutical Research*, vol. 17, 490 – 493, 2000

3. P. Molyneux, and H.P. Frank, "Interaction of polyvinylpyrrolidone with aromatic compounds in aqueous solution. 1. Thermodynamics of binding equilibria and interaction forces", *J. American Chemical Society*, vol 83, no15, pp 3169-3174, 1961;

4. M.C. Lonergan , E.J. Severin, B.J. Doleman , S.A. Beaber, R.H. Grubb, and N.S. Lewis, "Array based vapor sensing using chemically sensitive carbon black polymer resistors", *Chemistry of Materials*, vol 8, no 9, pp 2298-2312, 1996

5. R. Kessick and G. Tepper, "Electrospun polymer composite fiber arrays for the detection and identification of volatile organic compounds", *Sensors and Actuators B – Chemical*, vol 117, pp 205-21, 2006,

6. Y. Li, S. Zhang, Y. Li, and C. Sun, "Amperometric Nitrite Sensor Based on PVP-Os Entrapped in Titania Sol-Gel Matrix", *Electroanalysis*, vol 16, no 19 pp 1637-1641, 2004

7. A.A.A. de Queiroz, S.A.W. Soares, P. Ttrzesniak, and G.A. Abraham, "Resistive-type humidity sensors based on PVP-Co and PVP-I$_2$ complexes", *Polymer Science Part B: Polymer Physics*, vol. 39, no 4, pp 459-469, 2001

8. A. Liu and J. Anzaai , "Use of Polymeric Indicator for Electrochemical DNA Sensors: Poly(4-vinylpyridine) Derivative Bearing [Os(5,6-dimethyl-1,10-phenanthroline)2 Cl]2$^+$", *Analytical Chemistry*, vol. 76, no.1, pp 2975-2980, 2004

9. H. Zeng, U. Jiang, G. Xie, and J. Yu, "Novel Piezoelectric DDVP Sensor Based on Self-Assembly Method", *Analytical Letters*, vol. 40, no.1, pp 67-76, 2007

10. T.N. Ermolaeva, TL. Lavrent, AE Seredkin, and TJ Korenman, "A Sensitive Piezoelectric Crystal Sensor for Analyzing Phenols in Air", *Russian J. Applied Chemistry*, vol 74, no 2, pp 199-204, 2001

11. A. Zhao, Z. Huang, C. Wang, Q. Zhao, H. Sun, and D. Wang, "Preparation of PVP/MEH-PPV composite polymer fibers by electrospinning and study of their photoelectronic character", *Materials Letters*, vol 61, no 11-12, pp 2159-2163, 2007

12. D. Li, A. Babel, S.A. Jenekhe, and Y. Xia, "Nanofibers of Conjugated Polymers Prepared by Electrospinning with a Two-Capillary Spinneret", *Advanced Materials*, vol 16, no 2, pp 2062-2066, 2004

13. Q. Yang, Z. Li, Y. Hong, Y. Zhao, S. Qiu, C. Wang, and Y. Wei, "Influence of solvents on the formation of ultrathin uniform poly(vinyl pyrrolidone) nanofibers

with electrospinning", *Journal of Polymer Science Part B: Polymer Physics*, vol 42, no. 20, pp 3721-3726, 2004

14. J. Stejskal, P. Kratochvil, and M. Helmstedt, "Polyaniline dispersions .5. Poly(vinyl alcohol) and poly(N-vinylpyrrolidone) as steric stabilizers", *Langmuir*, vol. 12, pp. 3389-3392, 1996

15. S. Armes, "Handbook of Conducting Polymers", ed. T. Skotheim, R. Elsenbaumer, and J. Reynolds, Marcel Dekker Inc., pp. 423-436, 1998

16. P. Somani, "Synthesis and characterization of polyaniline dispersion", *Materials Chemistry and Physics*, vol 77, no 1, pp 81-85, 2003

17. R. Murugesan, G. Anitha, and E. Subramanian, "Multi-faceted role of blended poly(vinyl pyrrolidone) leading to remarkable improvement in characteristics of polyaniline emeraldine salt", *Materials Chemistry and Physics.*, vol 85, no 1, pp184-194, 2004

18. P. Ghosh, S.K. Siddhanta , and A. Chakrabarti, "Characterization of poly(vinyl pyrrolidone) modified polyaniline prepared in stable aqueous medium", *European Polymer Journal*, vol 35, no 4, pp 699-710, 1999

19. N.V. Blinova, I. Sapurina, J. Klimovic, and J. Stejskal, "The chemical and colloidal stability of polyaniline dispersions" , *Polymer Degradation and Stability*, vol 88, no 3, pp. 428-434, 2005

20. K. Ogura, A. Fujii, H. Shiigi, M. Nakayama, and T. Tonosaki, "Effect of hygroscopicity of insulating unit of polymer composites on their response to relative humidity", *J. Electrochemical Society*, vol. 147, no. 3, pp. 1105-1109, 2000

21. Conversations with Mr. Mark Flezar on FTIR, Benet Laboratories, U.S. Army Research, Development, and Engineering Command, Watervliet Arsenal, Watervliet, NY

22. L. Tarachiwin, P. Kiattibutr, L. Ruang Chuay, A. Sirivat, and T Schwank, "Electrically conductive response of polyaniline films to ethanol water mixtures", *Synthetic Metals*, vol 129, pp 303-308, 2002

23. W. Zheng, M. Angelopoulous, A.J. Epstein, and A.G. MacDiarmid, "Experimental evidence for Hydrogen bonding in polyaniline: mechanism for aggregate formation and dependency on oxidation state", *Macromolecules*, vol 30, pp. 2953-2955, 1997

24. R. Kostic, D. Rakovic, I.E. Davidova, and LA Gribov, "Vibrational spectroscopy of the leucoemeraldine form of polyaniline: theoretical study", *Physical Review B*, vol. 45, no 2, pp 728-733, 1992

25. S. Quillard, S. Louarn, S. Lefrant, and A.G. MacDiarmid, "Vibrational analysis of polyaniline- A comparativity study of leucoemerladine, emeraldine, and pernigraniline bases", *Physical review B*, vol 50, no.17, pp. 12496-12508, 1994

26. D. Yang, P.N. Adams, L. Brown, and BR Mattes, "Impact of H bonds in polyaniline AMPSA/acid solutions", *Synthetic metals*, vol 156, no 18-20, pp 1225-1235, 2006

27. J.P. Joshi, N.S. Saxena, T.P. Sharma, V. Dixit, and S.C.K Misra, "Band gap determination of doped polyaniline materials from reflection measurements", *Indian J. of Pure and Applied Physics*, vol. 41, no. 6, pp. 462-465, 2003

28. S. Saravanan, M.R. Anantharaman, S. Venkatachalam, and D.K Avasthi, "Studies on the optical band gap and cluster size of the polyaniline this films irradiated with swift heavy Si ions", *Vacuum*, vol 82, no. 1, pp. 56-60, 2008

29. J. Tauc, *Amorphous and Liquid Semiconductors*, Plenum Press, London, 1974

30. S.T. Mcgovern, G.M. Spinks, and G.G. Wallace, "Micro-humidity sensors based on a processible polyaniline blend", *Sensors and Actuators B-Chemical,* vol 107, no.2, pp. 657-665, 2005

31. K. Ogura, T. Saino, M. Nakayama, and H. Shiigi, "The humidity dependence of the electrical conductivity of a soluble polyaniline-poly(vinyl alcohol) composite film", *J. Materials Chemistry,* vol 7, no. 12, p. 2363, 1997

32. J.E. Albuquerque, L.H.C. Mattoso, D.T. Balogh, R.M. Faria, J.G. Masters, and A.G. MacDiarmid, "A simple method to estimate the oxidation state of polyanilines", *Synthetic Metals*, vol 113, no 1-2, pp 19-22, 2000

33. J. Elizalde-Torres, H Hu, and A. Garcıa-Valenzuela, "NO$_2$-induced optical absorbance changes in semiconductor polyaniline thin films", *Sensors and Actuators B – Chemical*, vol 98, pp 218-224, 2004

34. M. Angelopoulous, R. Dipietro, W. Zheng, A.G. MacDiarmid, and A.J. Epstein, "Effect of selected processing parameters on solution properties and morphology of polyaniline and impact on conductivity", *Synthetic. Metals*, vol 84, no 1-3, pp. 35-39, 1997

35. X.B. Yan, Z.J. Han, Y. Yang, and B.K. Tang, "NO$_2$ gas sensing with polyaniline nanofibers synthesized by a facile aqueous organic interfacial polymerization", *Sensors and Actuators B*, vol.123, pp. 107-113, 2007

36. M.K. Ram, O. Yavuz, and M. Aldissi, "NO$_2$ gas sensing based on ordered ultrathin films", *Synthetic Metals*, vol. 151, pp. 77-84, 2005

37. A. Pron, M. Zagorska, Y. Nicolau, F. Genoud, and M. Nechtschein , "Highly conducting composites of polyaniline with plasticized cellulose acetate", *Synthetics Metals*, vol 84, no 1-3, pp 89-90, 1997

38. J.L. Bredas and G. B. Street, "Polarons, Bipolarons, and Solitons in conduction polymers", *Accounts of Chemical Research*, vol 18, pp 309-315, 1985

39. C.N. R. Rao, Ultraviolet and Visible Spectroscopy, 3rd Ed. Butterworth and Co. Ltd, 1975

CHAPTER 5

5. Leucoemeraldine Base Polyaniline and Cellulose Acetate Composites

Cellulose acetate (CA) has been employed widely for filtration and reverse osmosis based applications [1-3]. Researchers have also employed the natural polymer as a support matrix for dissimilar materials (i.e. conducting polymers, ceramics, metal nanoparticles, etc.,). CA is traditionally produced by reacting the polysaccharide cellulose, $C_6H_{10}O_5$, with acetic anhydride $(CH_3CO)_2O$., which when hydrolyzed yields acetic acid. The transport properties of CA have been studied for applications ranging from wastewater treatment [4], chromatography [5], and biotechnology [6]. For conducting materials (i.e. ICPs, carbon nanotubes, metal oxides), it has shown to provide adequate pathways for charge transport within the composite matrix, yielding it to be a suitable base matrix for sensing and applications.

According to literature, cellulose acetate can be employed as a hole transport layer for polyaniline [8-15]. The advantage of CA is that it hydrophobic and more structurally stable against high levels of humidity unlike PVP. The water susceptibility of the polymer is dependent on the degree of substitution of acetyl groups (40% for CA employed in these studies). Thus, because CA is not soluble in water it is expected that hybrids of CA and LEB-PANI should retain their morphological character even after repeated exposures to humidity.

Using the electrospinning technique 8020 CA LEB-PANI composites were produced. Unlike the PVP base polymer, CA is inherently very viscous when dissolved

in acetone. The concentration of CA employed has been shown by [16-17] to be optimum for biosensing and tissue engineering applications. Higher concentrations of LEB-PANI would yield solutions that could not be electrospun. The following experiments reflect solely the chemical and structural analysis and sensor properties of 8020 CA LEB-PANI.

5.1. STRUCTURAL CHARACTERIZATION

5.1.1. *SEM*

SEM of the 8020 CA LEB-PANI composites, figure 5.1.1, reveals that there is a complete dissolution of the large agglomerated structures in figure 5.1.1a.
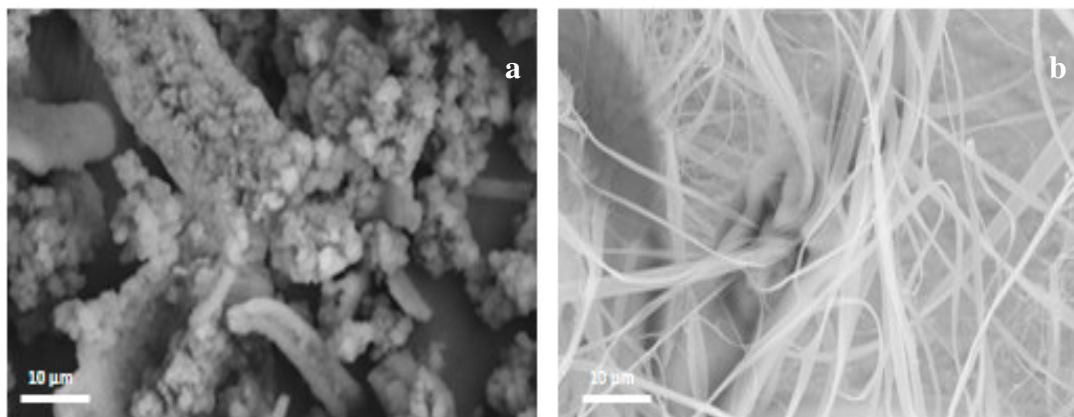
Figure 5.1.1 SEM of (a) as received LEB-PANI powders and (b) electrospun 8020 CA LEB-PANI composite

5.2. CHEMICAL EVALUATION OF 8020 CA LEB-PANI COMPOSITE

5.2.1. *FTIR*

Photo acoustic FTIR was employed to assess the molecular structure of the CA-LEB PANI composite. Figure 5.2.1 depicts the FTIR spectrum of the 8020 CA LEB-PANI composite. According to literature the characteristic peaks of CA are 3500 cm^{-1}, 2944 cm^{-1}, 2889 cm^{-1}, 1744 cm^{-1}, 1374 cm^{-1}, 1220 cm^{-1}, 1044 cm^{-1}, 906 cm^{-1}, and 602 cm^{-1} [8, 18-19]. In comparison, the characteristic peaks [20-21], of the 8020 CA LEB-PANI emulates the effects of oxidation of LEB-PANI and possibly doping by CA. In comparing the peaks of the 8020 PVP LEB-PANI (figure 4.2.1) composite with that of the 8020 CA-LEB-PANI composite, figure 5.2.1, it can be observed that the peak at 1555 cm^{-1} is sharper and medium strong, the peak at 1495 cm^{-1} is extremely weakened for the CA LEB-PANI mixture, the peak at 1163 cm^{-1} becomes medium weak as compared to the PVP alternative, and the peak at 849 cm^{-1} appears weaker for the 8020 CA LEB-PANI composite. The change in intensity of these peaks is expected with the increase in oxidation level of LEB-PANI. Thus the data presented suggests that CA can act as an oxidant for LEB-PANI. Another observation is the intensity of the characteristic bands around 1600 cm^{-1}, which represent the presence of the quinoid structures in polyaniline. Unlike the PVP composites, the CA composite exhibits strong vibrations around 1700 cm^{-1}. This may also represent the formation of quinoid-like structures in the composite. The weakening of the intensity of the bands around 1600 cm^{-1} may be due in part to the chemical nature of CA and its effects on LEB-PANI.

Several bands around 1500 cm^{-1} suggest the formation of bipolaronic structures. These peaks represent protonated imine species with oxygen anions. This suggests that acetate groups of CA may have disassociated and become bound to N sites along the LEB-PANI chain inducing the formation of these localized charge carriers. Table 5.1 (appendix E) details the vibration bands associated with the CA LEB-PANI composite.
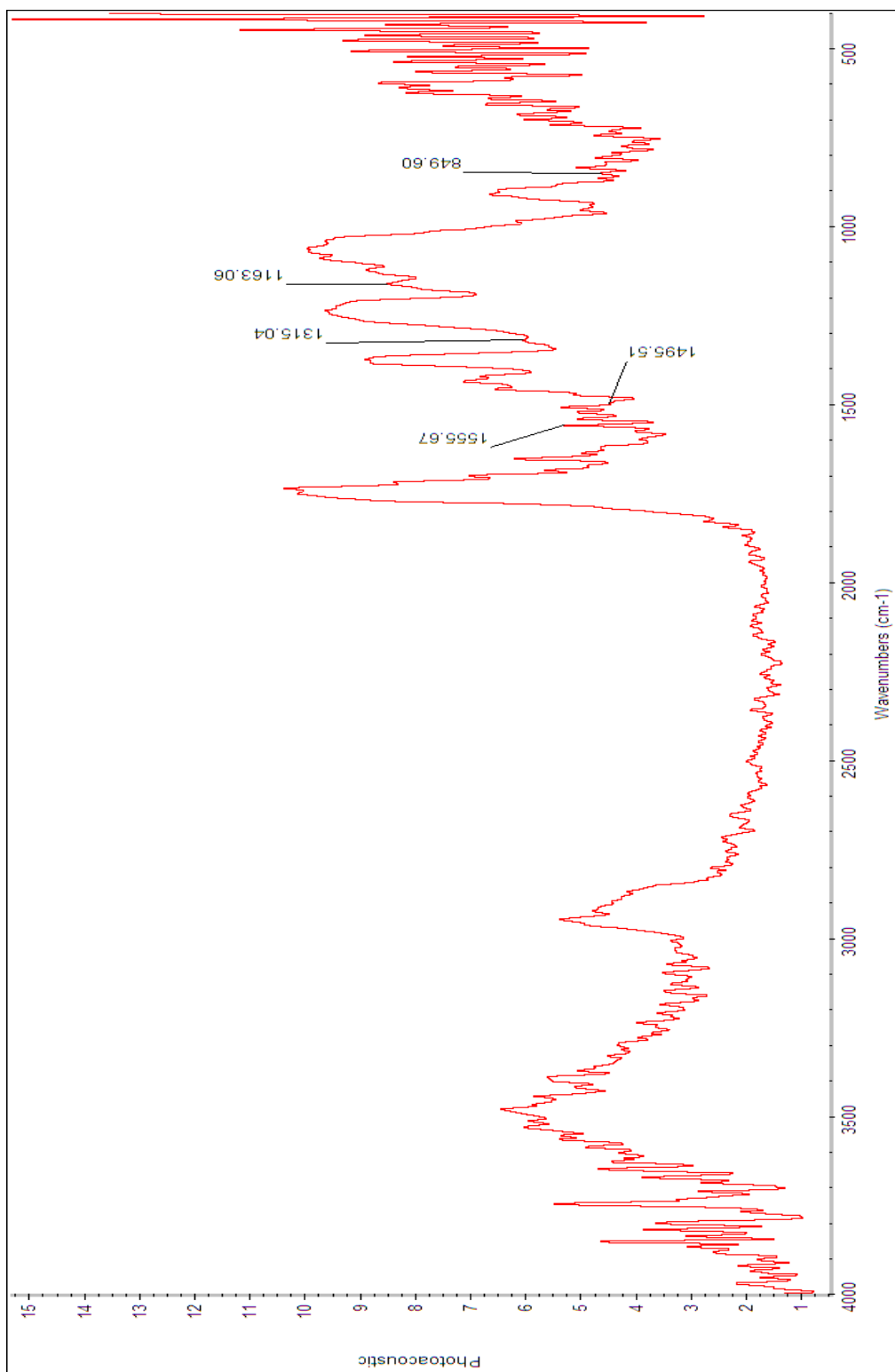
Figure 5.2.1 Photo acoustic FTIR Spectrum for 8020 CA LEB-PANI

5.2.2. UV-Vis Spectroscopy of 8020 CA LEB-PANI Composite

UV-Vis spectroscopy was employed to analyze the conformational structure of the CA LEB-PANI composite. Pron et. al [22] revealed from UV-Vis analysis of polyaniline blended with cellulose acetate the emergence of a sharp polaronic peak at 444 nm associated with a broad carrier tail around 800 nm. This is in agreement with the data represented in figure 5.2.2. The slight bathochromic shift in wavelength is attributed to the processing conditions of the CA LEB-PANI composite prepared for this study.

Several characteristic bands emerge from the polymer composite: 225 nm, 268 nm, 281 nm, 355 nm, 472 nm, 543 nm, and 651 nm. The peak at 225 nm reflects the high energy absorption band for cellulose acetate (like PVP, CA is transparent and does not absorb at any other wavelength). The peaks at 281 nm and 355 nm reflect the $\pi \rightarrow \pi^*$ transition for the benzenoid structure. The distinction between the two peaks was discussed in chapters 3 and 4. The peak at 268 nm is attributed to protonated amine structures. The band at 472 nm is a sharp polaronic peak reflecting the salt form of polyaniline. And the small absorption band at 543 nm is representative of bipolaron transitions along the polymer chain. This analysis is in agreement with the FTIR data presented in the previous section. The broad peak between 600 nm and 900 nm reflects delocalized polarons which may be associated with the absorption peak at 472 nm. Because of the sharp absorption edge at 930 nm it can be speculated that the LEB-PANI has a compact conformational structure.

The oxidation state can be calculated according to [23] (appendix D) where the calculated ratio of the absorption intensity of the peak at 355 nm (0.303) to the absorption

intensity of the peak at 651 nm (0.291) yields 1.04. This infers that the oxidation level of LEB-PANI has increased to a slightly higher oxidation level than EB-PANI.

Using the Tauc relation described in chapter 4, the band gap of the CA LEB-PANI composite was computed to be 2.8 eV. Figure 5.2.3 shows the Tauc plot for the CA LEB-PANI composite.
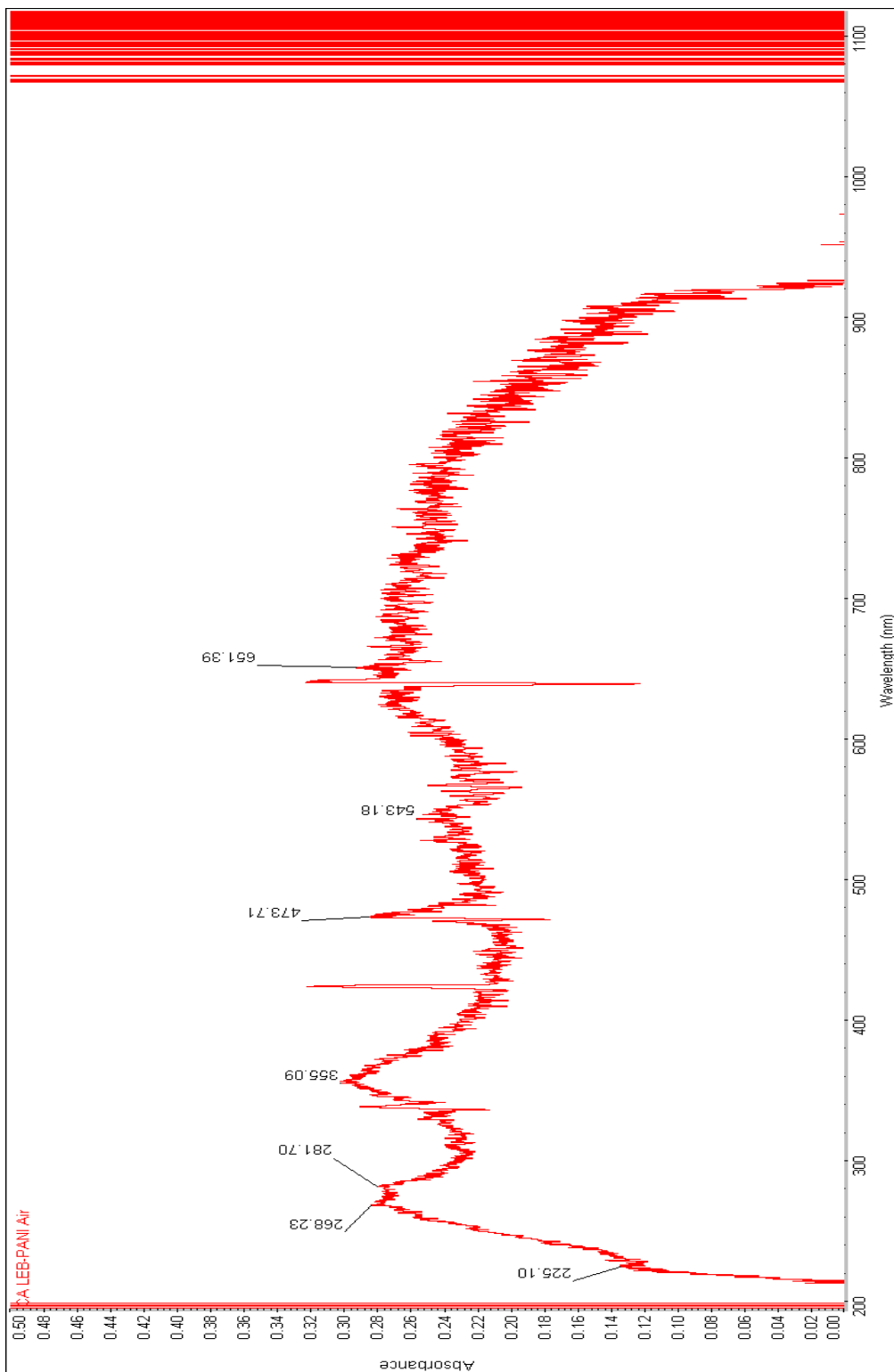
Figure 5.2.2 UV-Vis absorption spectra for 8020 CA LEB-PANI
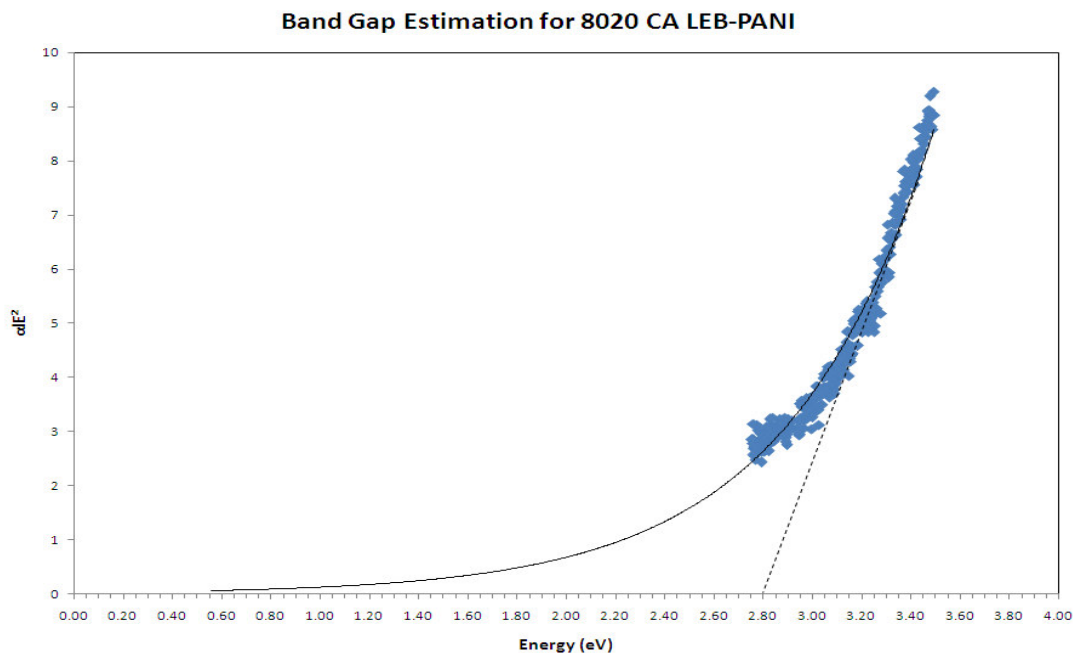
Figure 5.2.3 Band gap estimation for 8020 CA LEB-PANI

5.2.3. *XPS*

Complementary to the above spectrochemical analyses, XPS was used to identify the existence of protonated species, amines, and imines in the composite structure. Table 5.2 shows the representative XPS peaks associated with the N1s, C1s, and O1s spectra of the CA LEB-PANI composite. Figures 5.2.4, 5.2.5, and 5.2.6 reflect the N1s, C1s and O1s, spectra of the CA LEB-PANI composite, respectively.

The XPS data suggests that LEB-PANI has transformed into a higher oxidation state. This is evidenced by the reduced intensity of the -NH- peak at 399.6 eV. Although the matrix lacks in neutralized amine sites, the peak at 400.6 eV suggests that many of these sites have been protonated or transformed into polarons. [24-25] suggests

that the peak at 400.6 reflects $>C-N^+$ structures while the peak at 402.4 eV reflects $>C=N^+$ structures.

Table 5.2 XPS spectra data for 8020 CA LEB-PANI

Spectrum	Peak	B.E. (eV)	Compound	Rel. Area
N1s	A	398.9	=N-	70.5%
	B	400.6	$-N^+$	27.8%
	C	399.6	-NH-	1.1%
	D	402.4	$=N^+$	0.6%
C1s	A	285.1	C=N, C-N, C-H, C-C, C=C, possibly associated protonated species	59.1%
	B	288.8	COOH, C=O	18.7%
	C	286.8	C-O, C=O	21.7%
	D	283	C	0.9%
O1s	A	532..5	OH, H_2O	99.2%
	B	529	O_2, O_2-	1%

The rise in the number of protonated amines may be a consequence of protonation of quinoid imine units yielding N^+H through internal redox processes, protonation of the neutral amine structures by the acetate groups of CA, or polaron formation via reactions (protonation/oxidative doping) between the acetate groups of CA and LEB-PANI.   The peaks at 288.8 eV and 286.8 eV reflect the cellulose acetate groups in the composite which are responsible for the molecular modifications in LEB-PANI leading to the higher oxidation state and slightly doped structure.
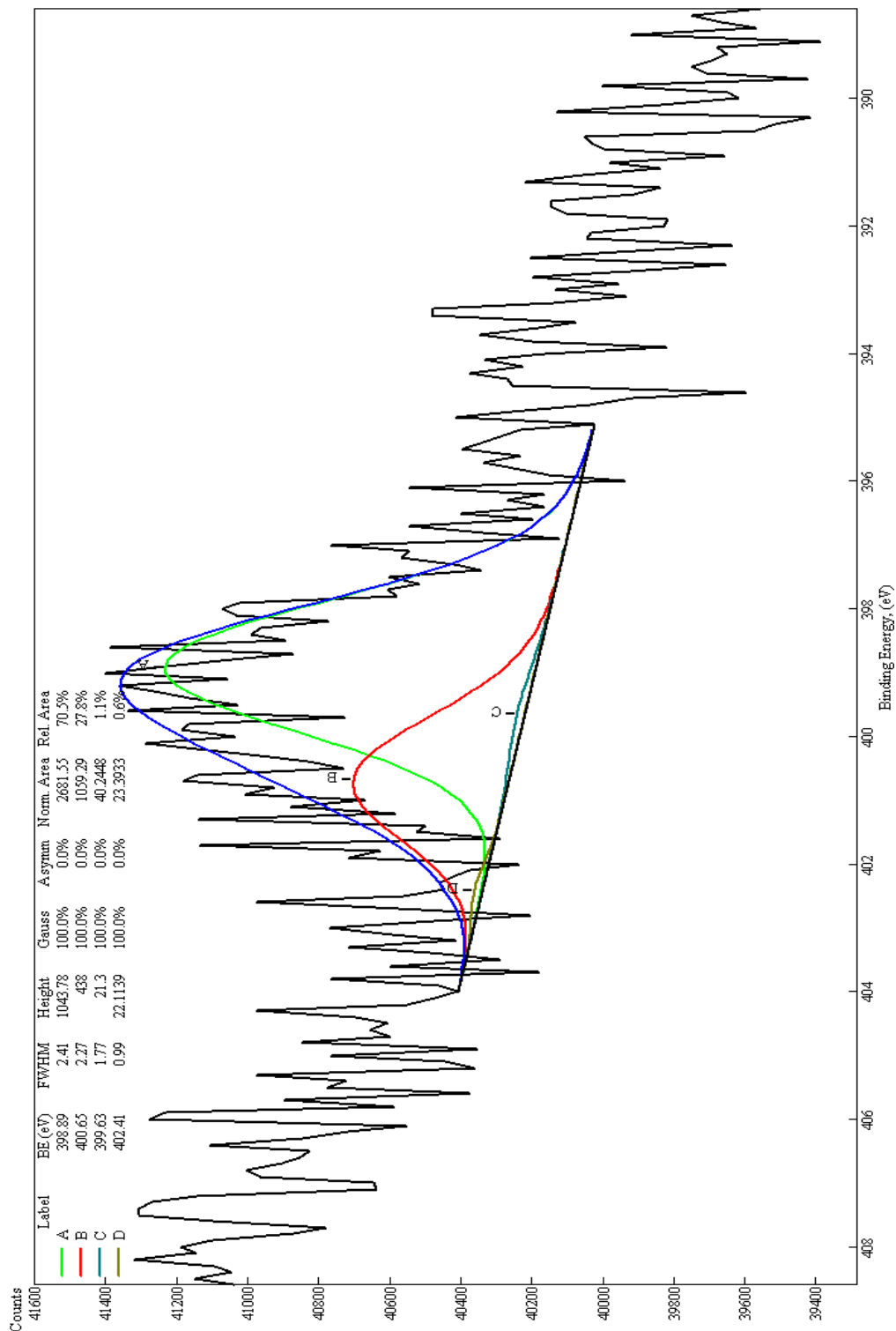
Figure 5.2.4 N1s core energy XPS spectra for 8020 CA LEB-PANI
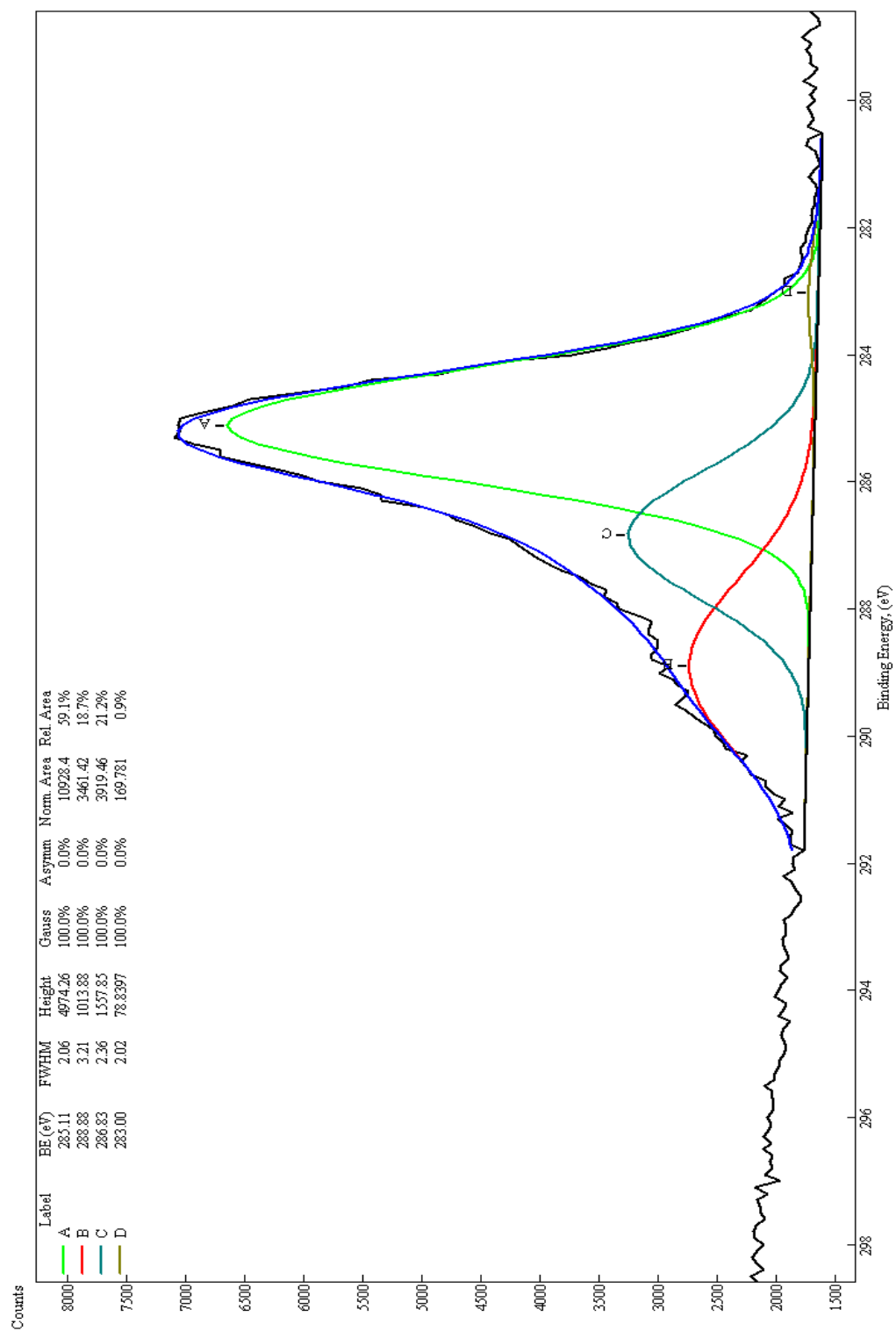
Figure 5.2.5 C1s core energy XPS spectra for 8020 CA LEB-PANI
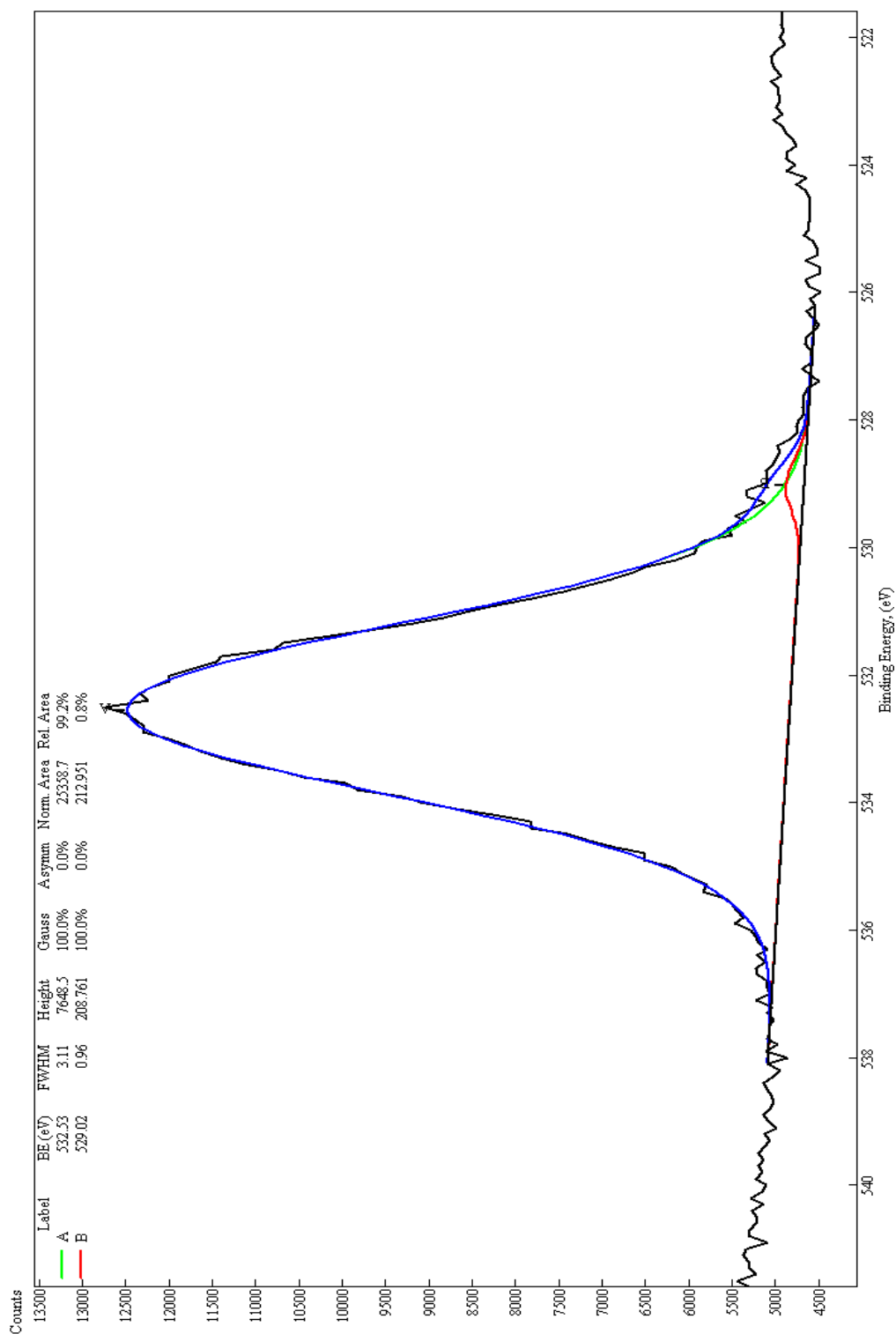
Figure 5.2.6 O1s core energy XPS spectra for 8020 CA LEB-PANI

5.3. GAS SENSING BASED ON CA LEB-PANI

Figures 5.2.7 and 5.2.8 reflect the response of the CA LEB-PANI composite to varying concentrations of NO_2 at 20% RH and 40% RH. Table 5.3 outlines the sensitivity, response and recovery times of the sensor.
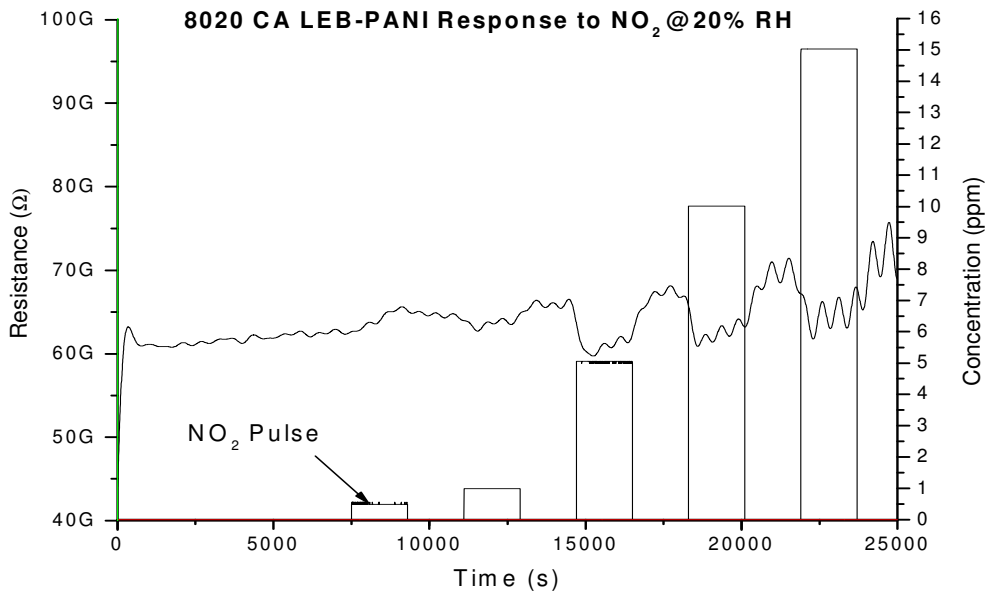
Figure 5.2.7 Response of 8020 CA LEB-PANI to NO_2 at 20% RH
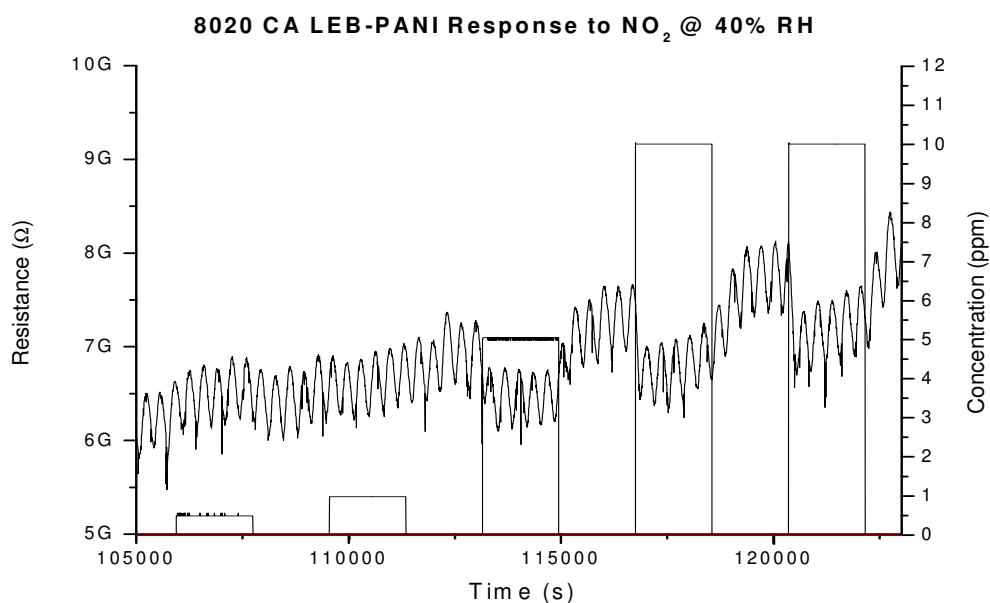
Figure 5.2.8 Response of 8020 CA LEB-PANI to NO_2 at 40% RH

Table 5.3 Sensitivity, Response, and Recovery times of 8020 CA LEB-PANI to NO_2

Concentration (ppm)	% RH	Sensitivity	Response Time (s)	Recovery Time (s)
0.5	20	0.05	1285	DNR
1	20	-0.08	105	185
5	20	-0.09	285	250
10	20	-0.12	70	155
15	20	-0.13	110	275
5	40	-0.09	340	15
10	40	-0.16	435	150

149

The data reflected in the figures above and table 5.3 reveal that on exposure to NO_2 the composite exhibits a decrease in resistance suggesting that during oxidation LEB-PANI becomes positively charge. This is associated with an increase in electrical conductivity and suggests that the charge carriers on the backbone of the film are positive (holes). Similarly to the effects of dissolution at low NO_2 concentrations on the 8020 PVP LEB-PANI composite (as discussed in chapter 4) at 0.5 ppm the film exhibits an increase in electrical resistance. The response and recovery times of the films vary suggesting that the adsorption and desorption of NO_2 is not stable due to possible poisoning of the sensor during exposure.

5.3.1. *Effects of Humidity*

Figure 5.2.9 depicts the effect of humidity on the sensitivity of the CA LEB-PANI composite to NO_2. As depicted, at low NO_2 concentrations (less than 5 ppm) there is no response to NO_2 at 40% RH. At higher levels of humidity and as the gas concentration increases the reactivity and sensitivity of the composite increases.

Figures 5.2.10 and 5.2.11 show the response of the CA-LEB-PANI sensor to humidity and its corresponding sensitivity, respectively. The data in figure 5.2.10 suggests that the relationship between humidity and resistance follows a power law and decreases by a factor of 3 with humidity.
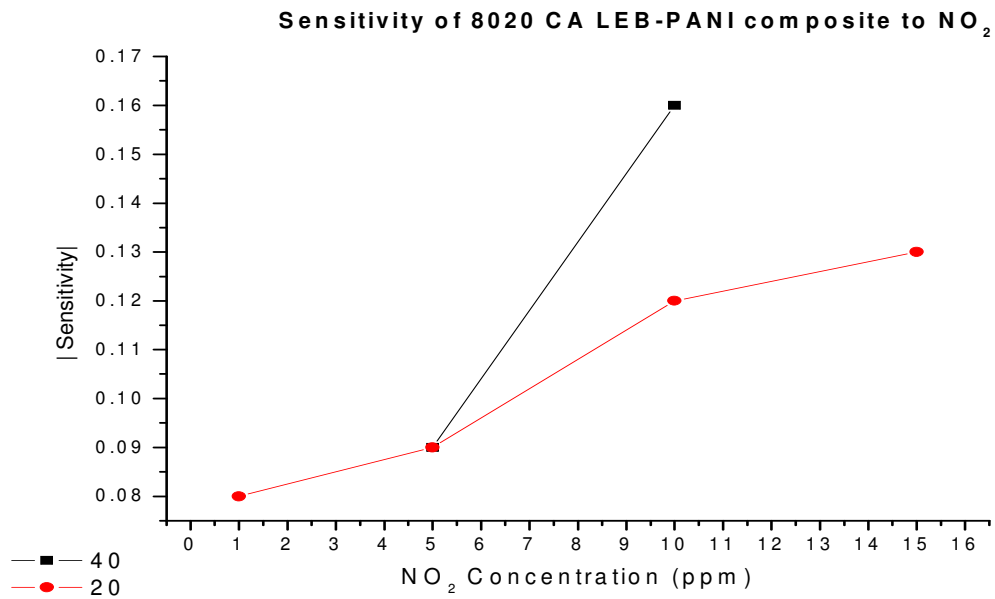
Figure 5.2.9 Sensitivity of the 8020 CA LEB-PANI composite to NO_2 at 20% and 40% RH
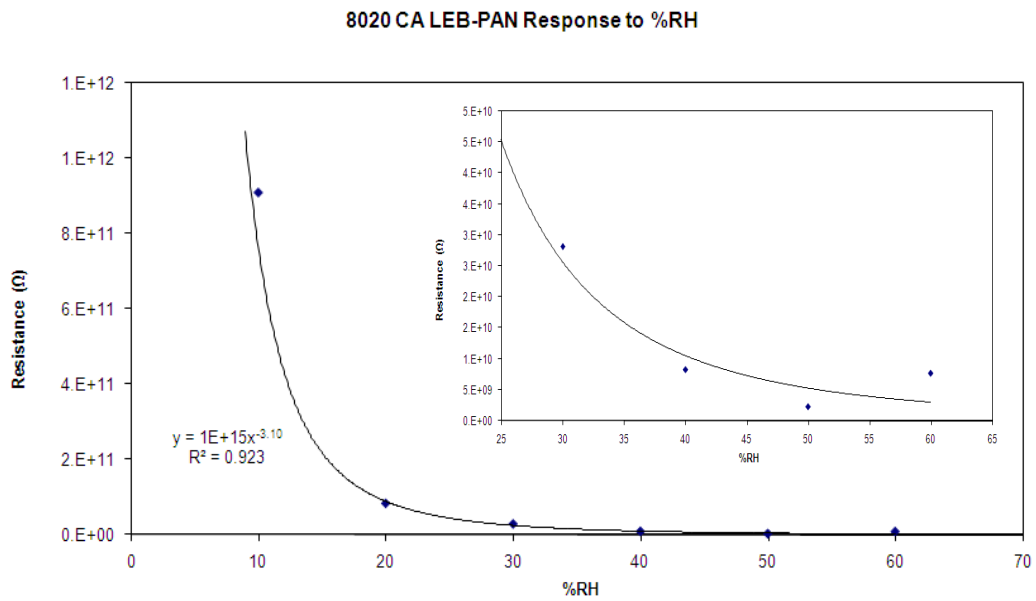
Figure 5.2.10 Response of 8020 CA LEB-PANI to humidity
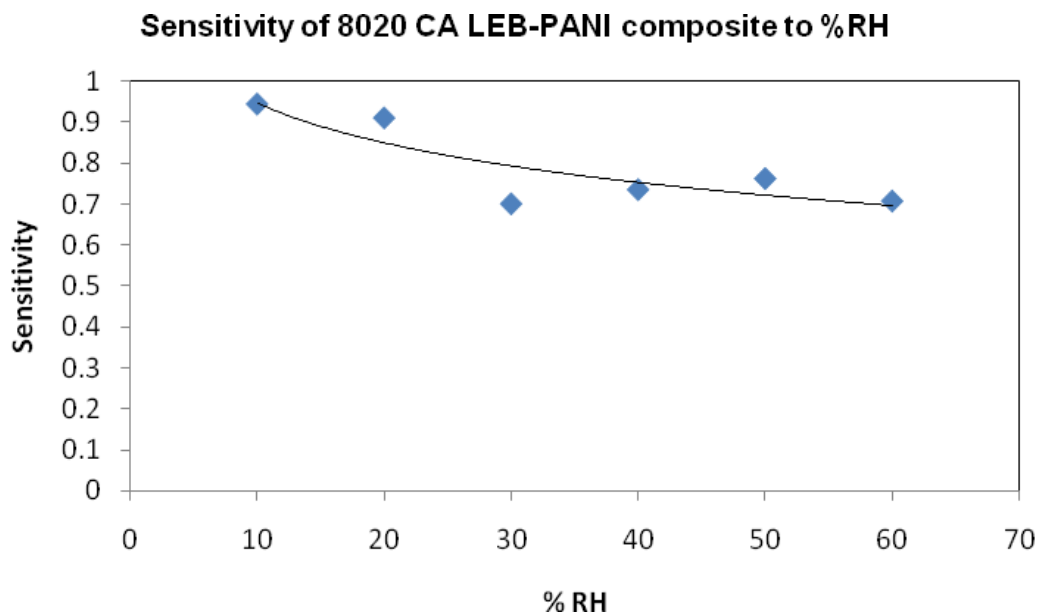
Figure 5.2.11 Sensitivity of 8020 CA LEB PANI to humidity

5.3.2. *In-Situ UV-Vis*

Figure 5.2.12 shows the in-situ UV-Vis spectra for the CA LEB-PANI composite at different levels of humidity ranging from 46% RH to 59% RH to 68% RH and during exposure to 20 ppm of NO_2. There are no significant changes in the spectra upon exposure to different levels of humidity and NO_2 except at the CA band which increases in absorption intensity with increasing water vapor and gas exposure. This suggests possible swelling of the polymer during water vapor and NO_2 absorption. Figure 5.2.13 shows the effects of NO_2 and humidity at 225 nm.
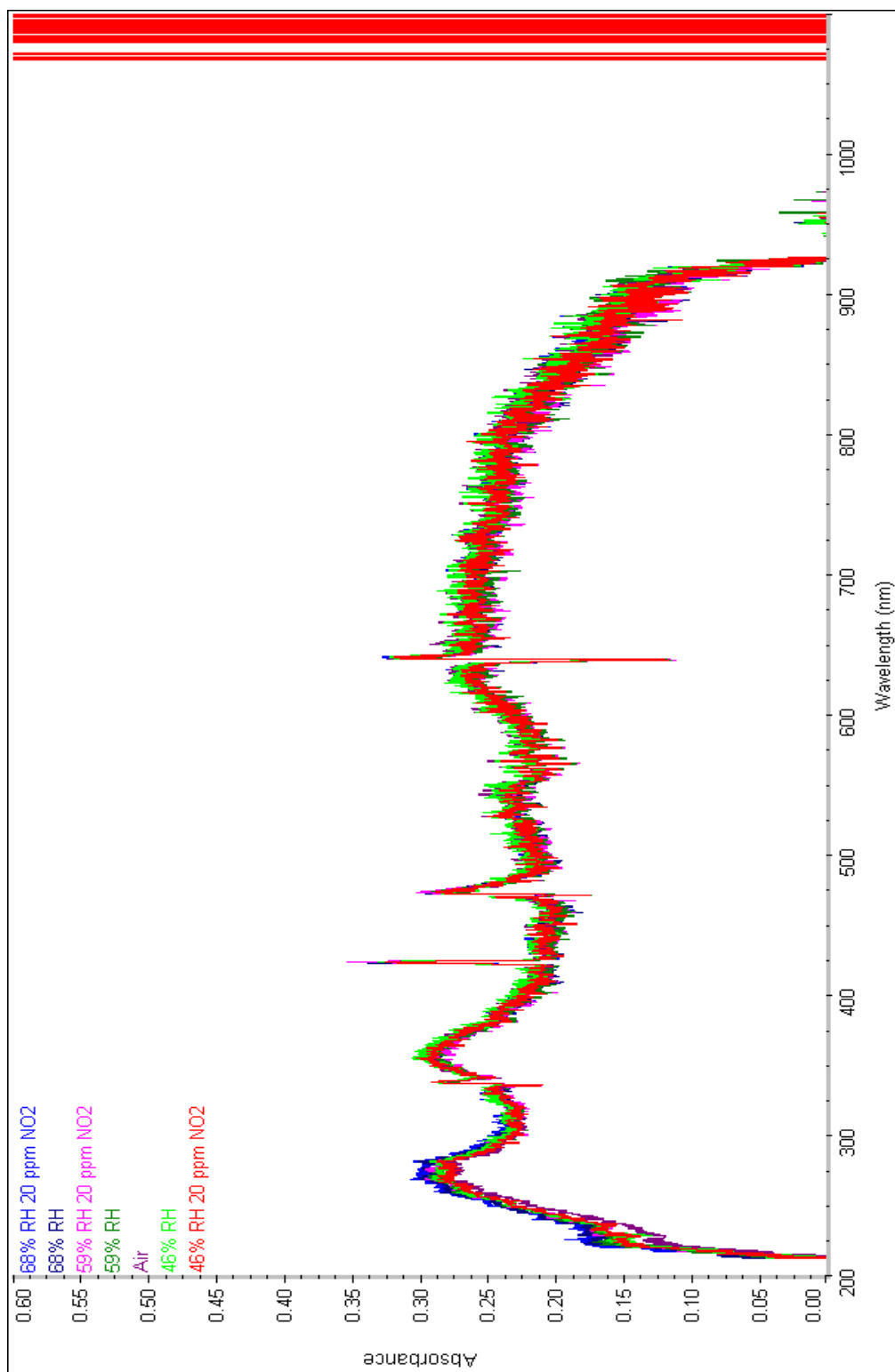
Figure 5.2.12 In-situ UV-Vis spectrum for 8020 CA LEB-PANI at 46% RH and 46% RH with 20 ppm of NO_2, 59% RH and 59% RH with 20 ppm NO_2, and 68% RH and 68% RH with 20 ppm NO_2.
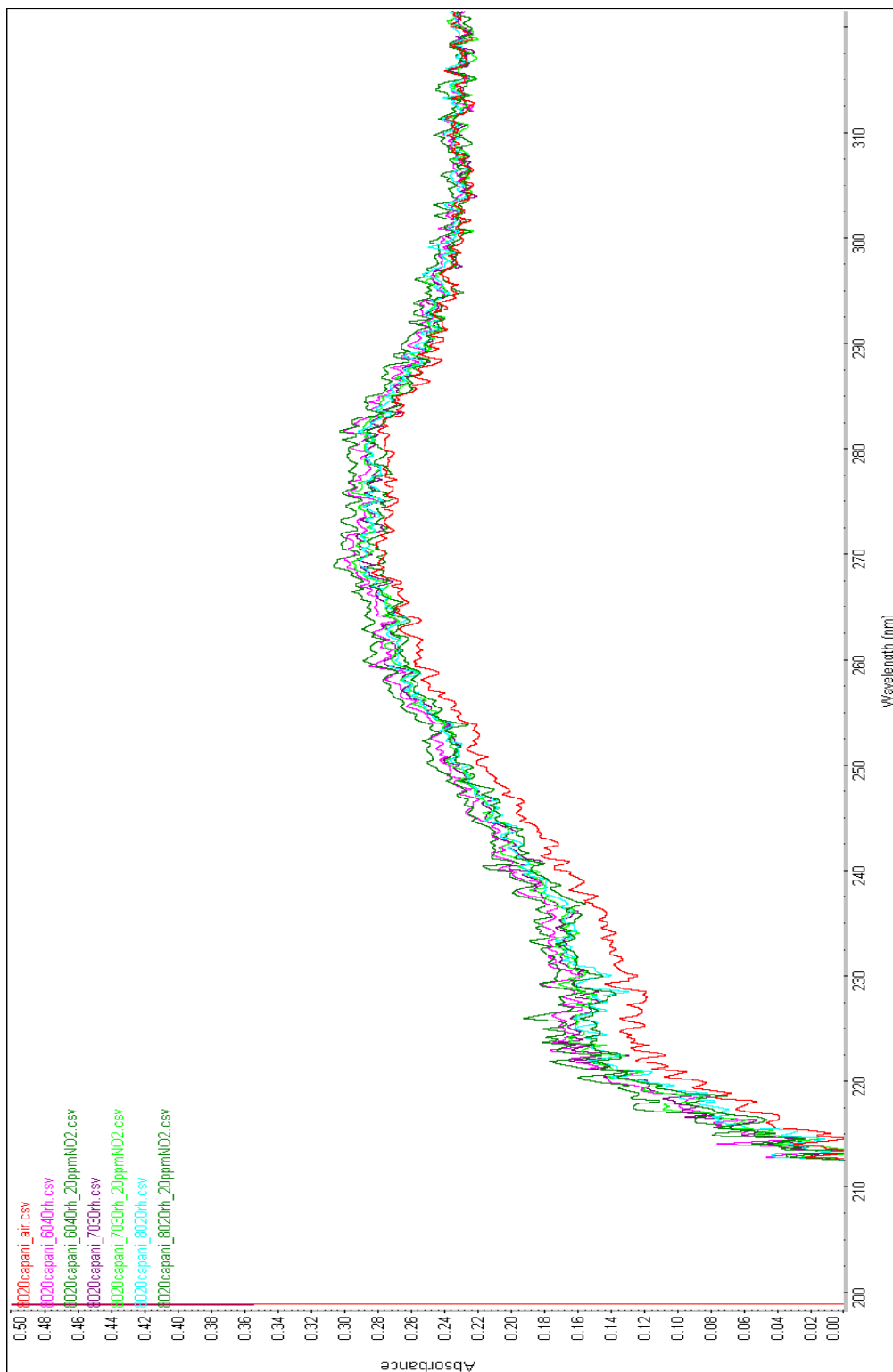
Figure 5.2.13 In-situ UV-Vis spectrum of 225 nm band of 8020 CA LEB-PANI at 46% RH and 46% RH with 20 ppm of NO_2, 59% RH and 59% RH with 20 ppm NO_2, and 68% RH and 68% RH with 20 ppm NO_2.

154

5.3.3. *Selectivity of 8020 CA LEB-PANI Composite*

Figures 5.2.14, 5.2.15, 5.2.16, 5.2.17, and 5.2.18 depict the response of the CA LEB-PANI composite to varying gas atmospheres as outlined in chapter 2. The graphs reveal that CA LEB-PANI exhibits no response to these interferents similar to the PVP LEB-PANI composites.
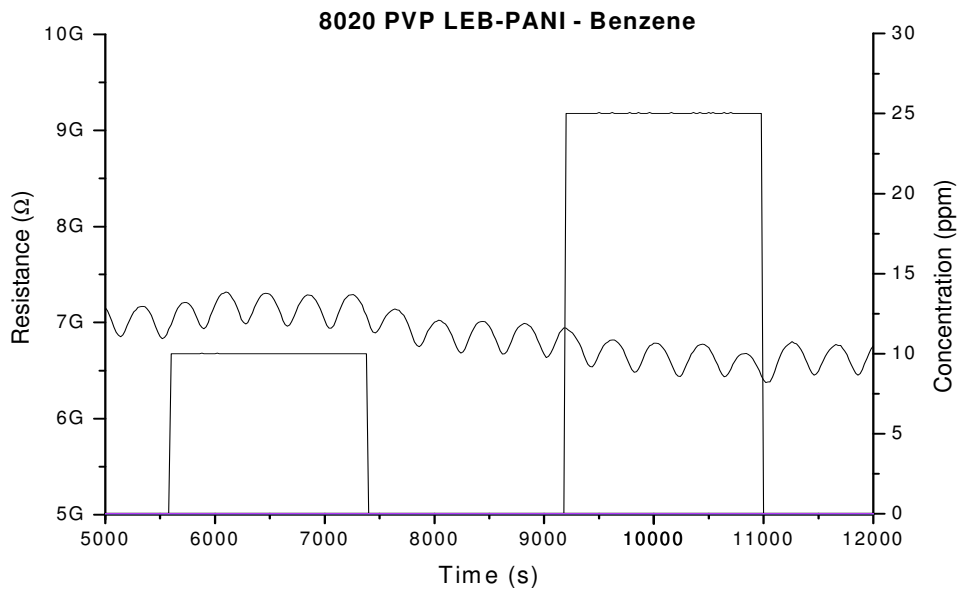
Figure 5.2.14 Response of 8020 CA LEB-PANI to Benzene
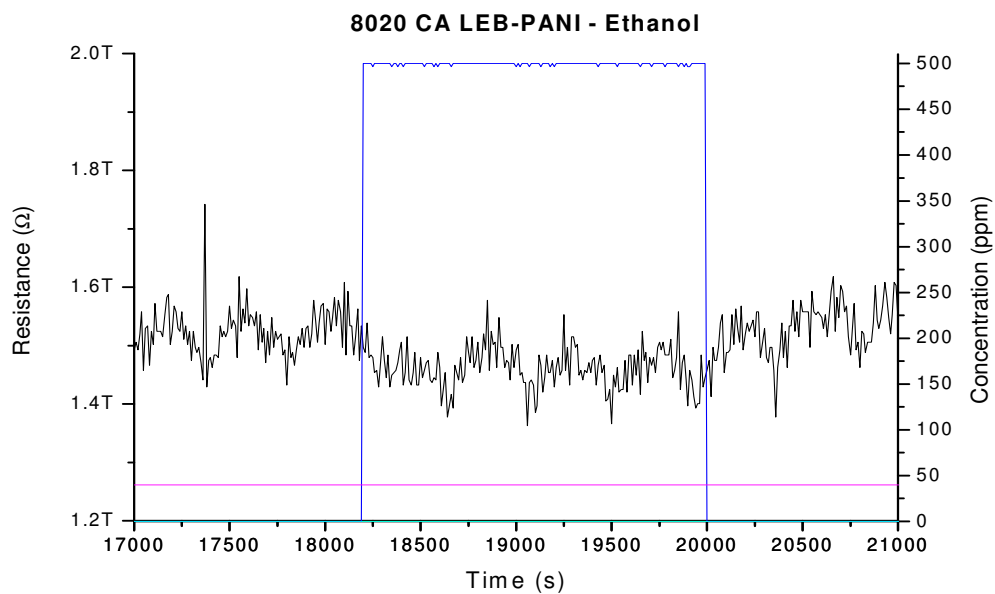
Figure 5.2.15 Response of 8020 CA LEB-PANI to Ethanol
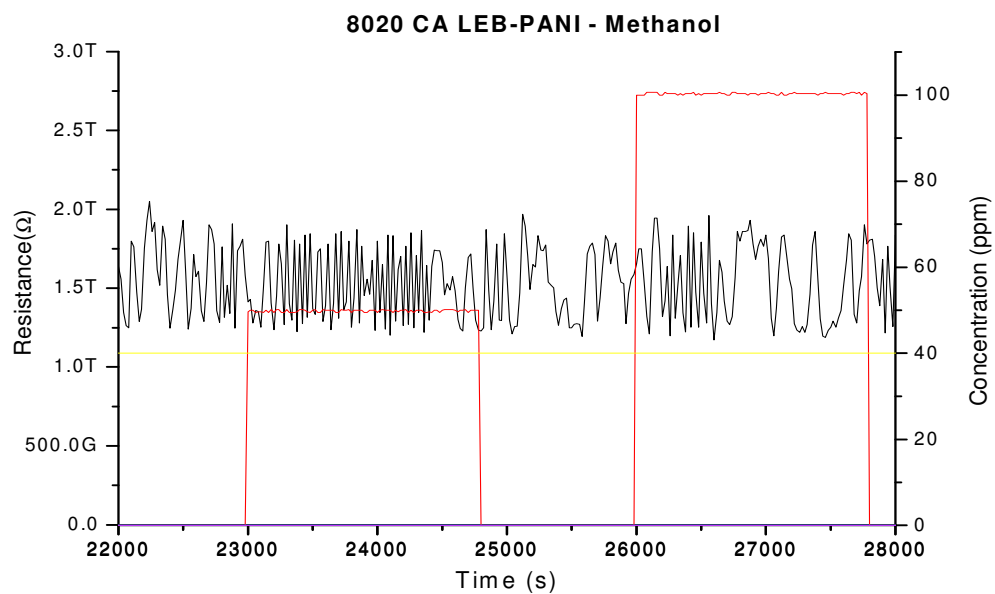
Figure 5.2.16 Response of 8020 CA LEB-PANI to Methanol
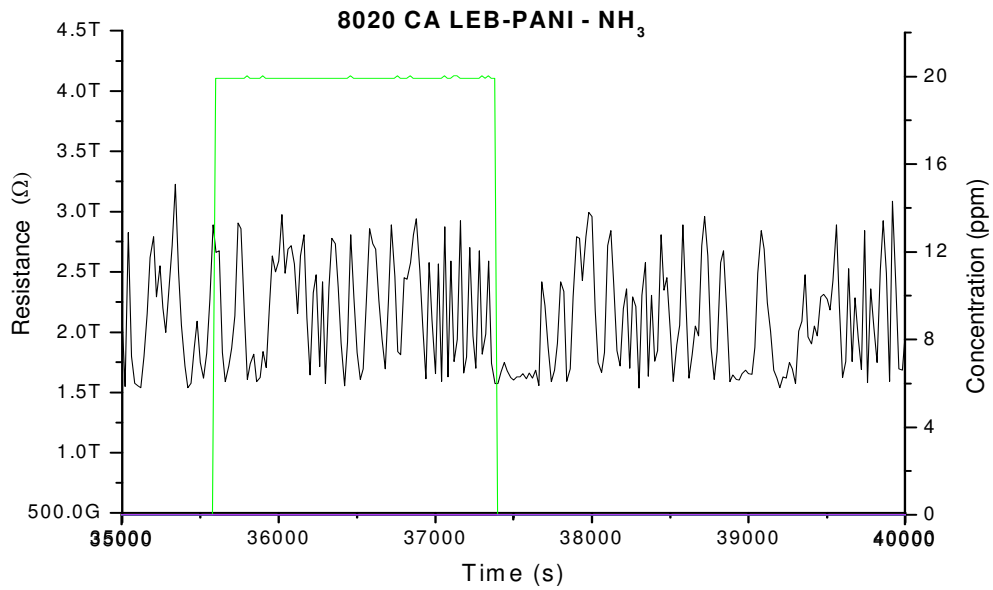
Figure 5.2.17 Response of 8020 CA LEB-PANI to NH$_3$
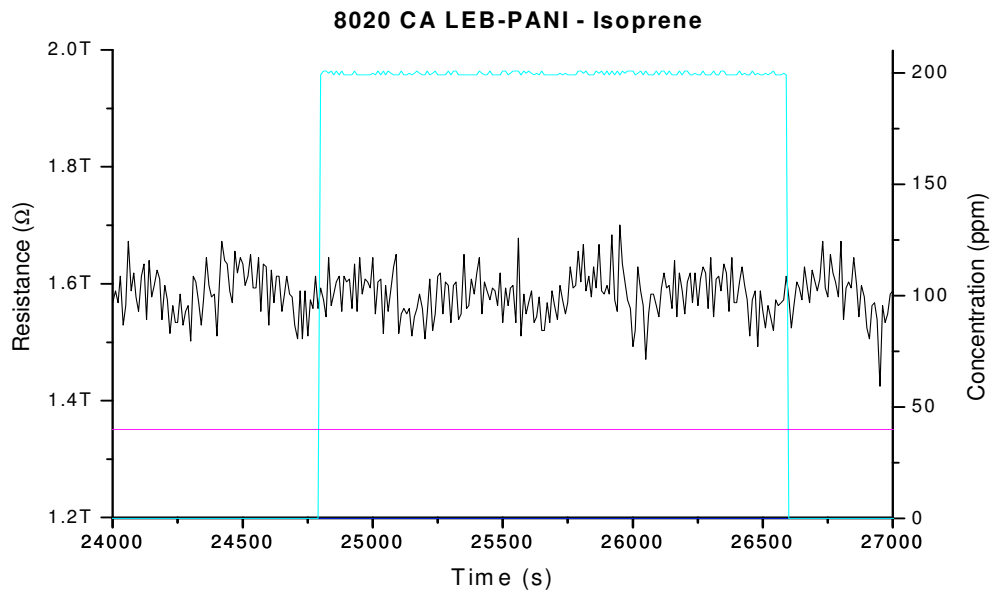
Figure 5.2.18 Response of 8020 CA LEB-PANI to Isoprene

Table 5.4 Selectivity of 8020 CA LEB-PANI

Gas	Response	Reason
Benzene	None	Analyte reflects structure of LEB-PANI
Methanol	None	Material treated in alcohol, thus will have no response to analyte
Ethanol	None	Material treated in alcohol, thus will have no response to analyte
Isoprene	None	Reducing agents will have limited effects on amine sites of LEB-PANI
CO	None	Reducing agents will have limited effects on amine sites of LEB-PANI
NH_3	None	Reducing agents will have limited effects on amine sites of LEB-PANI

5.3.4. *Stability Studies of 8020 CA LEB-PANI Composite*

Unlike PVP, CA does not dissolve in water. Thus it is expected to be stronger structurally under exposure to increased levels of humidity. The stability and reproducibility of the CA LEB-PANI sensor response was studied by cycling the sensing tests on the same sensor over the course of 2 days. Figures 5.2.19 and 5.2.20 depict the response of the same CA LEB-PANI sensor after each re-test. Figure 5.2.21 shows the effect of cycling on sensitivity. Table 5.5 outlines the sensitivities, response times, and recovery times of the LEB-PANI sensor on all three days.
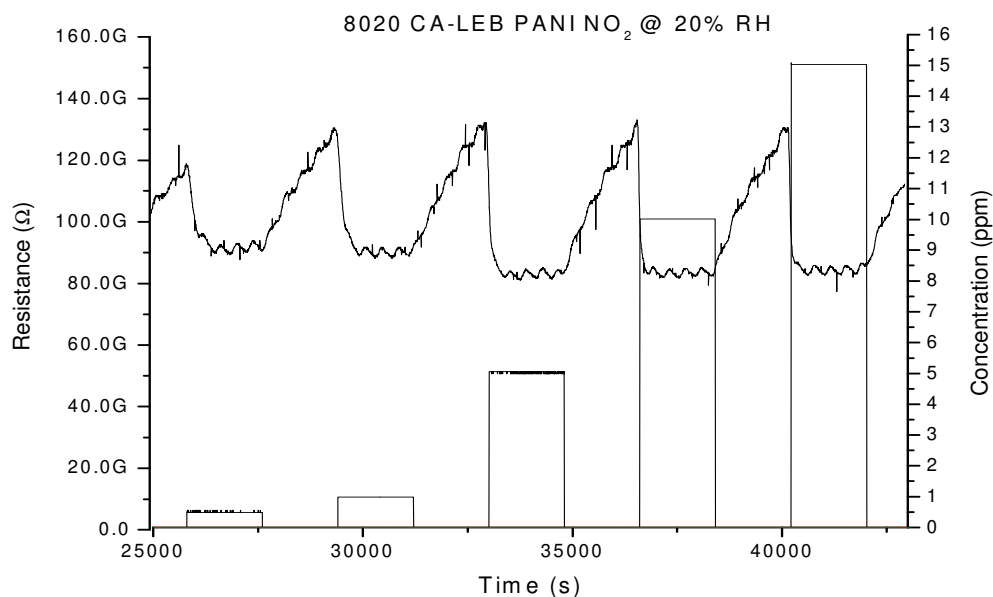
Figure 5.2.19 Sensor response of 8020 CA LEB-PANI to NO_2 at 20% RH during the 2nd test

Figure 5.2.21 shows that the sensitivity of the film to NO_2 increases by 78% from day 1 to day 3. The response times and recovery times have also stabilized as sensor is cycled under these conditions. As expected the sensor's response time will decrease with increasing gas concentration due to increase in rate of diffusion and surface reactions and its recovery time will increase with concentration due the increase in the amount of gas that needs to be desorbed out of the material.

The data collected from all tests reveal that the sensor response becomes saturated above 5 ppm of NO_2. This results in relatively the same level of sensitivity to 5 ppm, 10 ppm, and 15 ppm of NO_2.
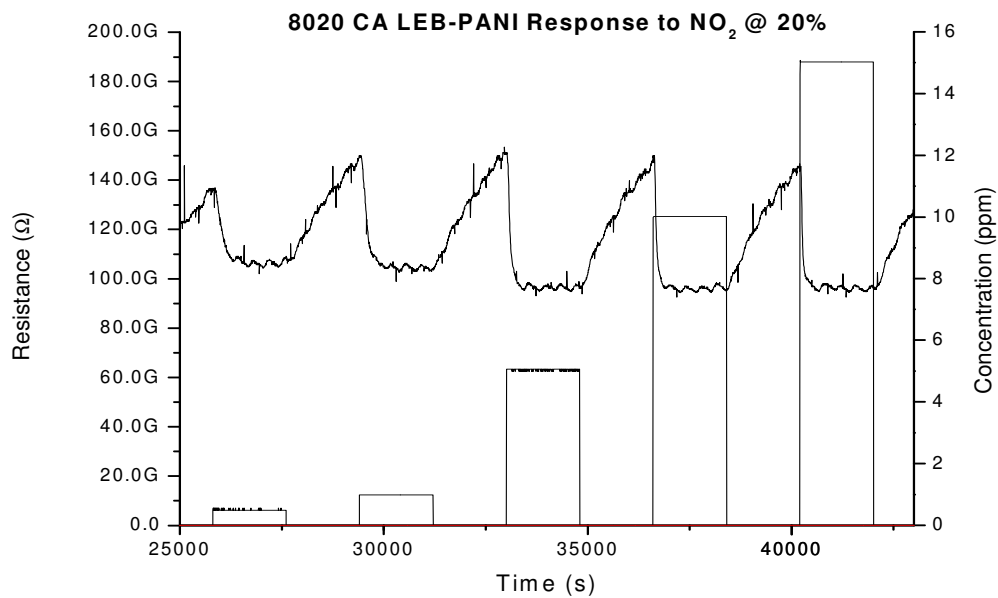
Figure 5.2.20 Sensor response of 8020 CA LEB-PANI to NO$_2$ at 20% RH during the 3rd test
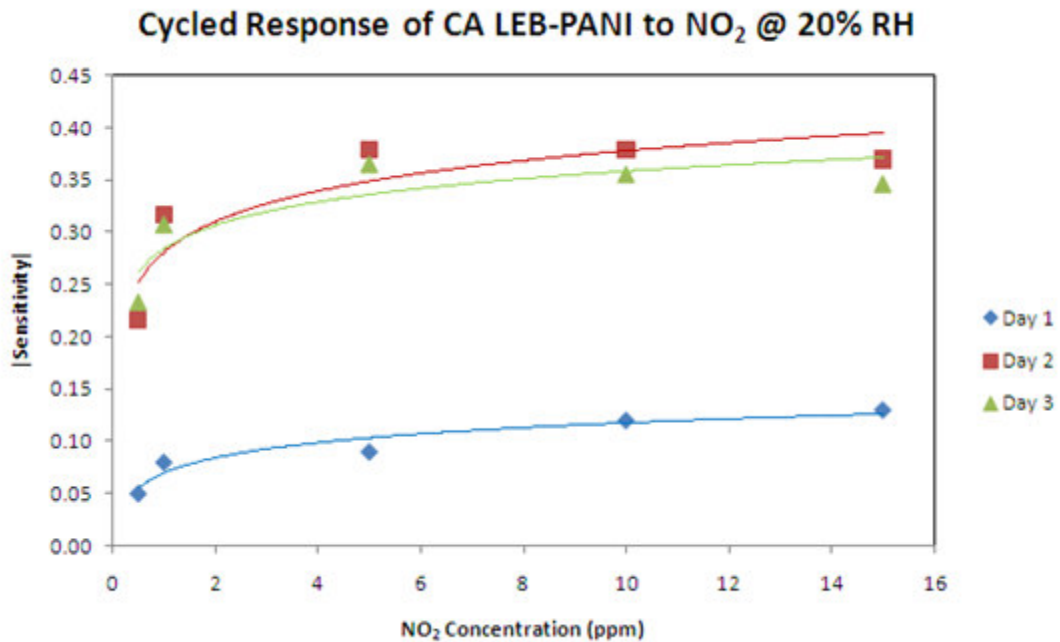
Figure 5.2.21 Sensitivity of all three sensing tests to varying concentrations of humidity

160

Table 5.5 Sensitivity, response, and recovery times of the 8020 CA LEB-PANI sensor
for the three test cycles

Concentration (ppm)	Sensitivity	Response Time (s)	Recovery Time (s)
Day 1			
0.5	0.05	1285	DNR
1	-0.08	105	185
5	-0.09	285	250
10	-0.12	70	155
15	-0.13	110	275
Day 2			
0.5	-0.22	580	520
1	-0.32	410	1015
5	-0.38	250	1055
10	-0.38	160	1200
15	-0.37	150	1075
Day 3			
0.5	-0.23	445	615
1	-0.31	430	980
5	-0.37	220	1090
10	-0.36	185	1170
15	-0.35	155	1030

REFERENCE

1. V.M. Sedelkin, G.P. Denisova, A.N. Surkova, L.F. Ramasaeva, and O.V. Pachina, "Rheological properties of spinning solution of cellulose acetate ultrafiltration membranes", *Fibre Chemistry*, vol 39, no 1, pp. 16-19, 2007

2. K.C. Ghanta, A.K. Ghosh, and V. Ramachandhran , "Separation characteristics of cellulose acetate blend (CAB) and aromatic polyamide hydrazide (PAH) reverse osmosis (RO) membranes for removal of phenol from phenol water-mixture", *J. Polymer Materials*, vol. 22, no 3, pp 313-319, 2005

3. K. J. Edgar, C. M. Buchanan, J. S. Debenham,. P. A. Rundquist,. B. D. Seiler, M. C. Shelton, and D. Tindall, "Advances in cellulose ester performance and application", *Progress in Polymer Science*, vol 26, no. 9, pp1605–1688, 2001

4. A.J.M. Valente, A.Y.A. Polishchuk, H.D. Burrows, and V.M.M. Lobo, "Transport properties of concentrated aqueous sodium dodecyl sulfate solutions in polymer membranes derived from cellulose esters", *Langmuir*, vol 16, no 16, pp 6475 - 6479, 2000

5. T.B. Meluch and D.R. Lloyd, "A comparative study of partition coefficients determined by sorption and liquid chromatography in alcohol water cellulose acetate systems", *Polymer*, vol 34, no 9, pp 1984-1987, 1993

6. T. H. Meltzer, K. Gutfreund, V. K. Kulshrestha, and A. M. Stake, "Optimized cellulose membranes for artificial kidney dialysis application", *American Society for Artificial Internal Organs Journal*, vol 14, no. 1 pp.12-18, 1968

7. E. Doelker, "Cellulose Derivatives", *Advances in Polymer Science*, vol. 107, pp. 199-265, 1993

8. A. Al-Ahmed, F. Mohammad, and M.Z.A Rahman, "Composites of polyaniline and cellulose acetate: preparation, characterization, thermo-oxidative degradation and stability in terms of DC electrical conductivity retention" , *Synthetic Metals*, vol. 144, no.1, pp. 29-49, 2004

9. A. Pron, Y. Nicolau, F. Genoud, and M. Nechtschein, "Flexible, highly transparent, and conduct polyaniline-cellulose acetate composite films", *J. Applied Polymer Science*, vol. 63, no. 8, pp. 971-977, 1997

10. J. Planes, A. Wolter, Y. Cheguettine, A. Pron, F. Genoud, and M. Nechtschein, "Transport properties of polyaniline-cellulose-acetate blends", *Physical Review B*, vol. 58, no. 12, pp. 7774-7785, 1998

11. J. Planes, Y. Cheguettine, and Y. Samson, "Nanostructure of polyaniline blends", *Synthetic Metals*, vol. 101, no. 1-3, pp. 789-790, 1999

12. A Wolter, E. Banka. F. Genoud, A. Pron, and M. Nechtschein, "Electronic transport in composites based on polyaniline blended with cellulose acetate - A DC-conductivity and ESR analysis", *Synthetic Metals*, vol 84, no 1-3, pp. 753-754, 1997

13. A.P. Marques, C.M.A. Brett, H.D. Burrows, A.P. Monkman, and B. Retimal, "Spectral and electrochemical studies on blends of polyaniline and cellulose esters", *J. Applied Polymer Science,* vol, 86, pp. 2182-2188, 2002

14. S. Karg, J.C. Scott, J.R. Salem, and M. Angelopoulos, "Increased brightness and lifetime of polymer light-emitting diodes with polyaniline anodes", *Synthetic Metals*, vol. 80, no 2, pp 111-117, 1996

15. R.W.T. Higgins, N.A. Zaidi, and A.P. Monkman., "Emeraldine base polyaniline as an alternative to poly (3,4-ethylenedioxythiophene) as a hole-transporting layer", *Advances in Functional Materials*, vol. 11, no 6, pp 407-412, 2001

16. D. Han and P. I. Gouma, "Electrospun Bio-Scaffolds that Mimic the Topology of Extracellular Matrix", *Nanomedicine*, vol. 2, pp. 37-41, 2006

17. D. Han, S. Goldgraben, M.D. Frame, and P.I. Gouma, "A novel nanofiber scaffold by electrospinning and its utility in microvascular tissue engineering", *Proceedings of Symposium on Nanoscale Materials Science in Biology and Medicine*, ed. C.T. Laurencin and E.A. Botchwey, Materials Research Society Symposium Proceedings, vol 845, pp. AA5.48, 2005

18. FTIR Spectra of Cellulose Acetate, Sigma Aldrich, http://www.sigmaaldrich.com/spectra/ftir/FTIR002032.PDF

19. D. Murphy and M.N. de Pinho, "An ATR-FTIR study of water in cellulose acetate membranes prepared by phase inversion", *J. Membrane Science*, vol. 106, no. 3, pp. 245-257, 1995

20. R. Kostic, D. Rakovic, I.E. Davidova, and L.A. Gribov, "Vibrational spectroscopy of the leucoemeraldine form of polyaniline: theoretical study", *Physical Review B*, vol 45, no 2, pp 728-733, 1992

21. S. Quillard, S. Louarn, S. Lefrant, and A.G. MacDiarmid, "Vibrational analysis of polyaniline- A comparativity study of leucoemeraldine, emeraldine, and pernigraniline bases", Physical Review B ,vol 50, no17, pp. 12496-12508, 1994

22. A. Pron, M. Zagorska, Y. Nicolau, F. Genoud, and M. Nechtschein, "Highly conductive composites of polyaniline with plasticized cellulose acetate", *Synthetic Metals*, vol. 84, no 1-3, pp 89-90, 1997

23. J.E. Albuquerque, L.H.C. Mattoso, D.T. Balogh, R.M. Faria, J.G. Masters, and A.G. MacDiarmid, "A simple method to estimate the oxidation state of polyanilines", *Synthetic Metals*, vol 113, no 1-2, pp 19-22, 2000

24. H.S.O. Chan, A. J. Neuendorf, S.Ng, P.M.L. Wong, and D.J. Young, "Synthesis of fully sulfonated polyaniline: a novel approach using oxidative polymerisation under high pressure in the liquid phase" , *Chemical Communication*s, vol 13, pp 1327-1328, 1998

25. J. Yue and A.J. Epstein, "XPS Study of Self Doped Conducting Polyaniline and Parent Systems", *Macromolecules*, vol 24, pp. 4441-4445, 1991

CHAPTER 6

6. Discussion

In this chapter the methodologies stemming from these studies will be discussed to provide a detailed description of the sensoric properties of the proposed LEB-PANI composites.

6.1. EFFECTS OF ELECTROSPINNING

Studies on the gas response of polyaniline composites have focused on the use of metal complexes[1], metal oxides [2-3], carbon nanotubes [4] or polymers such as polystyrene [5], poly (methyl methacrylate) [6], poly(butyl acrylate-co-vinyl acetate) [7], poly (vinyl acetate) [7], nylon-6 [8], and poly (vinyl alcohol) [9]. Of these only poly (vinyl alcohol), poly (methyl methacrylate), and polystyrene have been explored as base polymers for polyaniline based sensor devices. However, from this list, poly (vinyl acetate) is the only steric stabilizer for polyaniline. Poly-vinyl pyrrolidone (PVP) is also a well known steric stabilizer for polyaniline and, as discussed in chapter 4, can be employed to enhance processing of polyaniline. However, electrospun polyaniline nanocomposites with PVP as a base polymer have not been explored for gas sensing applications. As discussed in chapter 5 cellulose acetate (CA) is also a suitable secondary component for electrospinning polyaniline. These composites like those of PVP and polyaniline have also not been explored for gas sensing, although researchers

have shown enhanced and stable electrical properties of polyaniline with both polymers as secondary components.

It was researched by [10] that electrospinning induces charges on the polymer solution which dictate the miscibility of multiple components within the solution based on their surface charge. In chapter 3 it was shown that when processed in select solvents LEB-PANI incurs a surface charge that may inhibit aggregation. Complementary zeta potential measurements of the composites on the other hand were in-distinguishable because of the high solubility of the base polymer in the solvent. However, it is plausible to believe that the surface charge inflicted by the solvent can also be found on the neutral base polymer as it becomes solvated. Because of the presumed like charge on both polymers in the pre-spinning solution, both the PVP and CA based solutions have shown to present adequate dispersed colloidal suspensions of LEB-PANI.

During the electrospinning process a positive potential is applied to the spinning solution as it exits the needle. The work of Schreuder-Gibson et. al [10] has shown that charges inflicted on the solution as it leaves the needle can be retained in the deposited mat for up to several months. The retained charge may aid in the filtration potential of the base polymer. The more charged the material the more it will reflect like charged species.

6.2. NO$_2$ DETECTION WITH THE PROPOSED ELECTROSPUN MATRICES

6.2.1. *Effects of Solvent on the Structure of LEB-PANI*

Through a series of spectrochemical tests (FTIR and UV-Vis) it has been shown that both acetone and ethanol impart O and OH binding, respectively, at various sites along the LEB-PANI chains. The effects range from an increase in oxidation level and possibly substitution of these atoms on both the rings and N sites in the polymer chain to increased intermolecular H bonding. These adsorbed species can enhance the reactivity and selectivity of the polymer to select analytes. The effects of the solvent coupled with the effects of CA and PVP as base polymers is shown to improve the dispersion and colloidal stability of LEB-PANI (at low concentrations). In the case of the 8020 PVP LEB-PANI composite, the reduced leucoemeraldine state is preserved. This is attributed in part to PVP barriers formed on the surface of the LEB-PANI particles shielding the polymer from atmospheric contaminants.

6.2.2. *Effects of Water as a Primary Dopant*

Throughout this study water has been employed as a primary dopant for LEB-PANI. Traditionally when working with conducting polymers, scientists stimulate the electronic nature through reduction/oxidation or protonic acid doping mechanisms which entail the use of strong acidic agents such as HCl or H$_2$SO$_4$. However, the disadvantage of these types of dopants is that over time they begin to volatilize to the surface of the film blocking reactions between the analytes and polyaniline. Since the primary

contributor of the protonic agent is the H^+, water can also be exploited as a benign catalyst promoting charge transport along the polymer chain [11] similar to that of the protonic acid dopant

Reactions between water and polyaniline may involve: (1) polyaniline particles increasing in size with water adsorption on the surface [12], (2) insulating grain boundary barriers (between conducting sites – for highly doped polyaniline) breaking down with exposure to water vapor [13], (3) an exchange of protons between the water vapor and the polyaniline particles resulting in protonation of imines [34], and (4) changes in unit cell parameters and degree of crystallinity (also associated with highly doped polyaniline) [15]. It has been shown in the literature that water (aqueous or vapor state) may also promote conformational changes in polyaniline [11] and may adsorb at both the imine and amine centers through hydrogen bonding. According to literature the binding energy for H_2O at the imine center is ~15-18Kcal/mol while the binding energy of the water molecule at the amine center is ~3-5Kcal/mol [16]. The affinity of protons on these nitrogen centers are 268 kJ/mol and 217 kJ/mol respectively [17].

In this dissertation is has been shown that adsorbed atmospheric water and associated volatiles induces conformational changes in the LEB-PANI structure. Figure 6.1 depicts the molecular effects of adsorbed water on LEB-PANI. It can be concluded that water absorption into the composite matrix facilitates the transport of free protons in polyaniline, which may hop through hydrated moieties along the polymer chain via the Grotthus mechanism for proton transport. This supports the work Schmidt, De, and Aytac which suggests charge transport in polyaniline occurs via this phenomenon [18-21]. As the concentration of LEB-PANI increases so does uptake of water vapor into the

polymer (due to lack of surface coverage by PVP). [22] showed that polyaniline can absorb up to 40% its weight in water. At low LEB-PANI concentrations the effect of water on the polymer is enhanced by the base polymer matrix, especially for a polymer like PVP which is soluble in water. The adsorbed water may then act as a protonating agent by disassociating into H^+ and OH^- (in the presence of an applied electric field), where the latter acts as the anion and the couple can transform the N (most likely the imine) center into a reactant site for other molecular species such as NO and NO_2.

The imine N is most susceptible to protonation by water vapor. Through charge resonation and internal redox mechanisms these sites can be transformed into bipolarons and polarons (more energetically stable form). From UV-Vis spectroscopy of the 8020 PVP LEB-PANI composite, in chapter 4, the effects of increasing water vapor have a more pronounced effect on the quinoid transition band than the benzenoid band. While there is a slight bathochromic shift of the latter, suggesting some low level oxidation or more likely hydrogen bonding between O (from water) and the amine N, it is evident that the role of water vapor for the PVP LEB-PANI composites is as protonating agent for LEB-PANI (containing quinoid di-imine structures).
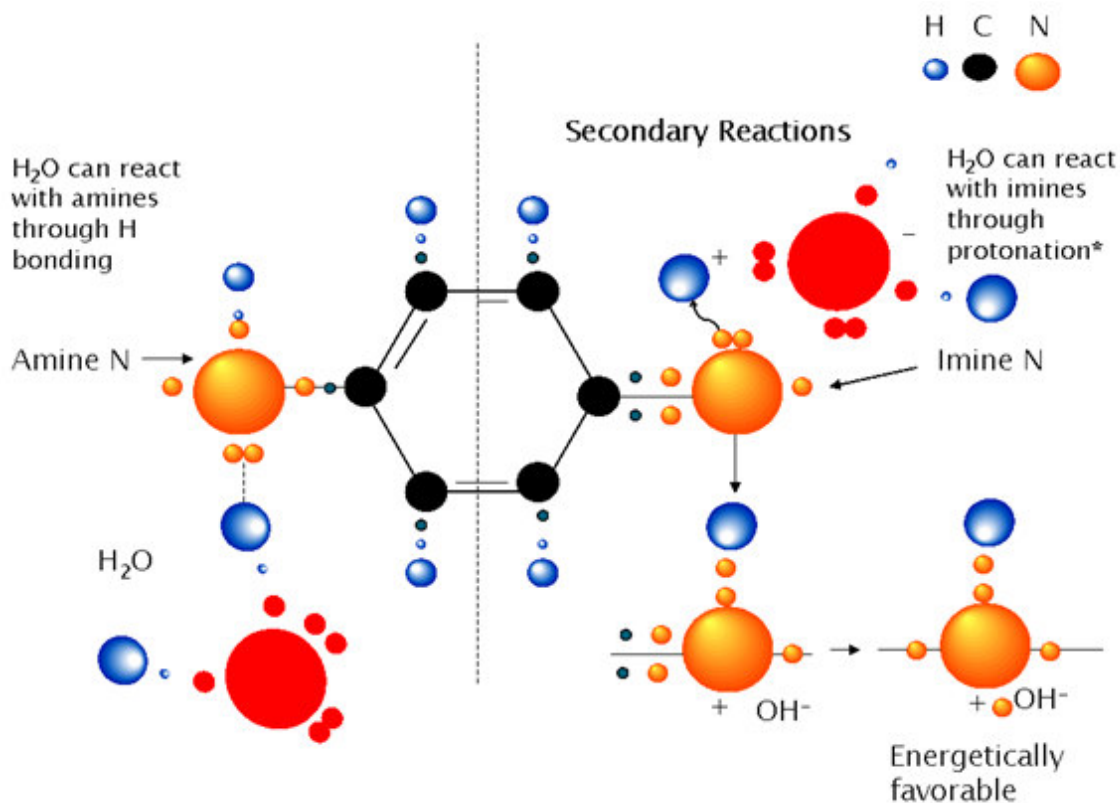
Figure 6.1 Effects of water vapor on LEB-PANI

6.2.3. *NO_2 Detection with Water as a Primary Dopant*

It has been demonstrated that water vapor is the dominant catalyst for sensing with LEB-PANI. In the presence of 0% and 10% RH no response to NO_2 is observed in all sensors. Only with the onset of water vapor above 20% RH is there any response to the analyte. Oxidation of the reduced polymer by NO_2 will yield the transformation from amine N to an imine N and benzenoid to quinoid structure, figure 6.2. It is important to note that reactions between the polymer and NO_2 are most likely to occur at the amine sites. However, unless coupled with a dopant ion no significant changes in electrical properties will be observed and the polymer will remain in an insulating base state. It is

likely that the OH⁻ of disassociated water acts as the anion during protonation of the imine N.   It can be presumed that increasing the level of humidity will yield an increase in the catalytic effect (i.e. doping) of the water vapor, and concurrently an increase in sensor reactivity (the OH⁻ creates a reaction site for oxidizing agents at the imine site). The data presented in chapters 4 and 5, reveal that the level of humidity used in the sensing setup has an effect on the sensor's response to NO_2. This is especially true for the 8020 CA LEB-PANI, the 8020 PVP LEB-PANI, and the 2080 PVP LEB-PANI composites.   Increasing the level of humidity on the former reveals an increase in sensitivity to NO_2 concentrations above 5 ppm. However no response was exhibited for lower concentrations at the higher humidity level. This may be due to competing effects of water vapor with NO_2. [23] showed that increasing levels of humidity decreased the response of polyaniline – polystyrene composites to NH_3. Due to lack of adsorption of water molecules on the intrinsic structure of CA at this humidity level it is possible for the CA LEB-PANI composite that more water vapor is available to react with NO_2 forming acidic byproducts that may not react with the CA LEB-PANI composite due to the type of substituted or adsorbed groups throughout the polymer chain (this will be explained in detail in the upcoming section). For the 8020 PVP LEB-PANI composite no significant response to NO_2 was observed for humidity levels below 40% RH. This may be a direct consequence of the composition of the 8020 PVP LEB-PANI sensor. At lower humidity levels water molecules may not diffuse adequately through the PVP matrix to the LEB-PANI particles. As for the 2080 PVP LEB-PANI composite, similarly to the results of [23] (which explore competing effects between the analyte and humidity), a decrease in the sensor's sensitivity to NO_2 was observed with increasing

humidity. As the level of humidity is increased, coupled with the blocked amine imine bound sites along the aggregated structure, the water molecules will bond to available amine (through H bonding) sites and may inhibit some of the reactions between NO_2 and polyaniline. At lower levels of humidity the polymer is less hydrated and the reactivity between NO_2 and amine sites along the polymer chain increases.

When NO_2 reacts with hydrated LEB-PANI, figure 6.2, it oxidizes the structure and electrons are transferred from the polymer to the gas. This was evidenced by small red shifts in the UV-Vis spectrum at the quinoid and benzenoid transition bands in the 8020 and 2080 PVP LEB-PANI composites.   Exposure to NO_2 has shown to induce transformations from the protonated imine species back to the neutral imine N for the high concentration LEB-PANI composite. Moreover several researchers have observed that for the emeraldine oxidation state, the sensor exhibits an increase in electrical resistance on exposure to NO_2. In many cases the response is irreversible. This oxidation level coupled with the reduction of the bipolaron charge carriers is associated with a shift in the response mechanism from decreasing electrical resistance on exposure to NO_2 for low LEB-PANI concentrations to an increase in electrical resistance on exposure to the gas for the 2080 PVP LEB-PANI composite.   The lack of response to NO_2 for the 5050 PVP LEB-PANI composite can be attributed to the oxidation level, the changing matrix morphology, and concentration of PVP.   At this oxidation level, it is likely that there exists an increase in the level of aggregation (H bonding between amine and imine sites) formed within the 5050 PVP LEB-PANI matrix.   This coupled with shielding effects of PVP and adsorption of water vapor (it is likely that H_2O uses H bonds to bind to the amine sites and disassociates into H^+OH^- to protonate imine sites - blocking

reactions between the polymer and other analytes) is likely to inhibit reactions between LEB-PANI and NO_2.

The CA LEB-PANI composite, however, behaves slightly different on exposure to NO_2 as compared to the PVP LEB-PANI composites. The water susceptibility of cellulose acetate has dependence on the degree of substitution of the acetyl groups (40% for CA employed in these studies, which has a high water resistance [24]). Although not soluble in water, it is likely that the polymer will undergo hydrolysis at these humidity levels yielding acetic acid as a byproduct. FTIR of the CA LEB-PANI composite reveals bonding between the acetate groups of CA and the benzenoid and quinoid rings of the polymer as well as at the imine N centers of LEB-PANI. It also shows several bands relative to the vibrations of the $C=N^+O^-$ structure. These groups can be formed from the interactions between CA and LEB-PANI or acetone and LEB-PANI giving rise to O^- anions. As these humidity levels, acetic acid may disassociate into COO- and H^+ or liberate a hydroxide or O^- which can bind to various sites along the LEB-PANI chain.

In chapter 5 it was determined that interactions between the gas and the CA LEB-PANI composite occur at the sites where the acetate groups have adsorbed. This presumption eludes from in-situ UV-Vis analyses of the CA LEB-PANI composite showing no significant affect of gas adsorption or water vapor adsorption on the conformational structure of LEB-PANI. Only an increase in the absorption intensity of the CA peak is observed. As NO_2 reacts with the composite it removes electrons from the acetate/acetic acid groups bonded throughout the polymer chain (through oxidation, protonation, substitution, or H bonding), forming positive charges along the polymer backbone. It is presumed that this will be the main interaction between NO_2 and the CA

174

LEB-PANI composites, as the adsorbed acetic acid and acetate groups may inhibit reactions with other like acids (i.e. the products of NO_2 dissolution). Moreover, although water vapor does not act as a primary charge carrier for this composite, it is still dire for the sensing mechanism such that water is necessary for the hydrolysis of CA yielding intrinsic doping of LEB-PANI within the composite matrix.

It has also been determined from these studies that at these humidity levels NO_2 may undergo dissolution forming acidic byproducts which can react with LEB-PANI via oxidation, protonation, and reduction. The first observation of this was the response of the 8020 PVP LEB-PANI composite to 0.5 ppm of NO_2. It has been observed that this composite decreases in electrical resistance on exposure to NO_2, however, at 0.5 ppm, the sensor exhibits an increase in electrical resistance. This is attributed to the complete dissolution of NO_2 at the water vapor concentration studied into HNO_2, H_3O^+, and NO_3^-. The adsorption of dissolved NO_2 is also evidenced during the in-situ optical spectroscopy of the 2080 PVP LEB-PANI composite under gas exposure. The emergence of a sharp polaronic peak on exposure to NO_2 was observed in the UV-Vis absorption spectrum for the 80% wt/wt LEB-PANI composite. This suggests that dissolved NO_2 might induce doping of LEB-PANI transforming the polymer into a light polaronic salt. The drawback of these reactions is the increase in baseline drift in the composite's response during gas exposure. This baseline drift has been observed for the 8020 and 2080 PVP LEB-PANI composites suggesting that the gas is poisoning the films.

$$-NH- + NO_2 \rightarrow =N- + NO_2^-$$
$$-NH-H_2O + NO_2 \rightarrow =N- + NO_2^- + H_2O$$
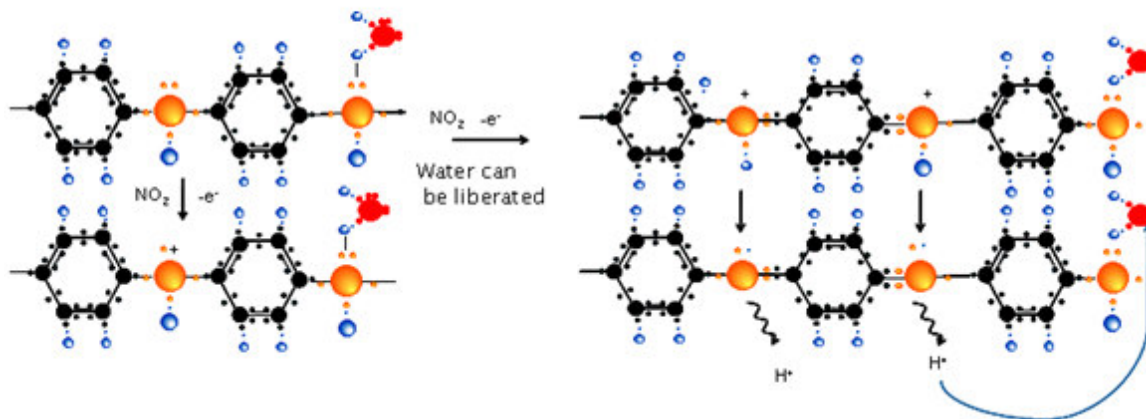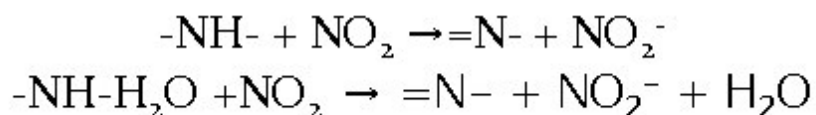
Figure 6.2 Effects of NO_2 on LEB-PANI - Water facilitates the transport of free protons in the polymer matrix hopping through hydrated moieties along the polymer chain via the Grotthus mechanism for proton transport

6.2.4. *Selectivity of LEB-PANI*

The selectivity of these films to NO_2 in the presence of the interferent gases explored in these studies is attributed to the processing of the pre-spinning solutions and the inherent structure of LEB-PANI. As discussed earlier, Miejerink et. al, [25] showed that post processing conditions of commercially available polyaniline powders can tailor the reactivity between the processed polymer and select analytes increasing selectivity and sensitivity of the polyaniline film to specific gases. If the films were post-processed using solvents similar to the analyte tested, they would become insensitive to the analyte. This is the case for the methanol and ethanol gases tested. This films are prepared in ethanol and acetone, thus according to the theory of [25] they are inhibited from reacting with sites along the polymer chain already bonded to similar groups or molecular

structures. The unresponsiveness of the composites to gaseous benzene suggests that it does not inflict any changes in the film's electrical properties. This may be attributed to the similarity in structure of benzene to that of the aromatic rings of LEB-PANI. Reducing gases such as CO, isoprene, and NH_3 were shown to have little to no effect on the low concentration LEB-PANI composites (for CA and PVP). In the presence of humidity reduction of protonated N centers (removal of H^+, as evidenced by the response of 8020 PVP LEB-PANI to NH_3 in chapter 4) may occur. This coupled with the transference of electrons from the reducing gas, such as NH_3, to the polymer may result in an increase in the sensors electrical resistance (as in the case of the 8020 PVP LEB-PANI composite). It has been observed for NH_3 that the response however does not recover.   It is possible that the oxidized PVP LEB-PANI composites will react with these gases as they can be reduced to lower oxidation levels. The 8020 PVP LEB-PANI composite, however, is already in the reduced state and thus does not have the ability to undergo further reduction.

The reactivity of the CA LEB-PANI composite to dissolved NO_2 can be explained by the work of [25] as well. With groups such as O^-, OH, COO^-, and H^+, from the acetic acid/acetate groups of CA, bonded to various sites along the conducting polymer chain it is possible that they may inhibit reactions between like species, such as the products of dissolved NO_2, and the polymer.

6.3. OPTIMIZATION OF LEB-PANI BASED SENSORS

The goal of this research was to develop a LEB-PANI sensor for selective NO_2 detection. The most promising candidates were determined to be the 8020 PVP LEB-PANI composite and the 8020 CA LEB-PANI composites. The main deviant between the two is that the former retains the reduced structure while the latter has transformed the material into a light emeraldine salt. None the less both sensors can be optimized to enhance sensitivity and response and recovery times. For the CA LEB-PANI sensor, it was shown in chapter 5 that stability, sensitivity, and response and recovery times may be optimized through conditioning of the sensor in the gas analyte. Previous studies on conditioning these samples according to ASTM D 618 – 05 *Standard Practice for Conditioning Plastics for Testing* showed that contamination by lab air over the 40 hour period poisoned the samples, such that they could not be tested. However from this work, it appears that if the samples are conditioned by the analyte in a closed atmosphere, improvements in the sensor's response mechanism may be achieved.

For the 8020 PVP LEB-PANI sensor, optimization of the sensor may involve alternative substrates. Current studies on the sensor response of the 8020 PVP LEB-PANI composite on silicon substrates show a 58% increase in sensitivity and 67% increase in response time to 5 ppm of NO_2 at 50% RH, as well as more stabilized response at higher humidity levels.

REFERENCE

1. G. Anitha and E. Subramanian, "Dopant induced specificity in sensor behaviour of conducting polyaniline materials with organic solvents, nanocomposite of Pd-polyaniline as a selective methanol sensor", *Sensors and Actuators B – Chemical,* vol. 92, no. 1-2, pp. 49-59, 2003

2. A.Z. Sadek, W. Wlodarski, K. Shin, RB Kaner, and K Kalantar-Zadeh, "A layered surface acoustic wave gas sensor based on a polyaniline/In$_2$O$_3$ nanofibre composite", *Nanotechnology*, vol 17, no 17, pp. 4488-4492, 2006

3. N. Parvatikar, S. Jain, SV Bjoraskar, and M.V.N.A. Prasad, "Spectroscopic and Electrical Properties of Polyaniline/CeO$_2$ Composites and Their Application as Humidity Sensor", *J. Applied Polymer Science*, vol 102, no 6, pp 5533-5537, 2006

4. Y. Wanna, N. Srisukhumbowornchai, A. Tuantranont, A. Wisitsoraat, N. Thavarungkul, and P. Singjai, "The effect of carbon nanotube CO gas sensing characteristics of polyaniline gas sensor", *J. Nanoscience and Nanotechnology*, vol 6, no 12, pp 1-4, 2006

5. D. Aussawasathien, J.H. Dong, and L. Dai, "Electrospun polymer nanofiber sensors", *Synthetic Metals*, vol. 154, no 1-3, pp. 37-40, 2005

6. K.M. Manesh, A..L Gopalan, K.P. Lee, P. Santhosh, K.D. Song, and D.D. Lee, "Fabrication of a functional nanofibrous ammonia sensor", *IEEE Transactions on Nanotechnology*, vol 6, no 5, pp 513-518, 2007

7. S.T. McGovern, G.M. Spinks, and G.G. Wallace, "Microhumidity sensors based on processible polyaniline blends", *Sensors and Actuators B – Chemical*, vol. 107, no. 2, pp. 657-665, 2005

8. K.H. Hong, K.W. Oh, and T.J. Kang, "Polyaniline nylon-6 composite fabric for ammonia gas sensor", *J. Applied Polymer Science*, vol. 92, no. 1, pp. 37-42 , 2004

9. Y. Wanna, S. Pratontep, A. Wisitsoraat, and A. Tuantranont, "Development of Nanofibers Composite Polyaniline/CNT Fabricated by Electrospinning Technique for CO Gas Sensor", *Proceeding of the Inter. Conference on Nanoscience and Technology,* 2007

10. H. Schreuder-Gibson, P. Gibson, P Tsai, P. Guptam and G. Wilkes, "Cooperative Charging Effects of Fibers from Electrospinning of Electrically Dissimilar Polymers", *International Nonwovens Journal*, pp. 39-45, 2004

11. O.N. Timofeeva, B.Z. Lubentsov, Ye.Z. Sudakova, D.N. Chernyshov, and M.L. Khidekel, "Conducting polymer interaction with gaseous substances, 1. Water, *Synthetic Metals*, vol. 40, no. 1, pp. 111-116, 1991

12. E. Tobolkova, J. Prokes, I. Krivka, M. Trchova and J. Stejskal, "Temperature- and humidity-related degradation of conducting polyaniline films", *Macromolecular Symposia,* vol. 212, p. 447-454, 2004

13. E.S. Matveeva, "Residual water as a factor influencing the electrical properties of polyaniline. The role of hydrogen bonding of the polymer with solvent molecules

in the formation of a conductive polymeric network" , *Synthetic Metals*, vol. 79 no. 2, pp. 127-132, 1996

14. K. Ogura, A. Fujii, H. Shiigi, M. Nakayama, and T. Tonosaki, "Effect of hygroscopicity of insulating unit of polymer composites on their response to relative humidity", *J. Electrochemical Society*, vol.147, no. 3, pp. 1105-1109, 2000

15. B. Lubentsov, O. Timofeeva, S. Saratovskikh, V. Krinichnyi, A. Pelekh, V. Dmitrenko, and M. Khidekel, "The study of conducting polymer interaction with gaseous substances 4. The water content influenced on polyaniline crystal structure and conductivity", *Synthetic Metals*, vol. 47, no. 2, pp. 187-192, 1992

16. M.E. Jozefowicz, A.J. Epstein, J.P. Pougetm J.G. Masters, A. Ray, Y. Sun, X. Tang, and A.G. MacDiarmid, "X-ray structure of polyanilines", *Synthetic Metals*, vol. 41, no. 1-2, pp. 723-726, 1991

17. M. Can, N.O. Pekmez, and A. Yildiz, "Theoretical investigation of the proton effect on electropolymerization of aniline", *Polymer*, vol. 44, no. 8, pp 2585-2588, 2003

18. V.M. Schmidt, D. Tegmeyer, and J. Heitbaum, "Transport of protons and water through polyaniline membranes studied with on-line mass spectrometry", *J. Eletroanalytical Chemistry*, vol. 385, pp 149-155, 1995

19. S. De, A. Dey, and S.K. De, "Electrical transport and optical properties of vanadyl phosphate polyaniline nanocomposites", *J. Physics and Chemistry of Solids*, vol.

68, no. 1, pp 66-72, 2007; "Large polaron tunneling and anomalous dielectric response in complex layered systems", *J. Applied Physics*, vol. 100, no.2, 2006

20. N. Agmon, "The Grotthus mechanism", *Chemical Physics Letters*, vol. 244, pp. 456-462,1995,

21. A. Aytac, M. Kabasakaloglu, B. Sari, and M. Talu, "Ion-Selective Electrodes Prepared with Polyaniline Membranes", *Russian J. Electrochemistry*, 40(7), pp 732-735, 2004

22. S.C. Hobaica, "Stability of polyaniline in air and acidic water", *J. Polymer Science Part B: Polymer Physics*, vol. 41, no. 8, pp. 807-822, 2003

23. M. Matsuguchi, A. Okamoto, and Y. Sakai, "Effect of humidity on NH_3 gas sensitivity of polyaniline blend films", *Sensors and Actuators B: Chemical*, vol. 94, no. 1, pp. 46-52, 2003

24. M. Chanda and S.K. Roy, *Plastics Technology Handbook*, CRC press, pp. 4-130, 2006

25. M.G.H. Meijerink, D.J. Strike, N.F. de Rooij, and M. Koudelka-Hep, "Reproducible fabrication of an array of gas sensitive chemoresistors with commercially available polyaniline", *Sensors and Actuators B- Chemical*, vol. 68, no 1-3, pp. 331-334, 2000

CHAPTER 7

7. Conclusions and Future Work

7.1. CONCLUSIONS

Polyaniline has been extensively studied and employed for various sensing applications. The responsive nature of polyaniline (PANI) is highly dependent on the processing conditions, film composition, and morphology. The mechanisms employed in producing PANI films for chemical or biological sensing applications dictate the material's electrical conductivity, overall structure, and stability. The studies presented in this thesis have demonstrated the successful application of leucoemeraldine base polyaniline for selective NO_2 detection. From the analyses of these LEB-PANI composites several key points about the system can be made:

- The sensing mechanism for the LEB-PANI composite systems depends strongly on water as a catalyst for charge transport. It has been shown that water facilitates the transport of free protons in the polymer matrix hopping through hydrated moieties along the polymer chain via the Grotthus mechanism for proton transport. This mechanism is responsible for charge transport in the polyaniline composites studied.

- In these studies water has adopted the role of protonating agent for the PVP LEB-PANI composites and catalyst for intrinsic doping (via the hydrolysis of CA) in the CA LEB-PANI composite.

- NO$_2$ reacts with the hydrated polymer through several mechanisms: 1) it can oxidize the polymer, transferring electrons from the polymer to the gas yielding a positively charged system and 2) at the humidity levels studied it can dissolve into H$_3^+$O, HNO$_2$, and NO$_2^-$ which can perform as protonating and reducing agents.

- LEB-PANI can remain in the reduced state if PVP is employed as a base polymer and the concentration of LEB-PANI is kept low. Optimum concentration for these studies was determined to be 20% wt/wt.

This is the first study that details the sensing mechanism of LEB-PANI using optical spectroscopy and for the first time electrospun LEB-PANI composites with PVP and CA have been successfully employed for selective NO$_2$ detection. This work has proven that the LEB-PANI composites exhibit higher sensitivity (down to 0.5ppm) and selectivity as compared to the polyaniline NO$_2$ sensors listed in table 1.4.1.

In chapter 1, the detection range for environmental monitoring was set to 1-5 ppm for NO$_2$. The sensors developed here have shown to be operable at room temperature in that range. However, as discussed it is necessary to employ a humidity level of at least 20% RH for operability. For the 8020 PVP LEB-PANI sensor, the optimum operating conditions are 40-50% RH at room temperature. Above this range the sensor transforms structurally and will yield variability and degraded responses. Below this range the sensor cannot create adequate charge along the polymer chain because the diffusion of water vapor to polyaniline is slower at low humidity and may just be absorbed completely by PVP. It has been determined that the mechanism which dominates the reactions between leucoemeraldine base polyaniline and NO$_2$ is the oxidation of amine centers. Interferents

however such as the dissolved NO_2 products were shown to poison the sensor decreasing its sensitivity to NO_2. Because this sensor has exhibited instability after repeated exposures as a consequence of the aforementioned interferents and base polymer degradation, it is best suited for single use NO_2 detection applications.

The CA LEB-PANI sensor on the other hand is likely to be operable at various levels of humidity making it possibly more suitable for breath analyses. As described in chapter 1, inflammation and oxidative stress in the lungs can by monitored by measuring the changes in the concentration of NO and its products NO_2- (nitrite) NO_3- (nitrate) [3-5]. In the case of asthma related illnesses, the concentration of NO_x in exhaled breath may increase from 0.22 ppm in healthy patients to 0.38 ppm for asthmatic patients [10]. Direct breath measurements center on a high humidity environment (~90%). Because CA is more water resistant than PVP it may be employable for such applications. It has been observed that CA exhibits high sensitivity (~0.22) down to 0.5 ppm with adequate reproducibility. The effect of humidity on polyaniline may be deemed negligible as observed from the in-situ UV-Vis experiments, which suggests that increasing humidity only affects rate or extent of hydrolysis of CA. The more water content available the more acetic acid is produced causing an increase the oxidation and doping level of LEB-PANI which yields enhanced electrical properties.

The primary focus of this dissertation was to implement a LEB-PANI based composite for selective NO_2 environmental and health monitoring applications. The 8020 PVP LEB-PANI and 8020 CA LEB-PANI composites have exhibited high sensitivity and selectivity in the presence of interfering gases such as hydrocarbons and

reducing gases like CO and NH_3 as well as fast response and recovery times (as fast as 40 s and 155 s, respectively).

7.2. FUTURE RESEARCH DIRECTIONS

7.2.1. *Applications*

•   It was observed above that the 5050 PVP LEB-PANI composite exhibits little to no response to NO_2.   Further studies on this composite revealed an increase in sensitivity to NH_3 (which acts as a deprotonating agent for polyaniline). During exposure, NH_3 removes protons (resulting in deprotonation of the film) from imine sites of the polymer chain and forms NH_4^+ resulting in a decrease in film conductivity (increase in resistance). Gas sensing of the composite films reveals that the 5080 PVP LEB-PANI hybrid increases in resistance with exposure to NH_3, as expected. This study demonstrated that the 5050 LEB-PANI PVP composite can be used for NH_3 detection down to 5 ppm. At low humidity levels (20% RH) the sensor can be employed as an 'on-off' sensor. At high humidity levels the sensor can exhibit up to a 50% increase in sensitivity to NH_3. Further research into the selectivity of the sensor against other reducing agents is necessary to ascertain possible applications.

•   It has been demonstrated that pH found in human breath condensate correlates to certain gas constituents of exhaled breath. The advantage of measuring pH is related to the decomposition or mixing of gaseous biomarkers resulting in false positives and ambiguity in sensor response. The pH of the condensate has been shown to be directly

related to the acidity of airway surface liquid which changes with an increase in oxidative stress associated with certain pulmonary diseases. In all studies to date the polymer based sensors are used in electrochemical sensing tests. It is proposed in this research, as an alternative, to employ conductimetric hybrid systems consisting of cellulose acetate and ES-PANI fabricated using the electrospinning technique for *'headspace analyses'* of solutions containing different pH levels. Results from the initial sensing tests with pH buffer solutions ranging from 4 to 7 to 10 reveal that as the pH increases, thus decreasing [H^+], the films exhibit an increase in resistance by 1.7-2.0 x10^{-7} Ω per pH unit (which correlates to a tenfold decrease in [H^+]). This increase in resistance is associated with reduction of the electroactive sites along the polymer chain by the basic headspace. As [H^+] increases the films become highly protonated along the imine sites yielding a decrease in the films resistance on exposure to the headspace of lower pH. The CA ES-PANI fiber composites are shown to be promising candidates for this application. Further work however is necessary to study the effects of pH in the range of interest (pH levels in the range of 7-8 represents the deaerated exhaled breath condensate of healthy people and people inflicted with illnesses such as bronchitis, asthma, and chronic obstructive pulmonary disease).

7.2.2. *Optimization of LEB-PANI Sensors*

• In an effort to improve the processing of LEB-PANI the use of an alternative solvent such as N- methyl pyrrolidone (NMP) may be used. Initial studies reveal an increase in the dissolution of LEB-PANI after processing with NMP. Treatment of the

polymer in n-methyl pyrrolidone might prove to reduce the occurrence of aggregated structures. Moreover, it may allow for electrospinning of pure LEB-PANI. This may improve the sensitivity of the films if pure polyaniline films are used as the sensing element versus the bi-component systems discussed in this thesis. This may also lead to enhanced inherent selectivity of LEB-PANI to target agents.

- In order to determine the bonds formed during exposure to NO_2 and humidity (the latter of which may deflect the laser), in-situ FTIR may be employed. This will provide a detailed analysis of gas – polymer reactions and confirm the manifestation of dissolved NO_2 and its proposed effects on LEB-PANI.

- The stability analyses performed on the CA LEB-PANI composite suggests that pre-conditioning the sensor in the analyte environment may improve the response and stability of the sensor matrix to the analyte. This is suggested as an optimization process for NO_2 detection with 8020 CA LEB-PANI. For an improved response to select analytes this may also be a useful technique for tailoring the selectivity of the CA LEB-PANI hybrid.

- Because the sensors are processed using benign solvents and biocompatible polymers it is possible that these materials can be employed for biosensing applications. Previous studies have shown that the electrospun PVP LEB-PANI matrix can be used to immobilize the enzyme urease. The enzyme has shown to retain its activity in the presence of urea even after exposure to the high potentials associated with the electrospinning process. On exposure to urea, reactions between the enzyme and urea liberate ammonia. The ammonia released can in turn be measured using the 5050 PVP

LEB-PANI matrix. The composite can be employed as a single system acting as both the receptor and transducer.

- The resolution of the in-situ UV-Vis setup depends on the slit width inside the HR4000 detector. An improvement in the sensitivity of UV-Vis can be achieved by decreasing the size of the slit width to resolve other transitions that are not observable with the current setup. Calculations on the evolution of the material's band gap as a function NO_2 exposure and humidity can then be accurately performed. Initial results show no significant differences in the size of the band gap during exposure. This is attributed to the lack of resolution in the UV-Vis system.

APPENDIX A

1.   Certificate of analysis for Fluka LEB-PANI Powders, 81303-5g

2.   Certificate of analysis for Sigma Aldrich LEB-PANI powders

SIGMA-ALDRICH

Sigma-Aldrich Production GmbH
CH-9471 Buchs/Schweiz
www.sigma-aldrich.com

Telefon ++41 81 755 2511
Telefax ++41 81 756 5449
Email: fluka@sial.com

Fluka

Certificateof**Analysis**

PRODUCT BRAND	**Fluka**
PRODUCT-NO.	81303
PRODUCT	POLYANILINE
	-
FORMULA	
MOLECULAR MASS	
CAS-NUMBER	25233-30-1

LOT	410463/1

Test	**Result**
APPEARANCE	DEEP BLUE POWDER
LOSS ON DRYING	1.7% (50 C, 4 HOURS)
CARBON CONTENT	63.90 %
HYDROGEN CONTENT	6.13 %
NITROGEN CONTENT	6.98 %
INFRARED SPECTRUM	CORRESPONDS

DATE OF QC-RELEASE	10/APR/00

Dr. G. van Look, Manager
Quality Control
Buchs, Switzerland

Sigma-Aldrich guarantees the 'Sales-Specification' values only, additional lot specific tests may be included for further information. The current 'Sales-Specifications' sheet is available on request. For further inquiries, please contact our Technical Service.
Sigma-Aldrich warrants, that its products conform to the information contained in this and other Sigma-Aldrich publications. Purchaser must determine the suitability of the product for its particular use. See reverse side of invoice for additional terms and conditions of sale.
The values given on the 'Certificate of Analysis' are the results determined at the time of analysis.

SIGMA-ALDRICH

Certificate *of* **Analysis**

Product Name	Polyaniline (leucoemeraldine base)
Product Number	530670
Product Brand	Aldrich
CAS Number	25233-30-1

TEST	**LOT 06527DD RESULTS**
APPEARANCE	VERY DARK BLUE POWDER
INFRARED SPECTRUM	CONFORMS TO STRUCTURE.
ELEMENTAL ANALYSIS	CARBON 78.64%
	HYDROGEN 5.57%
	NITROGEN 14.77%
QUALITY CONTROL	MAY 2005
ACCEPTANCE DATE	

Barbara Rajzer, Supervisor
Quality Control
Milwaukee, Wisconsin USA

APPENDIX B

1.   Sensing apparatus of University of Brescia

Gas sensor test system : type 1
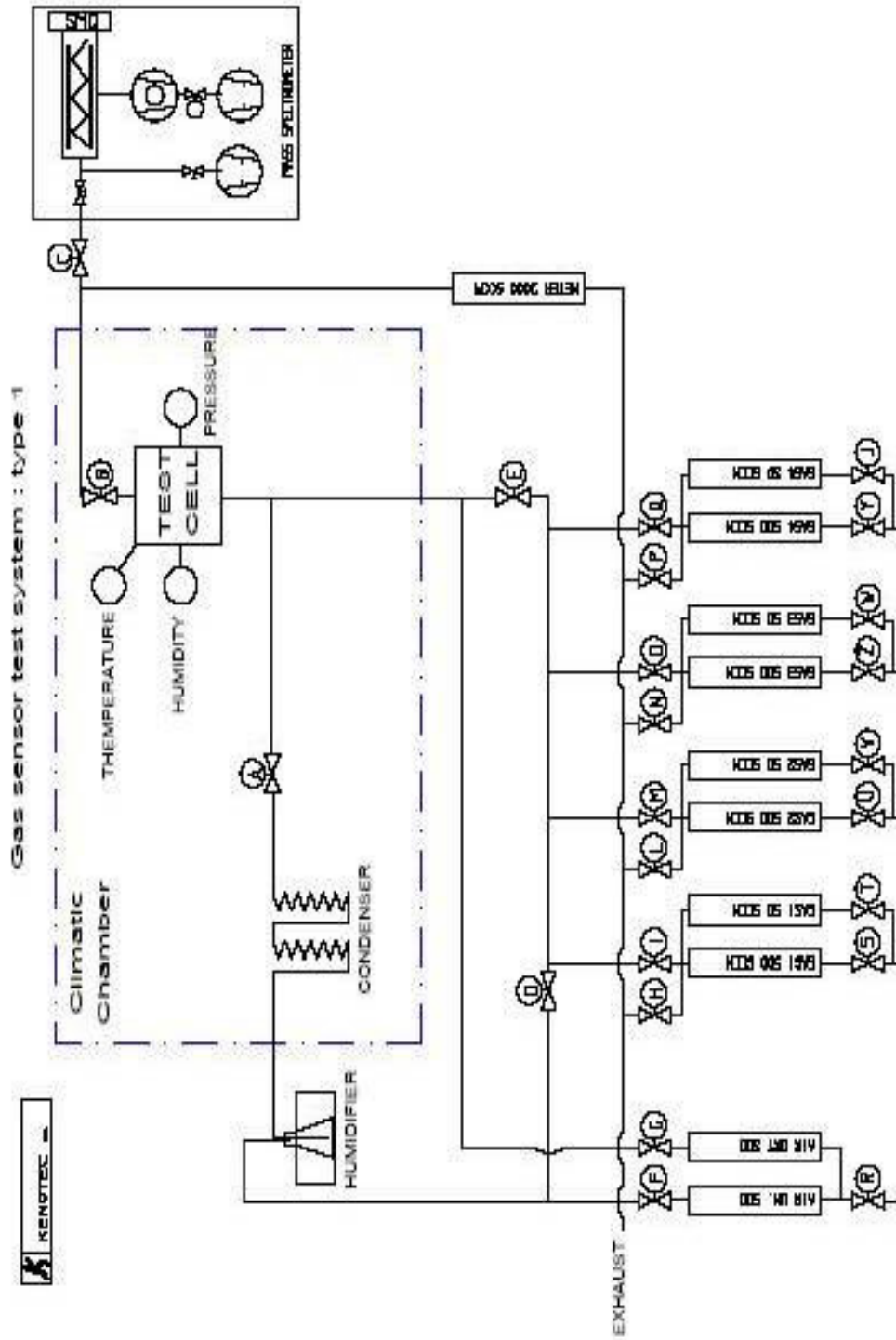
APPENDIX C

1.   Humidity Calibration for In-Situ UV-Vis setup

An Extech 44550 pocket humidity temperature pen was used to calibrate the humidity setup for the humidity range 20-70%. The modified gas sensing setup consists of 2 1000 ppm N_2 tanks, 1 1000ppm O_2 tank, and 1 1000 ppm NO_2 in N_2 tank. To measure humidity, the Extech pen was placed in a quartz tube. The ends of the tube were connected to the inlet of the gases and outlet to the fume hood. For 20 ppm NO_2, which is the lowest concentration that can be achieved with this current setup, the total N_2 gas used in the background (with O_2 to formulate synthetic air – O_2) was split by the two N_2 tanks. The flow from one tank flowed with the NO_2 and O_2 gases making it the dry N_2 and the other flow went through a 100 ml glass bubbler. The glass bubbler was filled with 100 ml of deionized water. The flow of gas is controlled using an MKS flow meter. Table 1 lists the settings for each channel on the flow meter. Figure 1 corresponds to the humidity level for each setting from 10% wet N_2 to 40% wet N_2 flow.

Table 1: Settings for MKS flow meter

Channel 3	**Gas (ppm)**	**20**
Channel 2	**O2 (ppm)**	**196**
Channel 1	100 Dry N	784
Channel 4	0 Wet N	0
Channel 1	90 Dry N	705.6
Channel 4	10 Wet N	78.4
Channel 1	80 Dry N	627.2
Channel 4	20 Wet N	156.8
Channel 1	70 Dry N	548.8
Channel 4	30 Wet N	235.2
Channel 1	60 Dry N	470.4
Channel 4	40 Wet N	313.6

Figure 1 Response of Extech humidity pen for each setting

APPENDIX D

1. Table 4.2 FTIR Table for LEB-PANI PVP Composites

2. Table 5.1 FTIR Table for LEB-PANI CA Composite

Table 4.2 FTIR vibrations for 8020, 5050, and 2080 PVP LEB-PANI composites

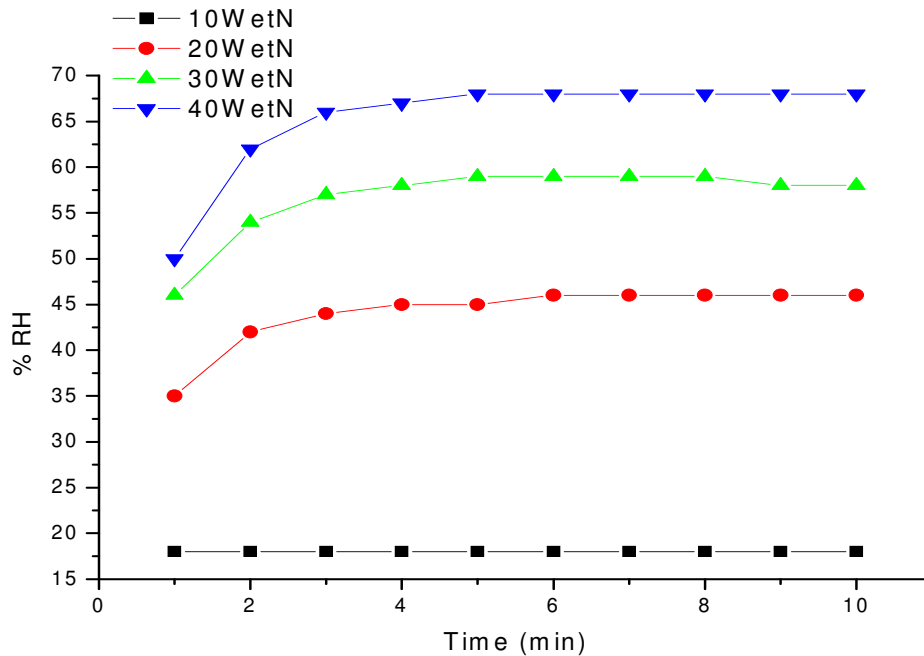| 8020 PVP LEB-PAN cm⁻¹	5050 PVP LEB-PAN cm⁻¹	2080 PVP LEB-PAN cm⁻¹	Forms of Vibration	Comments
3483	3467	3455	N-H Stretching; intermolecular H bonds	Can be found in all polymer composites and PVP
2966	2950	2951	CH_3 or CH_2 from residual ethanol	This is residual ethanol found in PVP fibers and adsorbed by PANI
2929	2915	2923	CH_3 or CH_2 from residual ethanol	This is residual ethanol found in PVP fibers and adsorbed by PANI
2879	2852	2886	CH_3 or CH_2 from residual ethanol	This is residual ethanol found in PVP fibers and adsorbed by PANI
		2774	O-H stretching vibration, intramolecular H-Bond; N-H stretching vibration	Suggests adsoprtion of atomosphere volatiles
		2672	O-H stretching vibration, intramolecular H-Bond; $C=N^+H$ or $C-N^+H_2$ or $C-N^+H$	Supports protonation of LEB-PANI by atmospheric water formulaing polaron and bipolaron structures
	2343	2357	$C=N^+H$ or $C-N^+H_2$ or $C-N^+H$	Supports protonation of LEB-PANI by atmospheric water formulaing polaron and bipolaron structures
		2338	$C=N^+H$ or $C-N^+H_2$ or $C-N^+H$	Supports protonation of LEB-PANI by atmospheric water formulaing polaron and bipolaron structures
		1843	$C=N^+H$	Supports protonation of LEB-PANI by atmospheric water formulaing polaron and bipolaron structures
		1821	$C=N^+H$	Supports protonation of LEB-PANI by atmospheric water formulaing polaron and bipolaron structures
		1791	C=C stretching of quinoid; C=O stretching in PVP	Characteristic peak of PVP and oxidized polyaniline
		1746	C=O Stretching in PVP; C=C stretching of Q	Characteristic peak of PVP and oxidized polyaniline
	1727	1729	C=O Stretching; C=C stretchingof quinoid	Characteristic peak of PVP and oxidized polyaniline
		1719	C=O Stretching in PVP	Characteristic peak of PVP
1696		1696	C=O Stretching in PVP	Characteristic peak of PVP
1682		1682	$C=N^+H$ or C=C stretching	C=N Peak most pronounced in 8020 PANI PVP composite, suggests formation of bipolaron structure
1672	1676	1670	C=O Stretching in PVP; and C=N stretching	C=N Peak most pronounced in 8020 PANI PVP composite
1647		1651	C=N stretching in imine and NH deformation in amine	C=N peak well pronounced in 8020 PANI PVP composite; NH peak small and broad in 8020 PVP PANI composite
		1615	C-H Vibration; NH in plane bending; C=C stretching in quinoid	Shoulder peak 8020PANPVP

8020 PVP LEB-PAN cm^{-1}	5050 PVP LEB-PAN cm^{-1}	2080 PVP LEB-PAN cm^{-1}	Forms of Vibration	Comments
	1572	1575	C=C Stretching ; C=N stretching in C=N$^+$O$^-$; NH bending in C=NH$_2$ and CH	Suggests protonation by water disassociation where O is the anion. Bipolaron formation is observed
	1565		C=N Stretching in C=N$^+$O-; NH in plane bending in imine; NH deformation in amine	Shoulder peak only pronounced in 5050 PVPPAN; Suggests protonation by water disassociation where O is the anion. Bipolaron formation is observed
1555	1552	1555	CH ring in plane bend; NH in plane bend; C=N stretch in C=N$^+$O$^-$; NH bending in imine;	CH and NH vribrations belong to quinoid imine unit; C=N Peak most pronounced in 8020 PANI PVP composite, weak peak in both 5050 and 8020 PVP PANI composites
		1538	N-H deformation vibrations; NH bending in imine; C=N Stretching	The NH deformation vibrations are weak; strong NH bending peak
	1528		C=N stretching in imine and NH bending in imine	Characteristic peak of oxidized structure
		1518	NH bending in C=NH$_2$; N=O stretching, C=N stretching	Possible protonation from water moleculed presorbed into structure during processing
	1509	1504	Benzenoid Ring Vibrations; C=C and CH Stretching in qunioid	Characteristic peak of oxidized structure
1491	1494	1495	C=N Stretching in quinoid; C-C strethcing in benzenoid; CH bending; NH and CH stretching	B; Bonding between N in amine/imine/PVP evident here
1456	1460	1462	NH in plane bend, CH ring in plane bend; CH deformation in N=CH$_2$ of PVP; CH and C=C stretching in benzenoif	This is peak is most defined in 8020 PANiPVP
1437		1434	CH deformation in CH-OH (adsorbed water)	This peak is most defined in 8020 PANI PVP suggesting that water is adsorbed best on this composite
	1421	1420	CN stretch; CH and NH deformation	This peak reflects adsorbed water
1415			CH-OH	Bonded alcohol
	1390		OH deformation in C=N-OH ; CO stretch & CH deformation in CHOH	This peak reflects adsorbed water
1368	1372	1375	OH deformation and CH stretch in benzenoid with adsorbed OH attached	This peak reflects adsorbed water
1312	1315	1316	Ring vibration; CH deformation in amine; CN stretching; NH in plane bend	Characteristic peak of LEB-PANI
1289	1284	1288	CH deformation in CH-OH with OH from ethanol	This peak reflects adsorbed ethanol on the benzenoid ring
1266	1270	1271	CH deformation	Shoulder peak from ethanol adsorption
1227	1226	1220	CH deformation from adsorbed ethanol and C-O stretching on benzenoid ring	This peak reflects adsorbed ethanol on the benzenoid ring

8020 PVP LEB-PAN cm⁻¹	5050 PVP LEB-PAN cm⁻¹	2080 PVP LEB-PAN cm⁻¹	Forms of Vibration	Comments
1167	1164	1169	CH in plane deformation from amine	Characteristic LEB-PANI band, also reflects vibrations from PVP
		1127	C-O stretching and CH in plane deformations	Suggests adsorption of ethanil
1112			CH in plane deformation and CN stretching in amine	Characteristic LEB-PANI band
1102			CH in plane deformation and CN stretching in amine	Characteristic LEB-PANI band
		1096	CH in plane deformation and CN stretching in protonated amine C-O stretching from ethanol adsorption	Characteristic LEB-PANI band, also reflects vibrations from PVP
1073	1070	1071	C-N stretching CH in plane deformation; NH out of plane bend	Characteristic LEB-PANI band
1045			CN stetching	Characteristic LEB-PANI band, also reflects vibrations from PVP
1014	1015	1017	CH ring in plane bend; CN stretching	Characteristic LEB-PANI band
1001	997	1000	CH in plane deformation	Characteristic LEB-PANI band
		981	CH in plane deformation	Characteristic LEB-PANI band
928	931	930	CH ring out of plane deformation; NO stretching in C=N-OH	ring deformation in PVP and is most pronounced in the 8020PVP PANI composite
890	894	899	NH out of plane bend in amine; ring out of plane deformation	Characteristic LEB-PANI band
843	844	841	CH out of plane deformation	This peak also reflects the CH ring deformation in PVP and is most pronounced in the 8020PVP PANI composite
	810	812	CH out of plane deformation	This peak is most pronounced in 5050 PVPPANI composite
793		798	Out of plane bending of Benzene	Very weak peak in 8020 PANI PVP; shoulder peak to 843 cm⁻¹ in 8020 PVP PANI
789			CH ring out of plane bend; NH out of plane bending	Small shoulder peak in 8020 PVP PANI in agreement with references
		775	OH deformation CO Stretching; NH out of plane bending; ring out of plane deformation	This reflects adsorbed water on the polymer chain
741		750	NH deformation; CH ring out of plane bending	Shoulder peak on both composites found in agreement with reference for LEB PANI
732	734	732	NH amine wagging; NH deformation; CH ring out of plane bend	Characteristic LEB-PANI band

8020 PVP LEB-PAN cm^{-1}	5050 PVP LEB-PAN cm^{-1}	2080 PVP LEB-PAN cm^{-1}	Forms of Vibration	Comments
694	692		NH out of plabe bending; ring out of plane deformation	Most prominent in high concentration LEB-PANI structure
684		685	in plane ring deformation	weak shoulder peak, characteristic band of polyaniline
		666	NH out of plane deformation	Characteristic LEB-PANI band
646	648	646	NH out of plane deformation; ring in plane deformation	This peak also reflects the CH ring deformation in PVP and is most pronounced in the 8020PVP PANI composite

Table 5.1 FTIR vibrations for 8020 CA LEB-PANI composite

8020 CA LEB-PAN cm^{-1}	Forms of Vibration	Comments
3479	N-H Stretching; intermolecular H bonds; OH Stretching	Free NH of polyaniline; unacetlyated OH of CA
2947	CH$_3$ vibrations from acetone	This is residual acetone found in CA fibers and adsorbed by PANI
2920	CH$_3$ vibrations from acetone; O-H stretching vibration, intramolecular H-Bond	Bonding between OH group of CA and LEB-PANI benzenoid ring, Bonding of COOH group with LEB-PANI
1748	C=O Stretching in CA; C=C stretching of quinoid	Stretching of Cellulose, adsorbed acetone, and acetyl group. Sharp peak shifted from 1600 cm-1 series of peaks. This suggests high levels of oxidation due to adsorption of CA
1735	C=O Stretching of acetate; C=C stretchingof quinoid	Stretching of Cellulose, adsorbed acetone, and acetyl group. Sharp peak shifted from 1600 cm^{-1} series of peaks. This suggests high levels of oxidation due to adsorption of CA
1694	C=O Stretching in CA	Characteristic peak of CA
1682	C=N$^+$H, C=O, C=C stretching	Sharp shoulder peak suggests bonding of COOH group from CA to aromatic ring of LEB-PANI. Provides evidence of CA adsorption abd bipolaron/polaron groups.
1649	C=C, C=N stretching in imine and NH deformation in amine	Sharp medium strong peak
1631	C=C and C=N stretch, OH deformation in cellulose, NH deformation	Very weak shoulder peak
1595	C=C and C=N Stretch, NH deformations	Formulated from C=N$^+$O$^-$, provides evidence of the acetate groups of CA disassociating and protonating imine N of LEB-PANI

8020 CA LEB-PAN cm^{-1}	Forms of Vibration	Comments
1571	C=C Stretching ; C=N stretching in C=N$^+$O$^-$; NH bending in C=NH$_2$ and CH	Suggests diassociation of H containing groups of acetate groups in CA onto the imine N of LEB-PANI. Provides evidence of CA adsorption abd bipolaron/polaron groups.
1556	CH ring in plane bend; NH in plane bend; C=N stretch in C=N$^+$O$^-$; NH bending in imine;	CH and NH vibrations belong to quinoid imine unit; C=N Peak most weakened in this composite. Provides evidence of CA adsorption abd bipolaron/polaron groups.
1538	N-H deformation vibrations; NH bending in imine; C=N Stretching	The NH deformation vibrations are weak; strong NH bending peak
1518	NH bending in C=NH$_2$; N=O stretching, C=N stretching	Chemical bonding between imine N and Cellulose
1512	C=N stretch, NH bending in C=NH$_2$, NH deformation in amines, C=C stretching in quinoid	Chemical bonding between imine N and Cellulose
1495	C-N and C-C strethcing in B; CH bending; NH and CH stretching	This peak is extremely weakened with the adsorption of CA
1455	NH in plane bend, CH ring in plane bend; CH and C=C stretching in B	Sharp peak, park of group of bands over broader band
1434	CH deformation in CH-OH (adsorbed water)	This peak is most defined in 8020 PANI PVP suggesting that water is adsorbed best on this composite
	CN stretch; CH and NH deformation	This peak reflects adsorbed water
1416	CH-OH	Bonded alcohol
1315	Ring vibration; CH deformation in amine; C-N stretching; NH in plane bend	Weak shoulder peak
1235	CH deformation in CH-OH, CO and OH stretching in COOH, OH deformation in C=NOH, Cellulose, C-O stretching	Suggests reaction between imine N and acetate groups of CA

8020 CA LEB-PAN cm^{-1}	Forms of Vibration	Comments
1163	C-H in plane deformation from amine	Sharp shoulder peak of broader band, weakened as a result of oxidation by CA
1121	C-O stretching from alcohol adsorption and CH in plane deformations	Sharp weak peak associated with broad band, reflects adsorption of acetone possibly on ring structures
1087	C-O stretch COOH and CHOH, C-N stretch, Cellulose vibrations	Sharp weak peak associated with broader CA LEB-PANI
1060	C-O stretch, Cellulose vibrations	Sharp weak peak associated with broader CA LEB-PANI
1033	CH in plane deformation from amine; Cellulose vibrations- C-O-C, CO stretch in CHOH	Sharp weak peak associated with broader CA LEB-PANI
949	N-O stretching in C=NO, COOH out of plane deformation, ring out of plane deformation	Suggests chemical bond formation between cellulose and imine N
908	NH out of plane deformation, Benzenoid ring out of plane deformation	This is a characteristic peak of both structures
863	NH out of plane bending, Benzenoid ring out of plane deformation	This is a characteristic peak of LEB-PANI induced by CA adsorption
849	CH out of plane deformation	This is a characteristic peak of LEB-PANI induced by CA adsorption
830	CH$_2$ deformation in cellulose, NH out of plane bending, ring out of plane bending	This is a characteristic peak of both structures
818	CH out of plane deformation	This is a characteristic peak of both structures
803	NH out of plane bending, N$^+$H$_2$ rocking vibrations, ring out of plane deformations	Suggests protonation of amine peaks by diassociated acetate structures of CA
792	CH ring out of plane bend; NH out of plane bending	Small shoulder peak in 8020 CA PANI in agreement with references

8020 CA LEB-PAN cm^{-1}	Forms of Vibration	Comments
770	OH deformation CO Stretching; NH out of plane bending; ring out of plane deformation	Reflects adsorbed hydroxide from acetate groups of CA or atmospheric water
758	NH out of plane bending, NH deformation, ring out of plane deformation	Characteristic peak of LEB-PANI
738	NH deformation; CH ring out of plane bending	Sharp weak peak
731	NH amine wagging; NH deformation; CH ring out of plane bend	Characteristic peak of LEB-PANI
695	NH out of plane bending; ring out of plane deformation	Characteristic peak of LEB-PANI
680	in plane ring deformation	weak shoulder peak
653	NH out of plane bending; ring in plane deformation; O-CO in plane deformation of CA	Characteristic peak of LEB-PANI and CA
638	ring in plane deformation	Characteristic peak of LEB-PANI and CA
626	ring in plane deformation	Characteristic peak of LEB-PANI
608	O-CO in plane deformation for CA	Characteristic peak of CA